NORTHWESTERN UNIVERSITY

Histone Methyltransferase DOT1L Coordinates AR and MYC Stability in Prostate Cancer

A DISSERTATION

SUBMITTED TO THE GRADUATE SCHOOL

IN PARTIAL FULFILLMENT OF THE REQUIREMENTS

For the degree

DOCTOR OF PHILOSOPHY

Driskill Graduate Training Program in Life Sciences

By

Rajita Vatapalli

EVANSTON, ILLINOIS

MARCH 2020

ABSTRACT

The histone methyltransferase DOT1L methylates lysine 79 (K79) on histone H3 and is implicated in active transcription. Here we show that DOT1L is overexpressed in Prostate cancer (PCa) and is associated with poor clinical outcome. Genetic and chemical inhibition of DOT1L selectively impaired viability of androgen receptor (AR)-signaling competent PCa cells, including castration-resistant and enzalutamide-resistant cells. DOT1L inhibition led to loss of H3K79 methylation at distinct genomic loci in AR-positive compared to AR-negative PCa cells. The selective sensitivity to DOT1L inhibition is in part due to loss of MYC expression caused by displacement of AR and DOT1L at a distal enhancer. Furthermore, loss of MYC expression leads to upregulation of E3 ubiquitin ligases HECTD4 and MYCBP2, which promote AR and MYC protein degradation. This leads to further repression of the MYC pathway in a negative feed forward manner.

These results demonstrate that DOT1L selectively regulates the tumorigenicity of AR-positive PCa cells and provide a rationale for investigating DOT1L inhibition as a promising therapeutic strategy for PCa.

ACKNOWLEDGEMENTS

Firstly, I would like to express my sincere gratitude to my advisor Dr. Sarki Abdulkadir for the continuous support of my PhD study, for his patience, motivation, and immense knowledge. I appreciate all of our discussions and debates, especially when experiments failed or when I had trouble analyzing perplexing results. I truly would not have completed this PhD if he hadn't pushed me when I was flagging. I could not have imagined having a better advisor and mentor for my PhD study.

Besides my advisor, I would like to thank the rest of my thesis committee: Dr. Debabrata Chakravarti, Dr. Jindan Yu, and Dr. Julie Kim, for their insightful feedback and encouragement. I also want to thank all my lab mates in the Abdulkadir lab especially Huiying for all the stimulating discussions that have always helped me think about my project. I thank Vinay, Younga and Kenji for always being supportive in times of need. I am especially grateful for Yara for always encouraging me to smile through PhD troubles and Barbara for making the lab so much fun. I want to thank Krithika, Anant and Christie, my fellow PhD students for making grad school an enjoyable place and Krithika especially for always being around to commiserate about graduate school struggles. I truly would not have finished grad school without you. Also I thank my friends, the Nerdy Hallows, Shwetha, Krithika, Anant, Armaan and Nitin, for all the memorable times that helped keep me sane during my PhD.

Last but not the least, I would like to thank my family: my parents, Jagdish and Susheela and my sister, Shwetha for supporting me throughout my PhD and my life in general. Thank you for always being there for me and for encouraging me to follow my dreams. I wouldn't have completed my PhD without you. Thank you for always putting me first.

TABLE OF CONTENTS

TABLE OF FIGURES

CHAPTER 1: INTRODUCTION

Histone methyltransferases have emerged as important therapeutic targets in oncology but there is limited knowledge about their contributions to the pathogenesis of several malignancies (1). Disruptor of Telomeric silencing 1 Like or DOT1L is a histone methyltransferase that methylates Lysine 79 of histone H3(2). DOT1L mediated H3K79 methylation is mainly associated with active transcription, transcription elongation, and DNA repair response (3-7). Previous studies have uncovered an important role for DOT1L in driving pathogenesis of acute myeloid leukemias (AML) with mixed lineage leukemia (MLL) gene translocations (4, 8); however its role in prostate cancer is yet to be delineated. Prostate cancer is the most common adult malignancy in men and the second most common causes of cancer-related deaths (9). The mainstay treatment for advanced prostate cancer involves targeting of the androgen receptor signaling pathway(10). Although most patients initially respond to treatment, many progress to develop Castration-Resistant Prostate Cancer (CRPC) (11). At this stage, median survival rates is under 2 years (9). The main oncogenic driver of CRPC is sustained signaling by Androgen receptor (AR) which is pivotal for the survival of prostate cancer cells (12-16). AR regulates transcription of more than 1700 genes in humans which control important biological processes like cell proliferation, survival, communication, and lipid metabolism (17). While effective AR targeting therapies like Enzalutamide (ENZA) have improved clinical outcomes and prolonged survival of patients, drug resistance frequently occurs through various mechanisms including persistent activation of the AR pathway (14, 18-20). In addition to AR, deregulation of c-MYC has been observed in over 60% of CRPC patients and several reports have demonstrated that upregulation of c-MYC mRNA and protein contributes to prostate cancer progression (21-25).

Sustained MYC expression is required for the viability of CRPC cells (23) and crosstalk between MYC and AR at the level of target gene expression has been described (21). While MYC is recognized as a valued therapeutic target in CRPC, there no clinically viable inhibitors that directly target MYC, leading to significant interest in strategies targeting MYC by indirect mechanisms (26). Hence, there is a critical need to identify molecular drivers in prostate cancer and ERPC, and therapeutic targeting of these drivers may help control advanced disease.

Recently, DOT1L was reported to play a role in AR mediated transcription (27) however, this role was later contested by another group(28). Despite these studies, DOT1L mediated H3K79 methylation signature has never been defined in prostate cancer. Moreover, the role of DOT1L in prostate tumorigenesis still remains unclear.

1.1 Introduction to Prostate Cancer

Prostate cancer (PCa) is the most common cancer in men and a leading cause of cancer-related deaths in American men. One in every 7 men is diagnosed with PCa during their lifetime with currently 2 million men in the US alone. About 1,276,106 new cases were diagnosed in 2018 and almost 358,989 men died of prostate cancer worldwide (29). PCa represents 14% of all newly diagnosed cancers in the US (30). PCa incidence and risk is strongly tied with age. Risk is also increased in men with a history of prostate cancer in the family and men of African American descent. Prostate cancer is a slow growing cancer i.e. there are extended periods of time when the cancer is dormant or relatively indolent. The 5-year survival rate for localized prostate cancer is 100%, however that rate drops to 28% when cancer has metastasized to distant sites (15).

The discovery of Prostate specific Antigen (PSA) as a blood-based biomarker of disease in the 1980s' revolutionized the diagnosis of prostate cancers (31-33). Today, men with elevated PSA levels undergo a prostate exam and biopsy to determine the potential presence of prostate cancer. The tumor is then graded histologically and given a Gleason score based on disruption of prostate architecture and basal membrane invasion. (15) Common treatment options include surgical excision of the tumor (prostatectomy), irradiation or androgen deprivation therapy. Groundbreaking work by Nobel Prize winner, C.B. Huggins in the early 1940's demonstrated that androgen deprivation by removal of the testes (orchiectomy) caused regression of prostate cancer (34). This is because most prostate cancers are primarily hormone driven. Circulating androgens are essential for normal prostate development mainly through their interactions with the Androgen receptor (AR). AR is a pivotal transcription factor; its pathway is the central signaling axis that drives normal prostate growth and development. In prostate cancer, aberrant AR signaling promotes PCa growth and progression. Hence, till this date, the mainstay of prostate cancer treatment has been hormone deprivation therapy – either surgically or chemically.

After androgen deprivation therapy, the prostate cells undergo cellular apoptosis and tumor involutes into a regressed state. Therapy also restrains the growth of metastatic cancer cells (35). The castration therapy relieves all prostate cancer symptoms almost immediately. However, this inhibition lasts for an average of 12-33 months after therapy, after which many patients relapse to an incurable form - Castration-Resistant Prostate Cancer (CRPC). CRPC progression can be due to AR dependent and AR independent mechanisms. AR independent mechanism includes up

regulation of parallel growth signaling pathways like MYC (36), PTEN-AKT (37), etc. However most commonly there is unhindered androgen independent AR signaling characterized by elevation of PSA levels in plasma. As the disease progresses, the cancer ultimately metastasizes (preferentially to bone). At this stage even with advanced therapeutic intervention, overall survival rates decrease to below 2 years (13). The resistant cancers grow in a more aggressive manner eventually resulting in death. Treating CRPC presents as a major clinical challenge today. In 2012, Enzalutamide (ENZ), an anti-androgen receptor drug was approved by the FDA for extending overall survival in CRPC patients from 13 months to 18 months. (86, 87) However, despite its initial success, Enzalutamide resistant prostate cancers (ERPC) have been rapidly emerging over the last few years. Till date, enzalutamide resistance has been attributed to presence of AR variants, AR mutations and receptor switch to the Glucocorticoid receptor (GR), among other mechanisms. (14, 20) Moreover, these mechanisms of resistance may provide cross resistance to other anti-androgen therapeutic agents. Majority of prostate cancer research is now focused on understanding the basic molecular mechanisms of castration resistance, specifically to understand how AR activity is undiminished in the absence of androgens.

1.2 Prostate cancer development

The human prostate consists of three zones named peripheral, central and transition zone. The peripheral zone is very most prostate cancers arise (38). At the cellular level the prostate contains three types of cells: luminal, basal and neuroendocrine cells. The luminal cells are the secretory cells that express AR and are defined by Cytokeratin 8 (CK8) and cytokeratin 18 (CK18) expression. The basal cells don’t express AR and are defined by expression of CK5 and p63.

Neuroendocrine cells form a very small population of the prostate and express markers such as Chromogranin A and Synaptophysin but not AR. While initially researchers believed that luminal cells were the origin of prostate cancer, there is new evidence showing that both basal and luminal cells could give rise to cancer. (39-41)

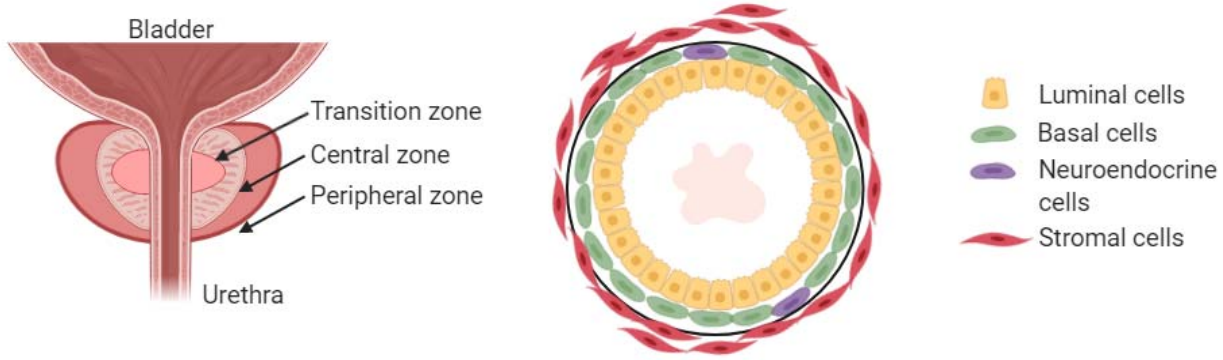

Figure 1.1. Anatomy and organization of the human prostate

Prostate tumorigenesis is a multistep process. The first step is the development of PIN or prostatic intraepithelial neoplasia which is the precursor to localized prostate cancer. PIN is marked by luminal cell hyperplasia, enlargement of nuclei, nuclear atypia etc. There may also be an increase in proliferation markers. Localized prostate cancer can give rise to advanced prostate cancer which is defined by invasion of the basement membrane and can give rise to metastatic prostate cancer. Metastases to the lymph nodes are often first followed by metastases to the liver, lungs and bones. (42)

More than 95% of all localized prostate cancers are usually classified as adenocarcinomas displaying a strong luminal phenotype. Other subtypes of PCa like ductal adenocarcinoma, mucinous carcinoma, and signet ring carcinoma are extremely rare. Less than 2% of PCa cases are neuroendocrine tumors that display neuroendocrine markers like Synaptophysin and Chromogranin A but not AR. They can be classified as small cell carcinoma or carcinoid tumor. However, in recent years, there has been a rise in the incidence of AR negative aggressive variant prostate cancer with neuroendocrine pathology (NEPC) after ADT. These are classified as treatment related neuroendocrine cancers as opposed to *de novo* neuroendocrine cancers. There is also a subset of tumors that displays non neuroendocrine features and don't express AR. These AR low cancers are inherently resistant to ADT (43).

1.3 Molecular alterations of Prostate tumorigenesis

Whole genome analyses have identified multiple molecular alterations including copy number changes, rearrangements and gene fusions. While copy number changes are abundant, mutations are sparingly observed in prostate cancer. (44, 45)

TMPRSS2-ERG translocations

TMPRSS2-ERG translocations were one of the first translocations identified in solid tumors (46). These translocations aim to upregulate the levels of ERG or other members of the ETS family of transcription factors by placing the promoter of an androgen responsive gene like TMPRSS2 upstream of the ETS gene (47). This translocation has been observed in almost half of all prostate cancers, suggesting that this might be an early event during cancer initiation. Recent

studies have shown that this translocation might be the result of DHT induced AR action that leads to recruitment of DNA topoisomerase which is critical for unwinding of DNA preceding the induction of DNA breaks (48, 49). ERG activation after the translocation promotes tumorigenesis alone or by cooperating with other tumorigenic events.(50, 51)

NKX3.1

NKX3.1 has been shown to be frequently deleted in prostate cancer (52). The region that contains NKX3.1 displays loss of heterogeneity frequently in PIN and prostate cancer, indicating that it is an early tumorigenic event (53). In the absence of deletion events, NKX3.1 is frequently repressed by epigenetic events like DNA methylation (54). NKX3.1 is a critical regulator of prostate epithelial differentiation (55) and its reduction leads to loss of protection against oxidative damage (56). Thus, NKX3.1 acts a ‘gatekeeper’ against prostate tumorigenesis.

PTEN

PTEN is a tumor suppressor that is frequently lost in prostate cancer (45, 57). This is an early event too like NKX3.1 reduction and cooperates with other tumorigenic events like MYC overexpression and TMPRSS2 fusions (51, 58, 59). PTEN loss is also a mark of castration resistant prostate cancer (60, 61). PTEN loss leads to hyperactivity of the PI3K/AKT pathway that controls cell survival, proliferation and energy metabolism.

1.4 Androgen Receptor: a prostate lineage factor

Since its discovery in the 1960s', AR has been extensively studied in prostate development and associated pathologies like prostate cancer (62, 63), breast cancer (64, 65), androgen-insensitivity syndrome (66), spinal bulbar muscular atrophy (67) and androgenetic alopecia (baldness) (68). The androgen receptor belongs to the steroid hormone family of nuclear receptors. This family includes glucocorticoid receptor (GR), estrogen receptor (ER) and progesterone receptor (PR). AR is an essential transcription factor in the prostate and is involved in normal prostate development as well as prostate cancer.

Androgen hormones like testosterone are produced in the testes, after which they circulate to different parts of the body. In the prostate, testosterone is converted to a more potent form, 5alpha – dihydrotestosterone (DHT) which then binds to AR in the cytosol through its ligand binding domain. In the absence of androgens, AR remains in an inactive state and is bound by heat shock proteins like HSP90, HSP70, HSP56 and HSP27. Upon binding with androgens, AR undergoes a conformational change, releases HSPs, dimerizes and then translocates to the nucleus. It then binds to Androgen response elements (ARE's) found all over the genome to induce a transcriptional program that helps maintains the normal prostate and when overexpressed often promotes prostate cancer initiation and progression (69, 70).

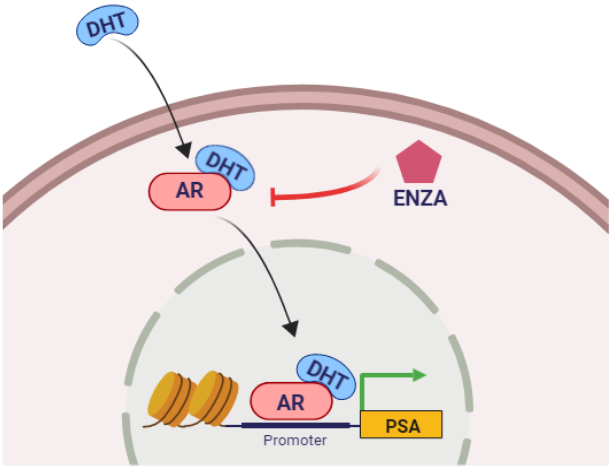

Figure 1.2. Mechanism of action of AR.

DHT enters the cell and binds to AR in the cytoplasm triggering AR's displacement into the nucleus. In the nucleus, AR binds to ARE elements in DNA and promotes gene transcription. ENZA or enzalutamide can inhibit AR action by preventing its binding to DHT and its subsequent translocation to the nucleus.

In the normal prostate epithelium, AR suppresses excessive cellular proliferation. However, in prostate cancer, it supports survival and proliferation and even promotes metastasis (15). AR regulates transcription of more than 1700 genes in humans (71) and these genes play a role in important biological processes like cell proliferation, cell communication, tissue development, cellular lipid metabolism etc. (72). AR associates with multiple coactivators at target genes to activate gene expression, for e.g. FOXA1, HOXB13, and NF-KB etc. Similarly, AR can cooperate with repressive transcription factors like NCOR2, EZH2 etc. to repress gene expression by modeling the chromatin environment (73).

Structure of AR

The AR gene is located on the X chromosome and spans eight exons. The gene encodes for a 110 KDa full length protein consisting of 919 amino acids. In addition to the full-length transcript, 20 other AR splice variants have been identified, among which AR-V7 is the most common. The full length receptor consists of four major domains (74): 1) a large amino-terminal transactivation domain, 2) a central DNA binding domain 3) followed by a hinge region (nuclear localization/degradation) and 4) a carboxy-terminal ligand binding domain. The AR variants are truncated versions of the full length receptor that function independently (75, 76). The NTD is mostly unstructured and contains one activation function (AF1) motifs which in turn has 2 transcriptional activation units (TAU). The TAU units are responsible for AR's androgen dependent and independent activity. The CTD has two zinc finger domains one of which interacts with AREs present in DNA and the other is critical for dimerization of AR. The hinge region connects the DBD with the LBD and is responsible for AR nuclear localization and protein degradation. The hinge region also contains the other activation function AF2 region in AR. LBD lacking splice variants have been recently identified as major players in prostate cancer and therapy resistance. They are independent of androgens and hence found mostly in the nucleus. They can keep target genes always 'on'.

AR transcriptional functions

The most well-known target of AR is PSA, which is also a prostate biomarker. PSA expression increases upon androgen stimulation (77). Upon binding to DHT, AR is recruited to ARE elements upstream of the PSA promoter namely ARE I and ARE II and a distant enhancer ARE III (78). While AR is bound to regions 'cis' to the promoter, it may also be bound at distal regulatory enhancers as seen in the case with PSA. A single gene might also be regulated by multiple distal AR bound enhancers, making gene regulation a more complicated affair.

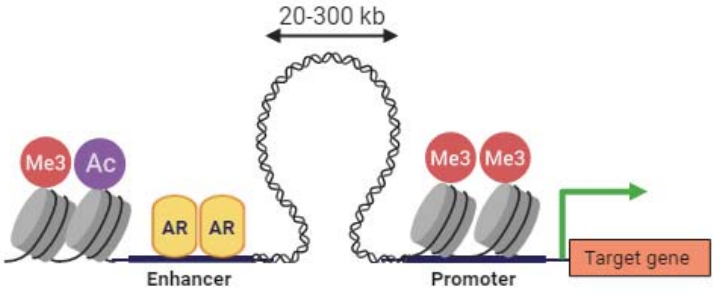

Figure 1.2. AR bound enhancer-promoter interaction.

AR target genes can be regulated by distant AR bound enhancers marked with H3K4me3 and H2K27ac. These enhancers come into contact with an accessible promoter through DNA looping to regulate the gene's expression.

In normal cells, AR regulates genes involves in differentiation and growth suppression. In cancer cells, AR does the opposite and promotes expression of proliferation and survival associated genes. AR controls a different transcriptional program categorized by elevation of cell cycle

genes specifically M-phase genes (79). There are several factors that reprogram AR's cistrome in normal cells vs cancer cells. It is widely established that AR can induce or repress expression of its target genes alone or by associating with/recruiting other transcriptional regulators. These include cofactors like FOXA1 and HOXB13 that are pioneering factors (80-82). They redistribute AR binding to regions that contain forkhead and homeodomain motifs. Additionally, AR can cooperate with specific epigenetic regulators like EZH2 that model the chromatin environment (71).

In CRPC, AR is most commonly activated through AR amplification or overexpression (83, 84), gain of function mutations (85, 86), ligand independent activation (87), increased intratumoral androgen synthesis (88), overexpression of AR coactivators, constitutively active splice variants (20). In addition to the above listed mechanisms, AR can undergo post-translational modifications like ubiquitination, phosphorylation, sumolyation, methylation and acetylation.(73, 89-91) These modifications can affect AR activity and stability. Ubiquitination of AR has important consequences on AR turnover and AR mediated gene transcription. Dysregulation of AR ubiquitination is an emerging mechanism of CRPC progression.

Ubiquitination of AR

Ubiquitination is one of the most common post-translational modifications in the cell and it can lead to either protein turnover or signal transduction. E3 ubiquitin ligases alone determine the specificity of the target substrate, making them critical enzymes for protein regulation in the cell. Several hundred ubiquitin ligases exist in eukaryotes; these are divided into 3 major sub-families

depending on their functional domains: the homology to E6-AP carboxyl terminus (HECT), the Really Interesting New Gene (RING) and U-box proteins (closely related to RING domain). The difference lies in the type of catalytic reaction: HECT proteins transiently bind the Ubiquitin molecule at the E3 active site whereas the RING proteins catalyze the direct transfer of ubiquitin from U2 to the target substrate (92) . The RING family of proteins consists of the largest family of E3 ligases; in fact, the number of RING ligases even exceeds that of kinases in the cell. The RING domain is structurally folded in a manner that binds Zn^{2+} through a four-point arrangement of conserved cysteine and histidine residues. RING proteins can function as monomeric E3 enzymes or can form multi-subunit complexes to carry out their E3 functions.

AR is ubiquitinated and regulated by a number of E3 RING ubiquitin ligases that alter its localization and turnover. These include Siah2, RNF6, MDM2, CHIP, NEDD4, SKP2 and CRL3- SPOP complex (93-95). AR activity and protein levels are therefore tightly regulated and aberrant activity of any of the above E3 ligases leads to prostate cancer progression. For e.g. SIAH2 was reported to play an important role in CRPC due to its role in degradation of AR protein that is associated with NCOR1 repressive complexes (96, 97). RNF6, another Ubiquitin ligase is required for AR mediated transcription of certain genes and consequently RNF6 expression has been reported as up regulated in CRPC (98).

1.5. MYC, a critical oncogene

MYC was first identified as a retroviral oncogene and later characterized in Burkitt's lymphoma as an essential tumorigenic event in cancer (99). In prostate cancer, Fleming at al. first found MYC mRNA to be elevated in prostate adenocarcinomas in comparison to normal tissue (100).

This observation was then confirmed by others establishing that MYC aberrations to be particularly important in PCa (101-104). Additionally, amplification of the chromosome region containing MYC (8q24) was frequently observed in patients with prostate cancer, more specifically in patients with aggressive/late-stage tumors (105). In fact, MYC has been estimated to be activated/over expressed in almost half of all human cancers (106).

C-MYC is the most widely characterized protein from the MYC family of 'super transcription factors'. L-myc and N-myc genes encode for the other two family members MYCL and MYCN that are completely distinct proteins from C-MYC. They all have high structural homology and they too target genes involved in protein translation, ribosome biogenesis, and metabolism. However, they differ in expression patterns: c-MYC is found in most solid tumors and blood cancers while N-MYC is expressed in most cancers with a neural origin (107) and L-MYC is mostly expressed in lung cancers(108).

Structure of MYC

All MYC proteins have the C-terminal basic region/ helix-loop-helix/ leucine zipper (BR/HLH/LZ) and the N-terminal conserved MYC boxes. The C-terminal contains the DNA binding region while the N-terminal contains the Transcriptional activation domain (TAD). Like other TADs, the MYC TAD is intrinsically unstructured in the absence of partners and is primarily responsible for signaling rapid degradation of MYC. The TAD contains the conserved sequence, MYC box 1 (MBI) which is a hotspot for oncogenic mutations in Burkitt's lymphoma (109). MYC box II (MBII) is extremely critical for MYC's transcriptional and more specifically oncogenic function as it interacts with the coactivator TRRAP and recruits Histone

acetyltransferases (at H4) to target genes for activation. Both MBI and MBII can bind to different Ubiquitin ligases to alter the stability of MYC protein. Much less is known about the other MYC boxes however MYCIIIa has been shown to play a role in transcriptional repression through recruitment of HDAC3. The C-terminal DNA binding domain is responsible for recognizing the E-box sequences in DNA. The C-terminal also plays a major role in MYC hetero-dimerization with MAX as it forms the leucine zipper between the two proteins. The central region of the protein contains the nuclear localization signal (NLS) which is responsible for MYC's strong expression in the nucleus (110).

MYC's transcriptional functions

MYC is a versatile transcription factor that regulates thousands of genes involved in multiple biological processes like cell growth, proliferation, differentiation and apoptosis. It usually cooperates and binds to MAX, another transcription factor to form a heterodimer (111). This MYC/MAX heterodimer then binds to DNA at E-box motifs at target gene promoters. E-box motifs are consensus sequences specific across species, most commonly, CACGTG. After MYC/MAX bind to these E-box sequences, they recruit other coactivators or corepressors to regulate gene expression like TRRAP, GCN5, TIP60 and TIP48 (112). Importantly, MYC/MAX's binding to E-box elements is dependent on multiple factors like the presence of proximal CpG islands, open chromatin states and active histone marks (113). The levels of MYC is also a critical determinant of MYC's cistrome in cells. While MYC and MAX are the main binding partners, MYC's cistrome can be influenced by other cooperators like WDR5, RAR alpha, etc (114, 115). MYC's transcriptional function has been recently characterized as an

'Amplifier' which means that it increases the expression of 'on' genes (116, 117). MYC has also been demonstrated to repress transcription via its association with MIZ-1 which subsequently prevents recruitment of activating factors like p300 and recruits DNMT3a instead to methylate DNA in target genes (118, 119). MYC can also mediate gene repression by sequestering transactivators like SP1 and C/EBP alpha. Furthermore, MYC proteins can also recruit histone deacetylases like HDAC1, HDAC3 and HDAC5 to target sites to induce heterochromatin formation (120).

MYC plays a role in many key processes that helps drive tumorigenesis. MYC acts as a cell cycle accelerator and causes cells to cycle more rapidly, particularly through G1 and G2 (121). MYC also reduces the growth factor requirements for cell cycle by directly activating cyclin/CDK expression (122). It also inhibits cell cycle checkpoints. On the other hand, forced expression of MYC in normal cells has also been shown to cause apoptosis (123). MYC also plays a major role in promoting cell growth during tumorigenesis. MYC overexpressing cells increase in size because of increased protein and RNA synthesis (124). MYC regulates genes involved in ribosome biogenesis and protein translation. It also activates RNA polymerase I to increase transcription and collaborates with mTOR to increase protein synthesis (125, 126).
Besides these major functions, MYC also increases the metabolic capacity of cancer cells enough to sustain rapid cell growth and divisions. MYC activates expression of genes involves in glucose uptake, glycolysis and glutamine metabolism (127, 128). MYC overexpression can also increase the levels of Reactive oxygen species (ROS) which can drive genetic instability by inducing DNA breaks (129). MYC can also promote amplifications and rearrangements at

certain loci and genome wide chromosomal abnormalities (130). MYC can also directly promote metastasis by promoting factors involved in invasion and decreasing expression of cell adhesion molecules (131, 132). MYC also regulates micro-RNAs that control EMT (133).

Due to MYC's critical role in transcriptional regulation, MYC levels are tightly regulated in normal cells and is upregulated by mitogen signals. Its expression is controlled at initiation and elongation steps as well as post transcriptionally. MYC protein has a very short half-life and so an important way of regulating MYC levels are through protein degradation.

Targeting MYC in cancer

Most cancer cells remain 'addicted' to MYC activity. Multiple animal studies have shown that even transient or even incomplete blockade of MYC activity is effective in inhibiting tumor growth (134). This implies that there is a therapeutic window in which we can target tumor cells but leave normal cells mostly unaffected. Strategies to target MYC include small molecule inhibitors that target MYC expression or activity directly or any of its downstream processes. Small molecule inhibitors that target MYC protein directly have been unsuccessful thus far mainly due to the inherently disordered structure of MYC that lacks a specific pocket for binding. Secondly, its location in the nucleus makes it difficult to target. Some small molecule inhibitors like 10058-F4 have been developed (135), however, these have failed due to their low bioavailability. Studies with drug screens have been conducted to target MYC alone or in conjunction with MAX which would give a better chance to find a binding pocket for small molecules. Molecules like IIA6B17 and 10058-F4 have been shown to disrupt MYC-MAX dimerization. Omomyc, another inhibitor is a mutant peptide that sequesters MYC from MAX

and prevents downstream pathway activation (136). So, to counteract these failings, strategies now target MYC expression and protein levels. Recently, BRD4 inhibitors have shown promise as they prevent BRD4 recruitment to the MYC super-enhancer and promote unfavorable chromatin states leading to lowered MYC expression (137). Inhibitors of CDK7 and CDK9 are also effective in reducing MYC expression (138). Inhibition of the PI3K/AKT/mTOR pathway also leads to decreased MYC levels due to a drop in mRNA translation through mTORC1 (139).

One of the major ways to target MYC is by targeting its protein stability. MYC protein levels are tightly regulated by multiple proteins in the Ubiquitin-proteasome system. When MYC is phosphorylated at T58, it's targeted for protein degradation by E3 ligases. One such protein is FBW7 (alpha and gamma) (140). On the other hand, several deubiquitinating enzymes like USP28, USP36 and USP7 help stabilize MYC and by targeting these enzymes, MYC levels can be leveled (141). Oncogenic partners that help stabilize MYC like AURKA can be targeted by small molecule inhibitors to indirectly decrease MYC (142).

Although many approaches to target MYC are available today, no inhibitors have been approved for clinical use. Hence, we need better therapeutic approaches that can be translated for future patient care.

1.6. Epigenetic alterations in Prostate cancer

Deregulation of genes involved in regulating epigenetic processes like DNA methylation and histone modifications have been frequently identified as a tumorigenic event in prostate cancer.

DNA methylation

DNMT1 can paradoxically act as a tumor suppressor in early prostate cancer and an oncogene in advanced cancers (143). This is partly due to its role in regulation of EMT (144). TET1 and TET2 also play a tumor suppressor role in prostate cancer (145). Due to AR's relationship with DNMTs, several AR target genes undergo changes in DNA methylation (146). DNA hypermethylation is observed in metastatic prostate cancer and neuroendocrine prostate cancer. However, DNA methylation inhibitors like Azacytidine and Decitabine have shown only modest potential in mouse models (147).

EZH2

The polycomb protein EZH2 is a SET domain containing methyltransferase. It is frequently upregulated in advanced prostate cancers through mRNA expression or gene amplification (148, 149). EZH2 methylates Histone H3 on Lysine 27 which leads to gene repression. One of its targets is NKX3.1 which is repressed in prostate cancer (150). It has been shown to play a major role in prostate cancer metastasis (151, 152).

1.7. DOT1L, a histone methyltransferase

DOT1L (Disruptor of Telomeric silencing 1 Like or KMT4) is a histone methyltransferase that can catalyze the transfer of one, two or three methyl groups to Lysine 79 of histone H3(6, 153). DOT1L mediated H3K79 methylation is mainly associated with active transcription, transcription elongation, and DNA repair response. (154) K79 is located in the histone core

rather than the histone tail like other commonly modified residues. K79 is found in the first loop of H3 and is in close vicinity of the interface between H3/H4 tetramer and the H2A/H2B dimer. While DOT1L is believed to be the only enzyme that modifies K79 there is some evidence that RE-IIBP can methylate K79 as well (155). This methylation is subject to dynamic regulation but is ultimately a very stable event partly since a specific demethylase for this site is yet to be identified.

Structure of DOT1L

DOT1L belongs to a unique class of methyltransferases that contains a catalytic methylase fold instead of the SET (Su (var) 3-9, Enhancer-of-zeste and Trithorax) domain commonly found in other histone methyltransferases (153, 156). DOT1L has an alpha-helical N-terminal domain and an open alpha/beta structure consisting of a seven-stranded beta sheet, an active site consisting of a SAM binding pocket. It methylates K79 in a non-processive manner i.e. DOT1L is a distributive enzyme.

DOT1L‘s functions

DOT1L was initially discovered in yeast as a protein that disrupts telomeric silencing when deleted or upregulated (157). In yeast, Sir protein complexes containing Sir2, Sir3 and Sir4 are protective at telomeres and alterations in DOT1L activity lead to Sir protein spreading throughout the genome leading to deprotected telomeres. A balance between Sir proteins and DOT1L is essential for heterochromatin formation at the telomeres in yeast (158). DOT1L is also critical for mammalian development as evidenced by the fact that DOT1L deletion leads to

embryonic lethality in mice because of heart defects and errors in yolk sac development (159).

H3K79 methylation has been shown to fluctuate with the different stages of the cell cycle however the mechanics of this process are yet to be understood. H3K79 methylation is localized within the gene body and correlates with the gene's expression level.(7, 160). It is now known that monoubiquitination of histone H2B at lysine 123 is required for H3K79 methylation to occur (161). This is further evidenced by the fact that DOT1L preferentially methylates K79 on whole nucleosomes rather than free histones indicating that it recognizes other features in the whole nucleosome. Genome wide analysis of H3K79 methylation agree that it associates with gene activation, however there are reports that H3K79me3 might correlate with gene repression. To support the notion of gene activation, DOT1L has been shown to directly interact with RNA Polymerase II (RNAPII) specifically its C terminal domain at phosphorylated Serine 2 and Serine 5. Moreover, H3K79 methylation is also found within the gene body of an expressed gene. However, these levels are not constant through the gene – methylation typically peaks within the first exon and then decrease gradually through the gene.

There is also evidence that H3K79 methylation plays a role in transcription elongation. Several RNAPII elongation complexes contain DOT1L and levels of AF9, AF4, AF10 have effects on H3K79 methylation levels as well. However, ultimately, mechanisms by which H3K79 methylation regulates transcription and elongation remain largely unclear.

H3K79 methylation has also been found in enhancers and recently a study has shown that H3K79 methylation at an enhancer is required for chromatin accessibility, histone acetylation

and transcription factor binding at the enhancer. Moreover, it is essential for promoter enhancer interaction by DNA looping. To support this, there is also evidence that more K79 methylation is associated with Histone variant H3.3 than canonical H3, which is typically enriched at enhancers and promoters. DOT1L also plays a role in DNA damage response in cells. DOT1L mediated H3K79 methylation at sites of double stranded breaks is bound by 53BP1 through its tudor domain to further recruit proteins to the site of DNA damage. This interaction is evolutionarily conserved.

Role of DOT1L in cancer

Recently many studies have implicated DOT1L in acute leukemias with MLL gene translocations. (162-165) MLL fusion products with AF4, AF9, AF6, AF10 and ENL aberrantly recruit DOT1L to target sites for transcriptional activation by H3K79 hyper methylation leading to leukemogenesis. By promoting K79 methylation at these sites, DOT1L prevents recruitment of SIRT1 and repressive complexes like SUV39H1, a H3K9 methyltransferase (166).

DOT1L was found to be significantly mutated in lung carcinomas(167) and DOT1L inhibition has been shown to inhibit proliferation of lung cancer cells (168). Furthermore, DOT1L was identified in a CRISPR knockout screen as an essential factor required for glioblastoma growth indicating that DOT1L inhibition could be effective in treating glioblastomas (169). In clear renal cell carcinomas, DOT1L expression correlated with poor overall survival (OS) and progression free survival (PFS) (170). In colorectal cancer, DOT1L was found to be highly expressed and promote expression of genes involved in stemness and tumorigenesis like

NANOG, SOX2, and Pou5F1 (171). DOT1L has also been reported to play a role in breast cancer progression.(172, 173) Cho et al. also reported that DOT1L cooperates with c-MYC to upregulate EMT genes leading to breast cancer metastasis. Recently, it was shown that DOT1L binds to and cooperates with the Estrogen receptor (ER) in promoting breast cancer progression (174). Moreover, inhibition of DOT1L has been shown to inhibit growth of breast cancer cells in various in vitro models (175, 176). Similar to what is seen in breast cancer, DOT1L cooperates with ER in promoting ovarian cancer as well (177). Recently, it's been shown that C/EBPβ co-opts DOT1L to promote expression of chemo resistance genes in ovarian cancer (178). Moreover, high DOT1L expression and K79 methylation were shown as markers for malignant ovarian tumors (179). However, there are also contradicting reports that DOT1L inhibition might lead to cell invasion and stemness of ovarian cancer cells (180).

Despite recent studies, the functional role of DOT1L in prostate cancer has not been fully examined. Yang et al. reported that DOT1L is recruited by the lncRNA PRNCR1 to methylate AR (27). However, Prensner et al. failed to find a role for the lncRNA PRNCR1 or evidence of the specific AR methylation in question in prostate cancer(28). Hence, DOT1L's role in PCa remains unclear.

CHAPTER 2: MATERIALS AND METHODS

2.1. Human Prostate Cancer Data

Prostate cancer Gene expression data were downloaded from the NCBI Geo for the following datasets: Grasso PCa dataset [GSE35988; benign (n=28), PCa (n=94)](181), Yu PCa dataset [GSE6919; Normal (n=60), PCa (n=81)](103, 182), Varambally PCa dataset [GSE3325; benign (n=6), PCa (n=13)](102), Taylor PCa dataset [GSE21032; Normal (n=29), PCa (n=150)](183), Roudier Prostate cancer dataset [GSE74367; primary cancers (n=11), metastatic cancers (n=45)](184), Gulzar Prostate cancer dataset [GSE40272; normal (n=66), prostate cancers (n=83)](185) and from cbioportal.org: Beltran dataset [CRPC adeno (n=15), CRPC-NE (n=34)](186)

Gene expression for other cancers was downloaded from NCBI GEO Datasets: Richardson Breast cancer dataset [GSE3971; Normal (n=7), Cancer (n=40)](187), Gaedcke Rectal cancer dataset [GSE20842; Normal (n=65), Cancer (n=65)](188), Murat Glioblastoma dataset [GSE7696; Normal (n=4), Cancer (n=80)](189), Hong Colorectal cancer dataset [GSE9348; Normal (n=12), Cancer (n=70)](190), Kohlmann CLL dataset [GSE13159; Normal (n=73), Cancer (n=448)](191), Kim Bladder cancer [GSE13507; Normal (n=68), Cancer (n=188)](192).

P value determined by Welsh's t-test. Survival analysis was performed using data from NCBI Geo: the Luca CancerMap prostate cancer dataset [GSE94767; Cut-off at 90th percentile, high DOT1L (n=19), low DOT1L (n=214)](193), Ross-Adams Discovery dataset [GSE70768; Cut-off at 75th percentile, high DOT1L (n=24), low DOT1L (n=84)](194), Grasso PCa dataset

[GSE35988; Cutoff at 75 percentile, High (n=11), Low (n=37)](181), Ross-Adams (Validation) dataset [GSE70768; Cut-off at 50th percentile, high (n=46), low (n=46)](194) and Gulzar Prostate cancer dataset [GSE40272; Cut-off at 50th percentile, high (n=41), low (n=41)](185) and from cbioportal.org: TCGA Provisional prostate cancer dataset [Cut-off at 90th percentile, high DOT1L (n=33), low DOT1L (n=463)](195), and TCGA Gleason 7 patients [Cut-off at 50th percentile, high DOT1L (n=121), low DOT1L (n=121)(195). Patient survival curves were assessed by the Kaplan–Meier method.

P values were determined by log-rank test. For Correlation analysis, the gene expression of DOT1L and MYC were analyzed using Spearman's rank correlation. Data used for this analysis was from the MSKCC dataset (n=150)(183), TCGA Provisional dataset (n=499)(195) and SU2C dataset (n=118)(196) downloaded from cbioportal.org.

2.2. Clinical Samples

RNA samples from normal prostate tissue (n=15) and hormone dependent prostate cancer (n=15) were obtained from Prostate Cancer Biorepository Network (PCBN). 30 RNA samples from prostate cancer metastases were kindly provided from Dr. Colm Morrissey from University of Washington, WA. All samples were de-identified and in compliance with ethical regulations and the approval of their respective Institutional Review Boards (IRB).

2.3. Immunohistochemistry

A Tissue MicroArray (TMA) with 80 cases and matched normal including a range of Gleason grade & pathology stage was acquired from PCBN. The TMA was processed for immunohistochemistry staining as described. H3K79me2 antibody from Abcam was used. After primary antibody incubation, slides were incubated with ImmPRESS HRP anti-rabbit (Vector#MP-7401). Expression was visualized by using AEC peroxidase substrate (Vector #SK-4200). Slides were incubated with Hematoxylin (Vector #3404) and mounted with Glycergel Mounting Medium (Dako #C056330-2). Images were visualized in TissueGnostics microscope at Northwestern Core facility Center for Advanced Microscopy. The number of epithelial cells showing nuclear staining was estimated per core and scaled: 0, no positive cells; 1, 1–25% positive cells; 2, 26–50% positive cells; 3, 51–75% positive cells; and 4, 76–100% positive cells. These scores were multiplied with an intensity scale (1, weak; 2, moderate; and 3, intensive staining), and the mean staining for a patient was calculated. TMAs were scored by three investigators in a blinded fashion.

2.4. Cell lines

LNCaP, C42B, 22Rv1, PC3, DU145 cells were grown in RPMI 1640 media (Gibco Life Technologies no. 11875-093) supplemented with 10% fetal bovine serum (FBS) - (Life Technologies no. 10437-028) and 1% penicillin/streptomycin antibiotic solution (Life Technologies no. 15140-122). RWPE-1 cells were grown in keratinocyte serum-free media supplemented with 0.05 mg/ml bovine pituitary extract, 5 ng/ml epidermal growth factor

(Thermo Fischer Scientific no. 17005042) and 1% penicillin/streptomycin antibiotic solution. For assays in charcoal stripped medium, cells were first hormone starved in RPMI 1640 media without Phenol red supplemented with 10% charcoal stripped fetal bovine serum (FBS) and 1% penicillin/streptomycin antibiotic solution for 48 hours before start of assay. All cells were verified as mycoplasma free and genetically authenticated by ATCC.

2.5. Mice

NOD-SCID mice (Jackson Laboratory) used in this study were housed in a pathogen-free animal barrier facility or a containment facility, as appropriate. When mice were 6–8 weeks old, they were injected subcutaneously with 2 million live LNCaP cells pretreated with either DMSO control or 10uM EPZ for 7 days (100µl, 1:1 with matrigel). Tumor volume was measured using calipers until they reached 1500mm^3. All experiments and procedures were performed in compliance with ethical regulations and the approval of the Northwestern University Institutional Animal Care and Use Committee (IACUC).

2.6. Cell growth assays

For long term clonogenic assays, cells were counted and plated in low density in 6 well plates and treated with different concentrations of EPZ004777 (Epizyme) or EPZ5676 (Selleckchem). After 12 days, colonies were fixed and stained with crystal violet and photographed. To assess cell viability, cells were plated in 10 cm culture dishes and treated with DMSO control or EPZ for 10 days. Media was replenished every 3-4 days. On day 10, cells were trypsinized, counted

and replated in 96 well plates (5000 cells per well). On day 12, viability was assessed using the CellTiter 96 AQueous One Solution Cell Proliferation Assay (Promega) as per manufacturer's instructions.

2.7. DNA constructs, Lentivirus production and lentiviral transduction of cell lines

MSCB-hDot1Lwt was a gift from Dr. Yi Zhang (Addgene plasmid # 74173). Flag tagged AR plasmid was kindly provided by Dr. Meejeon Roh. pSMP-Luc and pSMP-Dot1L_1 was a gift from George Daley (Addgene plasmid # 36339 and plasmid # 36394). FM1-YFP and FM1-AR-YFP were obtained from Dr. Kenji Unno (197). Halotag-HECTD4 was obtained from Promega (FHC24891). TRIM49 construct was obtained from GenScript (OHu03301D). pcDNA3.1 plasmid (EV) was a gift from Dr.Meejeon Roh. TRIM49 construct was obtained from GenScript (OHu03301D).

Viral particles were produced in 293T cells transfected with the expressing vector, Δ8.9 packaging vector (for lentivirus) or MMLV packaging vector (for retrovirus) and VSVG envelope vector (2:1:1) using Lipofectamine 2000 (Invitrogen) in Opti-MEM media (Gibco) as described (Anker et al., 2018). LNCaP cells were transduced with the virus and 1 μg/ml of puromycin was added to select stably expressing cells.

2.8. qRT-PCR

Total RNA extraction was performed using the TRIzol reagent (Life Technologies, Rockville, MD), according to the manufacturer's instructions. The reverse transcriptase polymerase chain

reaction (RT-PCR) was performed using Moloney murine leukemia virus reverse transcriptase (Invitrogen) as per manufacturer's instructions. qRT-PCR was performed using PowerUp SYBR Green Master Mix (Applied Biosystems). Primers used for qRT-PCR are listed in **Table 1**.

Table 1: Primers used for qRT-PCR

Name	Sequence
PSA_F	TGTGTGCTGGACGCTGGA
PSA_R	CACTGCCCCATGACGTGAT
TMPRSS2_F	GGACAGTGTGCACCTCAAAGAC
TMPRSS2_R	TCCCACGAGGAAGGTCCC
AR-FL_F	TCTTGTCGTCTTCGGAAATGT
AR-FL_R	AAGCCTCTCCTTCCTCCTGTA
DOT1L_F	CAAGTTCTCGCTGCCTCACT
DOT1L_R	GTCCTGAGGGCTCAGCTTC
18SrRNA_F	GTAACCCGTTGAACCCCATT
18SrRNA_R	CCATCCAATCGGTAGTAGCG
UGT2B15_F	GTGTTGGGAATATTATGACTACAGTAAC
UGT2B15_R	GGGTATGTTAAATAGTTCAGCCAGT
UGT2B17_F	TTTTGTCGCAGGAAAAAGGAAA
UGT2B17_R	AAGCCTGAAGTGGAATGACCAA
UGT2B7_F	TTTCACAAGTACAGGAAATCATGTCAAT
UGT2B7_R	CAGCAGCTCACTACAGGGAAAAAT
HERC3_F	CTCTGGCAGATCAGCATATCATT
HERC3_R	CAGCTTTTGTATTAACCTGGGCA
MYCBP2_F	AGTCTTGGTTAGGGTATGCTCA
MYCBP2_R	GGGCTTATCCTTATGGCTGTCAT
ELL2_F	CATCACCGTACTGCATGTGAA
ELL2_R	ACTGGATTGAAGGTCGAAAAGG
NDRG1_F	CTCCTGCAAGAGTTTGATGTCC
NDRG1_R	TCATGCCGATGTCATGGTAGG
ABCC4_F	AGCTGAGAATGACGCACAGAA
ABCC4_R	ATATGGGCTGGATTACTTTGGC
TRIM49_F	GAACGAAATGTGCCATAAACCAG
TRIM49_R	TGCAGAGTAATATGCACTCGGAA

HECTD4_F	GACCGAAGACAGCCCAAAGA
HECTD4_R	AGAACATGCAGGCTCGAACA
MYC_F	TTCGGGTAGTGGAAAACCAG
MYC_R	CAGCAGCTCGAATTTCTTCC

2.9. Microarray

LNCaP and PC3 cells were treated with DMSO control or 1uM EPZ for 8 days. Total RNA extraction was performed using the TRIzol reagent (Life Technologies), according to the manufacturer's instructions. RNA was cleaned up using the RNeasy Plus Mini Kit (Qiagen). RNA was submitted to the Genomics Core at the University of Illinois, Chicago for microarray analysis. RNA was hybridized to GeneChip® Human Transcriptome 2.0 arrays and raw data (CEL files) were processed and normalized using Robust Multichip Average (RMA) by Bioconductor oligo package. Differentially expressed genes (DEGs) were identified by the Bioconductor limma package. Heatmap view of differentially expressed genes was created by Cluster and Java Treeview. Gene set enrichment analysis (GSEA) was done using C2 curated and C6 oncogenic gene sets.

2.10. RNA interference

Cells were transiently transfected with HECTD4, MYCBP2, TRIM49, HERC3 siRNA or Non-targeted siRNA (Dharmacon Catalog no. D-001210-01-05) and DharmaFECT transfection reagent (Dharmacon), according to the manufacturer's protocol. Cells were analyzed for all experiments after 48 h. For DOT1L knockdown, Cells were transiently transfected with DOT1L targeting siRNA (Dharmacon MU-014900-01-0002) or Non-targeted siRNA (Dharmacon

Catalog no. D-001210-01-05) and DharmaFECT transfection reagent (Dharmacon), according to the manufacturer's protocol.

2.11. ChIP

LNCaP and PC3 cells were treated with DMSO control or 1uM EPZ for 8 days. Cells were cross-linked by adding 1/10 volume of Methanol free formalydehyde and incubated for 10 min. Cross-linking was stopped using 1/20 volume of 2.5 M glycine. Cells were isolated and resuspended in 1 ml of lysis buffer 1 (50 mM HEPES-KOH [pH 7.6], 140 mM NaCl, 1 mM EDTA, 10% glycerol, 0.5% IGEPAL-CA630, 0.25% Triton X-100, 1× protease inhibitors). Nuclei were recovered by centrifugation, resuspended in 1 ml of lysis buffer 2 (10 mM Tris-HCl [pH 8.0], 200 mM NaCl, 1 mM EDTA, 0.5 mM EGTA, 1× protease inhibitors). Nuclei were resuspended in 500 ul of lysis buffer 3 (10 mM Tris-HCl [pH 8.0], 100 mM NaCl, 1 mM EDTA, 0.5 mM EGTA, 0.1% sodium deoxycholate, 0.5% Sarkosyl, 1× protease inhibitors), and sonicated in using Bioruptor (Diagenode) for 8 cycles of 30 s on/off intervals. The sonicated chromatin was adjusted to 1% Triton X-100. After centrifugation, the protein concentration was determined by BCA assay, and chromatin was incubated overnight at 4°C with the indicated antibodies. Protein G Dynabeads were added for an additional 4 h. Beads were washed four times with 1 ml of ChIP-RIPA wash buffer (50 mM HEPES-KOH [pH 7.6], 500 mM LiCl, 1 mM EDTA, 1.0% IGEPAL-CA630, 0.7% sodium deoxycholate) and once with TE containing 50 mM NaCl. (198). For ChIP-qPCR, primers used are listed in **Table 2**. For ChIP-seq, barcoded sequencing libraries were generated using KAPA Library Preparation Kits (Kapa Biosystems)

according to the manufacturer's protocol. Libraries were quantified using a qPCR-based quantification (Kapa Biosystems) and sequenced on a NextSeq 500 instrument (Illumina). Sequence reads were aligned to the Human Reference Genome (assembly hg19) using Burrows-Wheeler Alignment (BWA) Tool Version 0.6.1. Peak identification, overlapping, subtraction and feature annotation of enriched regions were performed using Hypergeometric Optimization of Motif EnRichment suite (HOMER). Weighted venn diagrams were created by R package Vennerable. Differentially enriched genes were loaded into Enrichr website for ChIP Enrichment analysis (ChEA).

Table 2: Primers used for ChIP-qPCR

Name	Sequence	Purpose
PSA_F	CAGAGACCTTGATGCTTGGC	H3K79me2 peak
PSA_R	CCAGACTGAGGGACCCATTT	H3K79me2 peak
PSA_F	ACAGACCTACTCTGGAGGAAC	AR peak
PSA_R	AAGACAGCAACACCTTTTT	AR peak
TMPRSS2_F	TAGCAACACCCTCGGGTAAG	H3K79me2 peak
TMPRSS2_R	AAATAACCAGAGGCCGAGGT	H3K79me2 peak
TMPRSS2_F	TGGTCCTGGATGATAAAAAAAGTTT	AR peak
TMPRSS2_R	ACATACGCCCCACAACAGA	AR peak
UGT2B15_F	TCATGACCCCTCTGAACAAGC	AR peak
UGT2B15_R	CTCTGGAAGCTGTGGAAAGGT	AR peak
UGT2B17_F	TGAGCTGCATCAGCAGAAAGA	AR peak
UGT2B17_R	AAGCACTGCATAAGACCAGGA	AR peak
HERC3_F	GGGGACCAAGAAACACCTTT	AR peak
HERC3_R	GGAGGGAAAAGCACTGACTG	AR peak
ELL2_F	CCCATTCAGAACAGAAAGTCC	AR peak
ELL2_R	TTTGCTTGCAGTTACCCAAA	AR peak
ABCC4_F	TAGCTCTGCACGAAACTGGA	AR peak
ABCC4_R	TTGAGTCCCGTCTGTTTTCC	AR peak
MYC_F	GCAGGGAGGAAGTCAATGGT	Enhancer
MYC_R	TCATCTGCAGTTGCTCTTGG	Enhancer
FKBP5_F	ACCCTTCAGTGTGGTTCAGG	H3K79me2 peak
FKBP5_R	ACCACGAGCTCAAACTGCTT	H3K79me2 peak

NKX3.1_F	GATGGGTGGGAGGAGATGA	H3K79me2 peak
NKX3.1_R	TGTCTTGGACAAGCGGAG	H3K79me2 peak

2.12. Flow cytometry

LNCaP cells were transfected with ARE-GFP construct (Gentarget LVP912-R) using Lipofectamine and treated with vehicle or EPZ for 8 days. On Day 8, single-cell dissociation of LNCaP cells and flow cytometry was performed as described previously.(199)

2.13. Western blot

Cell lysates were prepared in RIPA buffer (Sigma) with protease and phosphatase inhibitors. Lysates were quantified and run by SDS-PAGE and transferred to PVDF membranes(200). Membranes were then blocked and exposed to the following antibodies: H3K79me2 (ab177184; Abcam), AR (RB-9030-P1; Thermo Fischer), PSA (A0562; Dako), Actin (sc-1616; Santa Cruz Biotech), Histone H3 (ab1791; Abcam), GAPDH (sc-20357; Santa Cruz Biotech), DOT1L (EMD Millipore MABE425, Abcam ab72454), MYC (Abcam ab32072), Halotag (Promega G9211), and Ubiquitin (Cell Signaling Technology 3936). Blots were then imaged using chemiluminescent substrate (Thermo Scientific) and ChemiDoc Imaging System (Bio-Rad).

2.14. Co-Immunoprecipitation assays

Briefly, cells were lysed using NETN buffer (20 mM Tris HCl [pH 8.0], 100 mM NaCl, 1 mM EDTA, and 0.5% Nonidet P-40). The insoluble pellets from the crude lysis step was treated with Enzymatic shearing cocktail from Nuclear Complex Co-IP Kit (Active Motif) for 90 min at 4 C°

to release nuclear proteins. Both cell lysis fractions were combined and then lysates were incubated with either AR (RB-9030-P1; Thermo Fischer) or Flag antibody (F1804; Sigma-Aldrich) overnight. Magnetic beads were added to the cell lysate and incubated for 2 hours. Beads were washed and bound fractions were eluted with 2x loading buffer. The eluted fractions were then analyzed by Western blotting.

2.15. Organoid culture and treatments

Organoid culture was performed as described previously.14, 15 Briefly; 2000 cells were resuspended in organoid media containing low percentage matrigel (5%) then plated in to 96-well ultralow attachment plates (Corning no. 3474). A 100ul of fresh media was added to the cultures every four days. Treatments were DMSO control, 1 and 10uM EPZ. Organoid growth was captured by brightfield microscopy using Zeiss Axioskop/Nuance microscope (Carl Zeiss Inc. Oberkochen, Germany). Organoid viability was evaluated using CellTiter-Glo® 3D Cell Viability Assay (Promega). Briefly, at the end of the experiment, organoids were collected and mixed with equal volumes of the reagent and incubated for 30 mins at the end of which luminescence was recorded.

2.16. CRISPR knockout

To stably express CAS9 in LNCaP and PC3 cells, we generated a CAS9 (Streptococcus pyogenes CRISPR-Cas) expressing lentivirus (Addgene 65655) from 293T cells. Lentiviral infection efficacy was >90% and cells were maintained with 2 μg/ml puromycin. 2 synthetic

guide RNAs (gRNAs) (CRISPR crRNA, Integrated DNA Technologies) were designed using the CRISPR Design Tool (crispr.mit.edu), those with off-target effects were excluded. gRNAs were ordered from Integrated DNA technologies (IDT) as g-blocks (455 bp fragment) that contains U6 promoter, gRNA target sequence, guide RNA scaffold and a termination signal. The sequence for gRNA 1 and 2 is CCCCCTGGTTGTCAAACTCTGGG and GCCTCCCATCAGTC-ATCCCAGGG respectively. They were delivered by transient transfection reagent Lipofectamine. Enhancer knockout was confirmed by genomic DNA PCR using the following primer sequences: F primer – TAAAGGAAAAGGGACTGTGGAA, R primer – CAGGTCTTCTCAGGTCTTTGCT.

2.17. Mass spectrometric analysis

LC-MS/MS analysis was performed by Northwestern Proteomics Core Facility. Briefly, LNCaP cells were treated with Vehicle or 1uM EPZ for 8 days followed by treatment with MG-132 for 6 hours. Cells were then lysed as described above. Lysates were quantified and equal amounts of protein were incubated with AR (RB-9030-P1; Thermo Fischer) overnight. Magnetic beads were added to the cell lysate and incubated for 2 hours. Beads were washed and bound fractions were eluted with 2x loading buffer. The pull-down samples were loaded onto stacking gel for 5min, and gel lane holding the total loaded proteins was cut and submitted to the facility. The proteins were digested with trypsin and analyzed by LC-MS/MS using a Dionex UltiMate 3000 Rapid Separation nanoLC and an Orbitrap Elite Mass Spectrometer (Thermo Fisher Scientific Inc, San Jose, CA) following the standard protocol in the Proteomics Core Facility. Scaffold (version

Scaffold_4.8.6, Proteome Software Inc., Portland, OR) was used to validate MS/MS based peptide and protein identifications. Peptide identifications were accepted if they could be established at greater than 90.0% probability by the Peptide Prophet algorithm with Scaffold delta-mass correction. Protein identifications were accepted if they could be established at greater than 99.0% probability and contained at least 2 identified peptides. Protein probabilities were assigned by the Protein Prophet algorithm. Proteins that contained similar peptides and could not be differentiated based on MS/MS analysis alone were grouped to satisfy the principles of parsimony. Protein probabilities were assigned by the Protein Prophet. Proteins that contained similar peptides and could not be differentiated based on MS/MS analysis alone were grouped to satisfy the principles of parsimony (version Scaffold_4.8.9). All identified proteins were filtered by Contaminant Repository for Affinity Purification (CRAPome) database following the workflow 1 instructions (www.crapome.org). The proteins with over 20% frequency in CRAPome database were considered as nonspecific bindings and removed from the list.

2.18. Statistical analyses

Statistical analyses were performed using unpaired two-tailed Student's t-test. Survival studies were analyzed by Log-rank (Mantel-Cox) test. Correlations were analyzed by Spearman's correlation coefficient (r). Data are presented as mean ± standard error of the mean (S.E.M.), unless otherwise indicated. For all analyses, results were considered statistically significant with $P < 0.05$, $*P < 0.05$, $**P < 0.01$, $***P < 0.001$, and $****P < 0.0001$.

CHAPTER 3: RESULTS

3.1. High DOT1L expression correlates with prostate cancer progression and poor disease-free survival

We investigated the oncogenic potential of DOT1L in prostate cancer progression by screening for DOT1L alterations in several publicly available PCa datasets. The analysis revealed that DOT1L was significantly upregulated in PCa when compared to normal prostate tissue and when primary tumors were compared to metastatic tumors. (**Figure 3.1**)

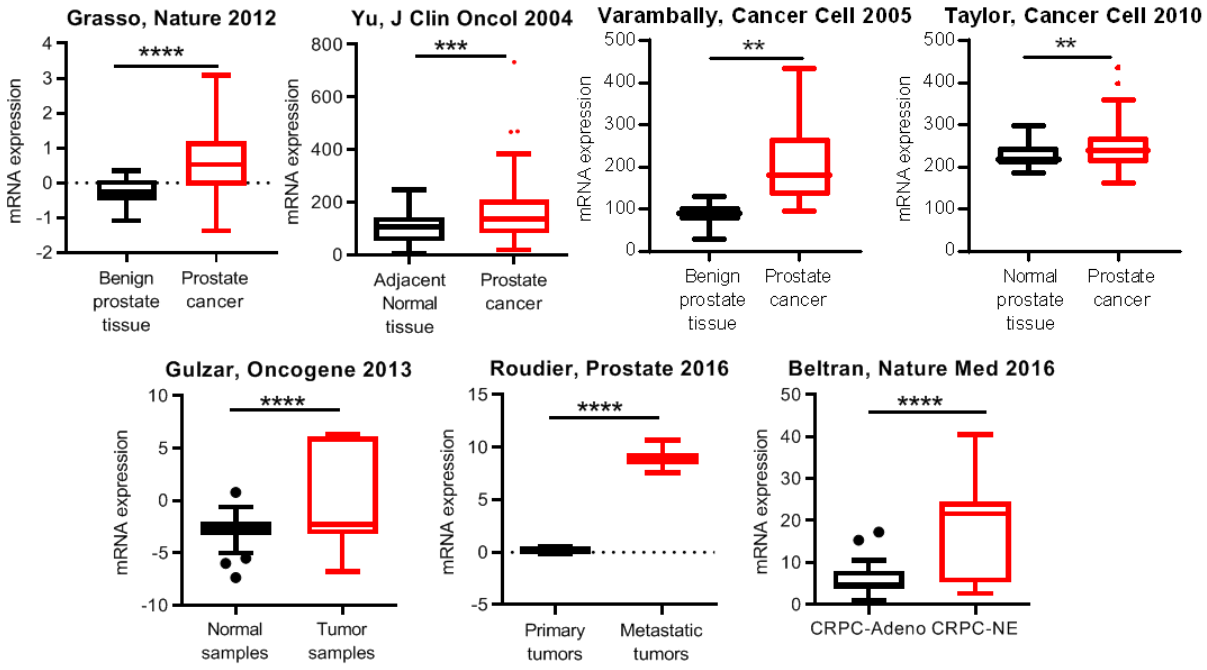

Figure 3.1: DOT1L expression is upregulated in prostate cancers.

Comparison of DOT1L expression in cohorts of prostate cancer patients' datasets. Data for this analysis was used from the Grasso PCa dataset [benign (n=28), PCa (n=94)], Yu PCa dataset [Normal (n=60), PCa (n=81)], Varambally PCa dataset [benign (n=6), PCa (n=13)], Taylor PCa dataset [Normal (n=29), PCa (n=150)], Roudier Prostate cancer dataset [primary cancers (n=11), metastatic cancers (n=45)], Gulzar Prostate cancer dataset [normal (n=66), prostate cancers (n=83) and Beltran dataset [CRPC adenocarcinomas (n=15), CRPC-Neuroendocrine cancers (n=31)]. P value determined by Welsh's t-test. Error bars represent minimum and maximum values. *p< 0.05, ** p<0.01, *** p<0.001, ****p<0.0001

We confirmed these results in an Independent validation set of benign and PCa patient samples by performing qRT-PCR for DOT1L mRNA and found that again DOT1L was dramatically overexpressed in prostate cancer in comparison to normal prostate tissue (**Figure 3.2**). These results imply that DOT1L is a putative oncogene that is consistently upregulated in prostate cancer.

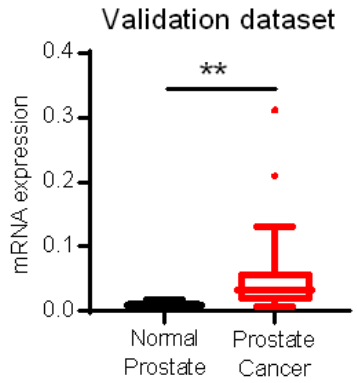

Figure 3.2: DOT1L expression is upregulated in prostate cancer in an independent validation dataset.

Comparison of DOT1L expression in an independent dataset with PCa patient specimens [benign (n=15), PCa (n=45)]. P value determined by Welsh's t-test. Error bars represent minimum and maximum values. ** $p<0.01$

We also found that when compared to their normal tissue counterparts, DOT1L was over expressed in other solid cancer types including breast cancer, glioblastomas and several others (**Figure 3.3**).

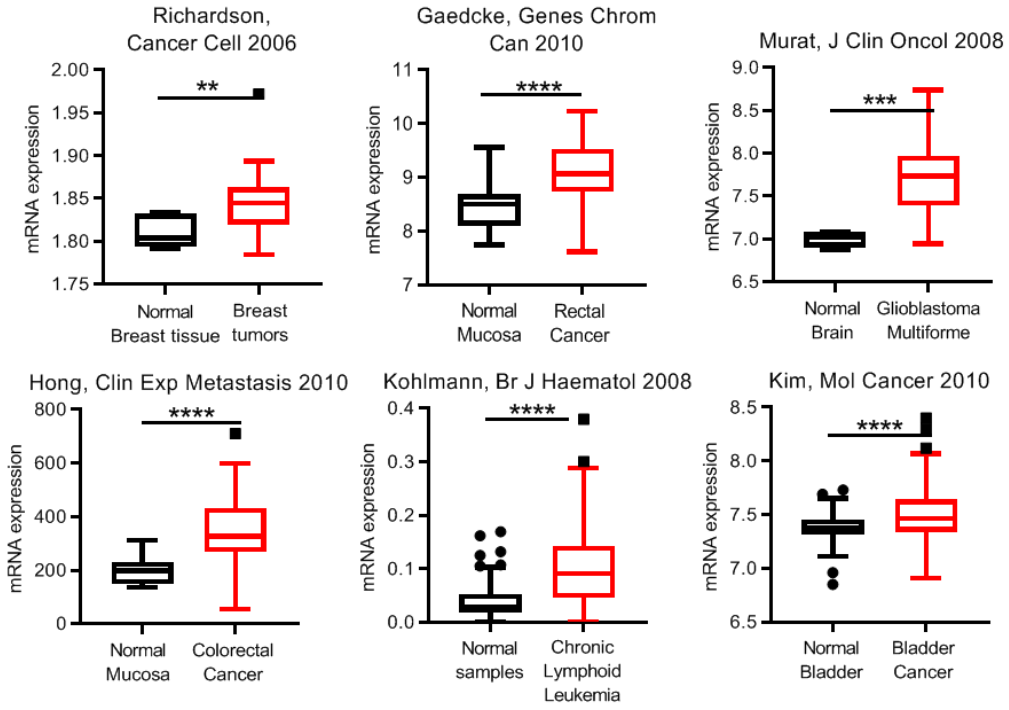

Figure 3.3: DOT1L expression is upregulated in different cancers when compared to normal tissue.

Expression of DOT1L in multiple cancer types. Data was used from Richardson Breast cancer dataset [Normal (n=7), Cancer (n=40)], GaedckeRectal cancer dataset [Normal (n=65), Cancer (n=65)], Murat Glioblastoma dataset [Normal (n=4), Cancer (n=80)], Hong Colorectal cancer dataset [Normal (n=12), Cancer (n=70)], Kohlmann CLL dataset [Normal (n=73), Cancer (n=448)], Kim Bladder cancer [Normal (n=68), Cancer (n=188)]. P value determined by Welsh's t-test. Error bars represent minimum and maximum values. *p< 0.05, ** p<0.01, *** p<0.001, ****p<0.0001

This indicates a selective pressure to elevate DOT1L expression during cancer progression, not limited to the prostate. We then probed the possibility that DOT1L expression is associated with poor survival in prostate cancer patients. Our analysis showed that high DOT1L expression is significantly associated with poor disease-free survival and overall survival (**Figure 3.4**) in multiple datasets. Moreover, in patients with cancers of intermediate grade (Gleason 7), high DOT1L expression was able to significantly predict poor disease-free survival.

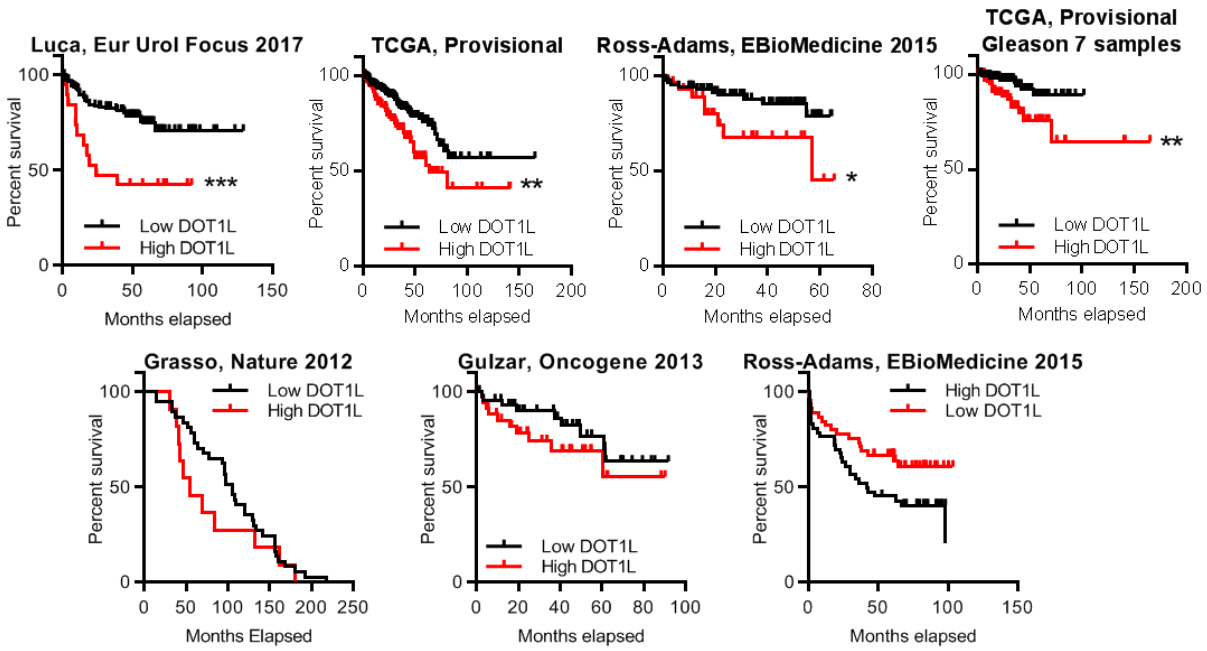

Figure 3.4: High DOT1L expression correlates with poor disease-free survival.

Survival analysis of independent cohorts of prostate cancer patients divided by expression of DOT1L. Data for this Disease free survival analysis was used from the Luca Cancer Map prostate cancer dataset [Cut-off at 90th percentile, high DOT1L (n=19), low DOT1L (n=214)], TCGA prostate cancer dataset [Cut-off at 90th percentile, high DOT1L (n=33), low DOT1L (n=463)], Ross-Adams prostate cancer dataset [Cut-off at 75th percentile, high DOT1L (n=24), low DOT1L (n=84)] and TCGA Gleason 7 patients, Ross-Adams Validation dataset [High(n=92), Low (n=92), p=0.0632], Gulzar dataset [High (n=83), Low (n=83), p=0.1535]. Overall survival data was used from Grasso dataset [High (n=48), Low (n=48), p=0.3118]. P value determined by Log-rank test.

DOT1L is the only enzyme known to catalyze H3K79 methylation, so we checked the levels of DOT1L-mediated H3K79 methylation in patient tissues. To this end, we performed Immunohistochemistry (IHC) for H3K79me2 in a tissue microarray (TMA) with 80 PCa patient specimens and found that H3K79me2 staining was indeed increased in prostate cancer tissue in contrast to normal tissues (**Figure 3.5**). This confirms that DOT1L activity is upregulated in prostate cancer and that H3K79me2 can be used as a predictive biomarker for DOT1L action.

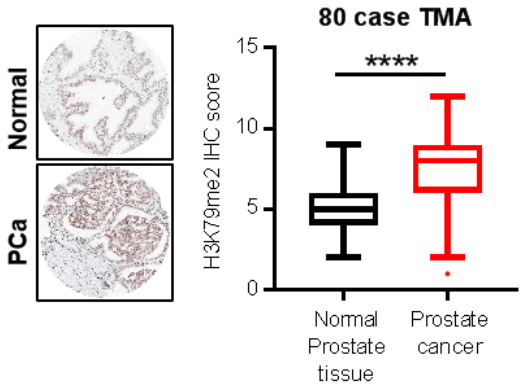

Figure 3.5: H3K79me2 expression is increased in prostate cancer compared to normal tissues.

Representative images (left) and comparison of average H3K79me2 staining scores (right) in tissue sections from a PCa TMA [Normal (n=80), PCa (n=80)].

3.2. DOT1L is required for viability of androgen receptor positive prostate cancer cells

To ascertain the functional role of DOT1L in prostate cancer, we treated a panel of prostate cancer cell lines with specific DOT1L inhibitor EPZ004777 (EPZ) and performed colony formation and cell viability assays. DOT1L inhibition led to a selective loss in colony formation and cell viability in AR positive cells compared to AR negative cells, indicating that response to DOT1L inhibition may depend on the AR signaling status of the cancer cells (**Figure 3.6** a-b). Sensitivity to DOT1L inhibition is seen in AR-positive cells including CRPC cells (C42B), AR variant AR-V7 expressing cells (22Rv1) and C42B enzalutamide resistant cells (**Figure 3.6** c). A second DOT1L inhibitor, EPZ5676 showed similar results as EPZ004777 (**Figure 3.6** d). Lentiviral-mediated shRNA knockdown of DOT1L in LNCaP cells also decreased colony formation (**Figure 3.6** e). We also used a 3D organoid model to confirm the effects of DOT1L inhibition on viability as it better recapitulates in vivo conditions compared to 2D cultures. Similar to 2D cultures, LNCaP but not AR negative PC3 organoids were sensitive to EPZ (**Figure 3.6** f-g).

a

Cell Line Name	AR signaling	IC50 for EPZ (nM)
LNCaP	Positive	250
22Rv1	Positive	250
C42B	Positive	500
DU145	Negative	>10,000
PC3	Negative	>10,000
RWPE-1	Negative	>10,000

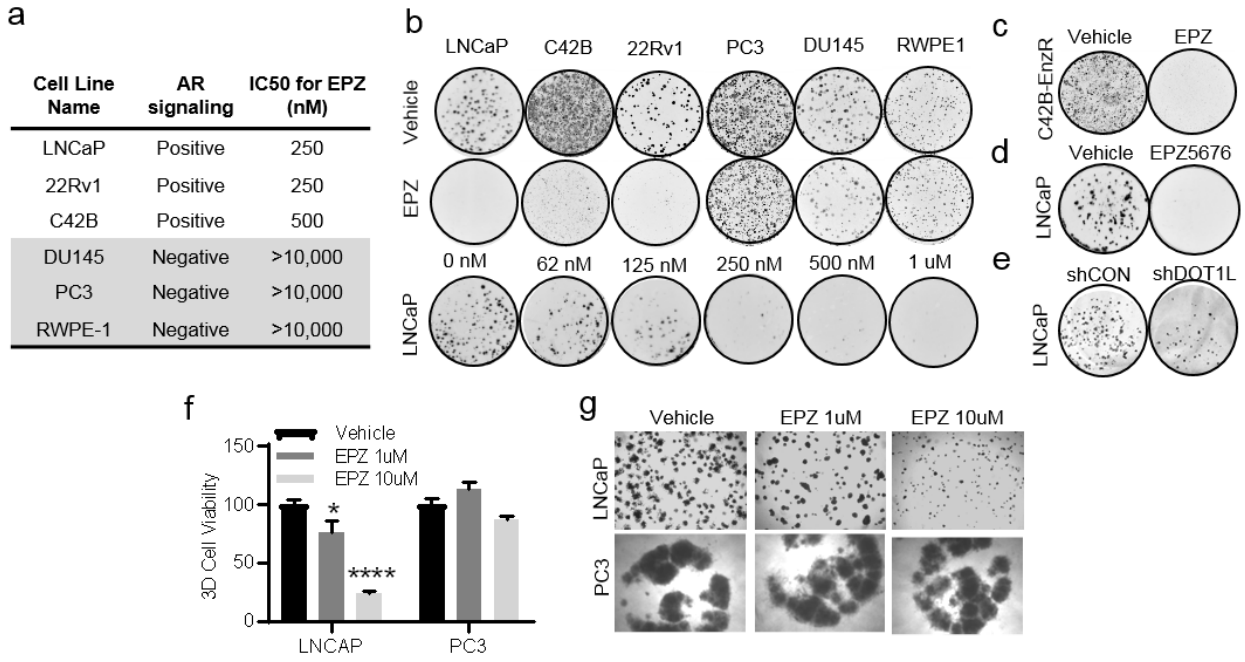

Figure 3.6: DOT1L inhibition leads to selective loss in cell viability in AR positive cells. (a) Comparison of Half maximum inhibitory concentration (IC50) for EPZ in 6 prostate cancer cell lines (b) (Top) Representative images of clonogenic assays performed for 6 prostate cancer cell lines treated with Vehicle or 10uM of EPZ for 12 days from 3 independent experiments. (Bottom) Representative images of clonogenic assay in LNCaP cells treated with increasing doses of EPZ for 12 days from 3 independent experiments. Colony formation assays performed in (c) C42B-ENZR cells treated with Vehicle or 10uM EPZ for 12 days (d) LNCaP cells treated with Vehicle or 10uM EPZ5676 for 12 days (e) LNCaP cells transduced with shControl or shDOT1L (f-g) 3D Cell viability assay in LNCaP and PC3 organoids after 12 days of EPZ treatment. Representative images shown (g).

Next, we sought to test the effects of DOT1L inhibition in vivo using a LNCaP subcutaneous xenograft model. However due to the poor pharmacokinetic properties of the drug, we resorted to an in vitro treatment model. We treated cells with EPZ for 7 days, then inoculated cells into mice subcutaneously. In vivo, the growth of EPZ pre-treated tumors was substantially inhibited compared to the control group. These results indicate that DOT1L inhibition has sustained effects on the prostate cancer cells, possibly by remodeling of the epigenetic landscape.

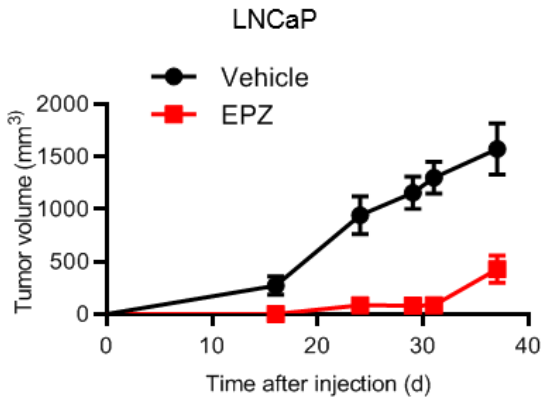

Figure 3.7: DOT1L inhibition leads to impairment of LNCaP tumor growth in vivo. LNCaP cells were treated invitro with Vehicle or 10uM EPZ and 2 million viable cells were injected subcutaneously in NOD-SCID mice and tumor growth was monitored. (n=5 per arm)

Due to the known long half-life of H3K79 methylation in cells, we performed the above experiments after 8-12d of inhibitor treatment or shRNA expression. Short term treatment with EPZ (**Figure 3.8 a-b**) or transient knockdown of DOT1L with siRNA had no effect on the cell viability of sensitive cell lines (**Figure 3.8 c**). These data suggest that the effect of DOT1L inhibition in AR-positive cells is dependent on loss of H3K79 methylation. This was supported by the observation that H3K79me2 was decreased only after long-term (8d) treatment with EPZ but not short-term treatment (**Figure 3.8 d**). These results support a model wherein the functional effects of DOT1L inhibition in the AR-positive cells require events that occur after loss of

H3K79 methylation such as dysregulated target gene expression in contrast to direct effects, such as modification of AR by DOT1L enzymatic activity or protein-protein interaction. The differential sensitivity to DOT1L inhibition between AR-positive and AR-negative cells was not due to lack of inhibition of DOT1L function in the resistant cells as 8d treatment with EPZ decreased H3K79me2 to the same extent in both LNCaP and PC3 cells (**Figure 3.8 d**). This was confirmed with the shDOT1L construct and EPZ5676 drug as well (**Figure 3.8 e-f**).

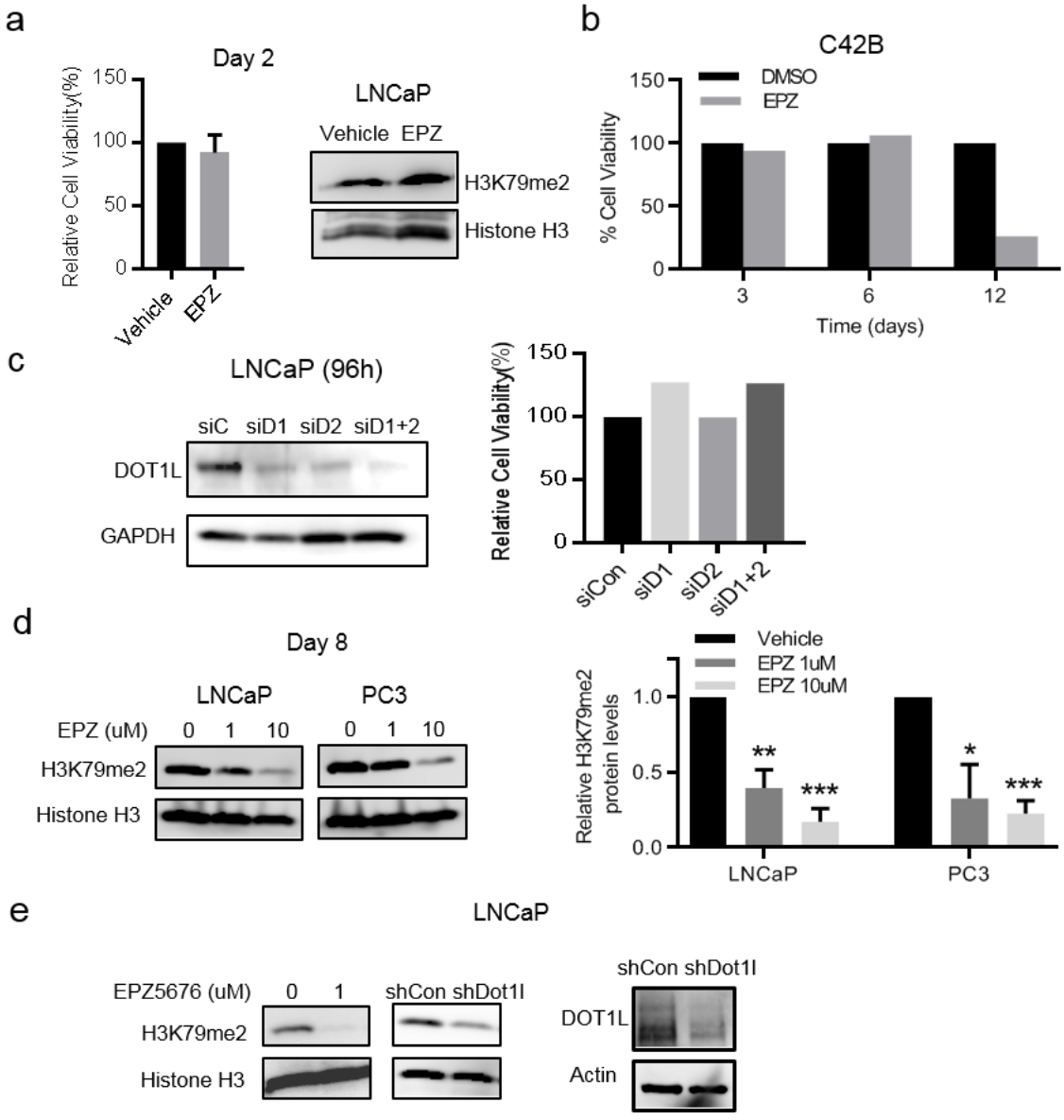

Figure 3.8: DOT1L inhibition leads to loss of H3K79me2 levels.

(a) Cell viability and H3K79me2 western blot analysis performed after 2 days of treatment with Vehicle or 10uM EPZ in LNCaP cells (b) Cell viability assays performed after 3,6 and 12 days of treatment with Vehicle or 10uM EPZ in C42B cells (c) DOT1L western blot (4 days) and Cell viability assays (12 days) in LNCaP cells transfected with Control or 2 single DOT1L targeting siRNA and 1 pool of DOT1L targeting siRNA (d) H3K79me2 western blot analysis performed after 8 days of treatment with Vehicle or EPZ (left) with quantitation of protein levels (right) (e) H3K79me2 western blot analysis in LNCaP after 8 days of treatment with (left) Vehicle or EPZ5676, (right) shControl or shDOT1L. DOT1L western blot in LNCaP cells transduced with Luciferase targeting shRNA or DOT1L targeting shRNA (4 days).

We next sought to determine if differential distribution of H3K79 methylation at baseline or after DOT1L inhibition may be related to sensitivity to EPZ. To this end, we performed Chromatin Immunoprecipitation-sequencing (ChIP-seq) for H3K79me2 in both LNCaP and PC3 cells. EPZ decreased the number of H3K79me2 marked peaks to the same extent (**Figure 3.9 a**); however, while a subset of sites was shared between the two cell lines, the majority of sites were unique to each cell line (**Figure 3.9 b**). Due to the association of H3K79me2 with active transcription, we speculated that the shared sites might be related to lineage associated or prostate cancer specific genes. To characterize the unique genes whose K79me2 was sensitive to DOT1L inhibition in each cell line, we performed ChIP Enrichment Analysis (ChEA). We found that these genes were associated with unique transcription factors that function exclusively in these cells. In LNCaP,

AR and FOXA1 associated genes were among the top hits (**Figure 3.9 c-d**). In PC3, top hits included neural lineage associated transcription factors including HOXC9 and MYCN. Together, these results show that AR positive cells are selectively sensitive to DOT1L inhibition and that distinct H3K79me2 marked sites in LNCaP might be responsible for this selectivity.

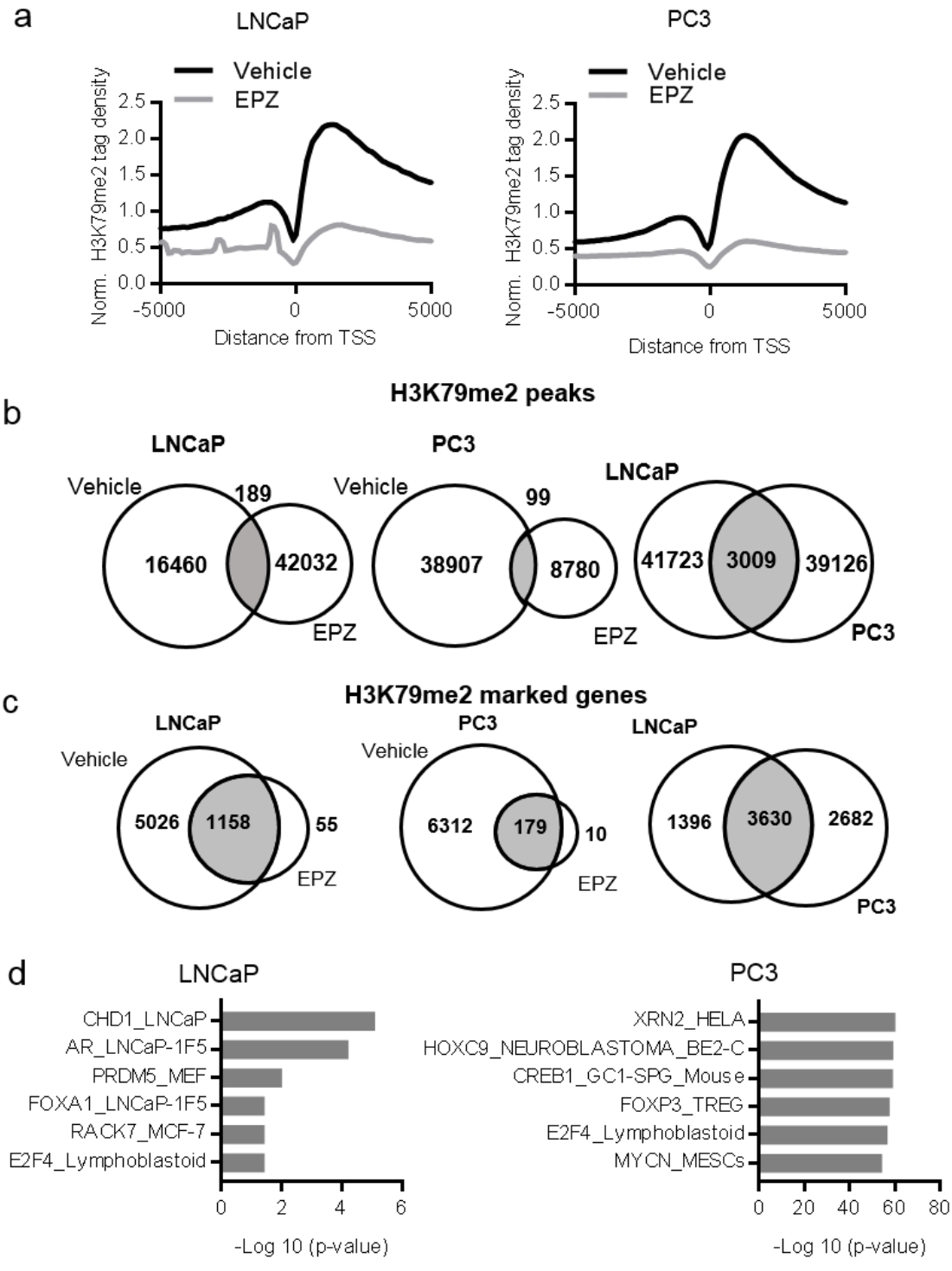
a
LNCaP
PC3
Vehicle
EPZ
Norm. H3K79me2 tag density
2.5
2.0
1.5
1.0
0.5
0.0
-5000
0
5000
Distance from TSS
b
H3K79me2 peaks
LNCaP
Vehicle
189
16460
42032
EPZ
PC3
Vehicle
99
38907
8780
EPZ
LNCaP
41723
3009
39126
PC3
c
H3K79me2 marked genes
LNCaP
Vehicle
5026
1158
55
EPZ
PC3
Vehicle
6312
179
10
EPZ
LNCaP
1396
3630
2682
PC3
d
LNCaP
CHD1_LNCaP
AR_LNCaP-1F5
PRDM5_MEF
FOXA1_LNCaP-1F5
RACK7_MCF-7
E2F4_Lymphoblastoid
0
2
4
6
-Log 10 (p-value)
PC3
XRN2_HELA
HOXC9_NEUROBLASTOMA_BE2-C
CREB1_GC1-SPG_Mouse
FOXP3_TREG
E2F4_Lymphoblastoid
MYCN_MESCs
0
20
40
60
80
-Log 10 (p-value)

Figure 3.9: DOT1L inhibition leads to loss of H3K79me2 levels globally in both LNCaP and PC3 cells.

(a) Histogram of H3K79me2 tags (within 10kb) centered on the TSS in LNCaP (left) and PC3 (right) Vehicle and EPZ treated samples. ChIP-seq performed after cells were treated for 8 days with Vehicle or 1uM EPZ (b) Venn diagrams comparing H3K79me2 enriched peaks in LNCaP and PC3 after treatment with Vehicle or 1uM EPZ for 8 days. (c) Venn diagrams comparing H3K79me2 marked genes in LNCaP and PC3 after treatment with Vehicle or 1uM EPZ for 8 days identified by ChIP-sequencing and Venn diagram comparing H3K79me2 marked genes in LNCaP and PC3 in non-treated controls (right). (d) ChIP Enrichment Analysis (ChEA) of unique H3K79me2 enriched genes from LNCAP and PC3 identified using Enrichr web tool.

3.3. DOT1L inhibition leads to impairment of the AR pathway

Since AR-positive cell lines were sensitive to DOT1L loss, we determined the status of the AR pathway after short-term and long-term DOT1L inhibition. AR protein levels were decreased upon treatment with EPZ in a dose dependent manner and DOT1L knockdown (**Figure 3.10 a**). However, this change in AR protein was observed only after 8 days of DOT1L inhibition, but not 2 days (**Figure 3.10 b**). This observation rules out the possibility of direct DOT1L-AR interaction having an effect on cell viability. Conversely, we found that in DOT1L overexpressing LNCaP cells, AR protein levels were upregulated (**Figure 3.10 c**). Moreover, LNCaP-DOT1L cells displayed an increased proliferation rate in charcoal stripped medium devoid of androgens (**Figure 3.10 c**). This implies that DOT1L promotes androgen independent growth of prostate cancer cells.

DOT1L does not regulate AR at the transcriptional level as we found no change in AR mRNA levels after EPZ treatment or DOT1L knockdown (**Figure 3.10 d**). We then tested the possibility that AR stability was altered upon DOT1L loss. AR protein half-life was reduced in LNCaP cells treated with EPZ when compared to DMSO treated cells in a cycloheximide chase assay (**Figure 3.10 e**).

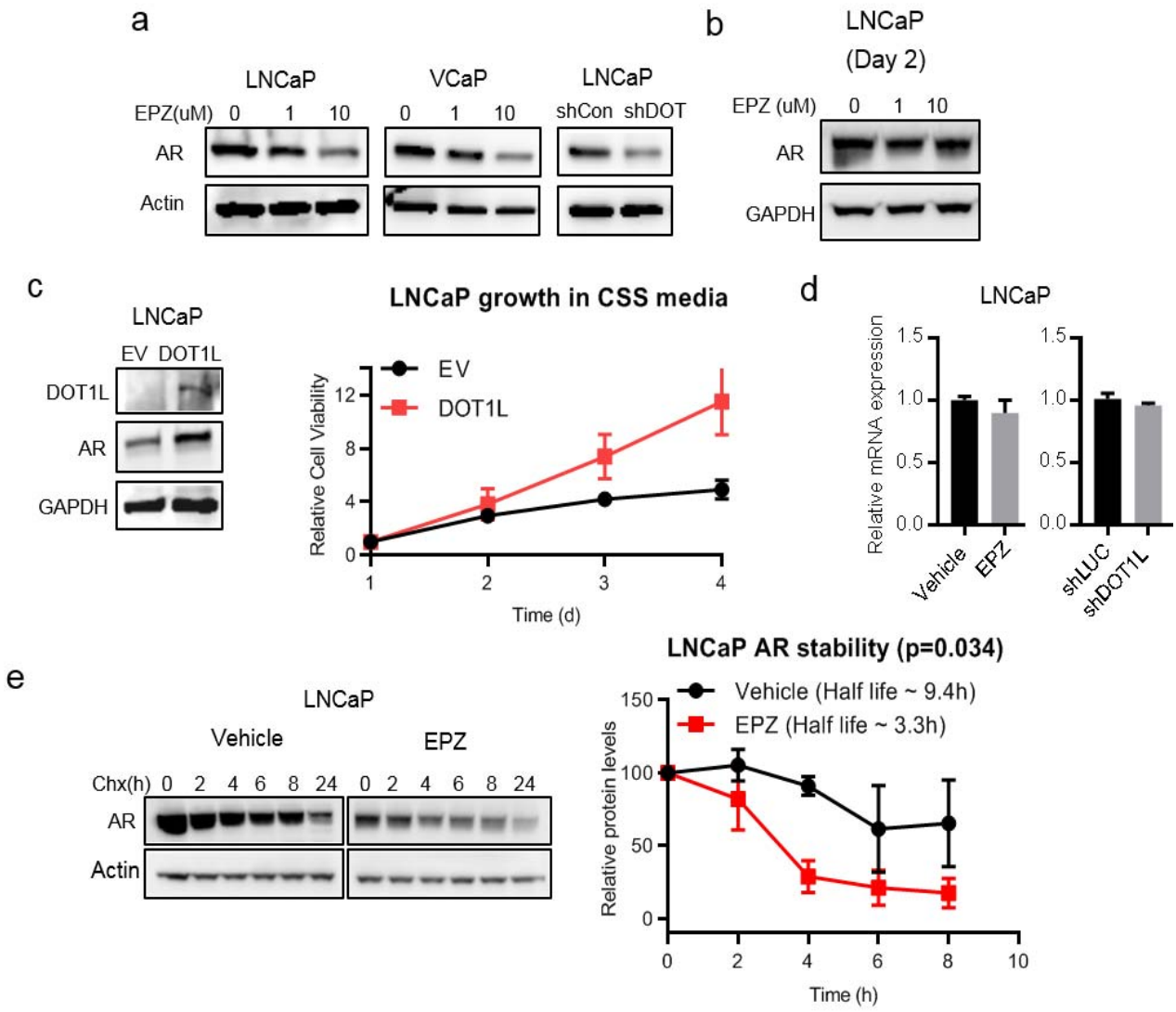

Figure 3.10: DOT1L inhibition leads to loss of AR levels by altering its protein stability.

(a) AR protein levels after EPZ treatment in LNCaP (left) and VCaP (middle) cells and shControl or shDOT1L transfected LNCaP cells (right). (Representative experiment shown from 3 independent experiments) (b) Western blot analysis of AR in LNCaP cells treated with Vehicle or EPZ for 2 days. (c) AR protein levels in EV or DOT1L overexpressing LNCaP cells (left). Proliferation assay of LNCaP cells with and without DOT1L expression in charcoal stripped

media (right) measured using MTS assays for 4 days. (d) mRNA expression of AR in LNCaP cells treated with Vehicle or EPZ for 8 days (left) and LNCaP cells transfected with shControl or shDOT1L (right) (e) AR western analysis after 50 ug/ml Cycloheximide treatment in LNCaP cells treated with Vehicle or EPZ for 8 days (left). Quantitation of AR protein levels from 3 independent experiments (right).

To further examine the status of the downstream AR pathway upon DOT1L inhibition, we first examined the levels of PSA, a canonical AR target gene. PSA protein levels were decreased in a dose dependent manner upon EPZ treatment (**Figure 3.11 a**). Additionally, by using an Androgen Responsive Element (ARE) promoter-GFP reporter expressing cell line to monitor AR pathway activation, we found a dose dependent decrease in AR transcriptional activity with long-term EPZ treatment (**Figure 3.11 b**). To further characterize the state of AR target genes globally, we performed whole genome expression profiling. Surprisingly, while a small subset of AR activated genes were suppressed by EPZ treatment as expected (e.g. PSA, TMPRSS2, KLK2), a larger subset was found to be upregulated in the Nelson_Response_To_Androgen_Up dataset, including ELL2, HERC3, ACSL3 (**Figure 3.11 c-d**). We confirmed these results using qRT-PCR after both EPZ treatment and shDOT1L expression (**Figure 3.11 e-f**). We further confirmed that AR binding at these target gene promoters was decreased upon EPZ treatment despite the increased expression (**Figure 3.11 g**). This discrepancy is not due to persistence of H3K79me2 levels at these upregulated AR target genes as determined by inspection of H3K79me2 ChIP-seq plots (**Figure 3.11 i**).and by ChIP-qPCR (**Figure 3.11 h**).

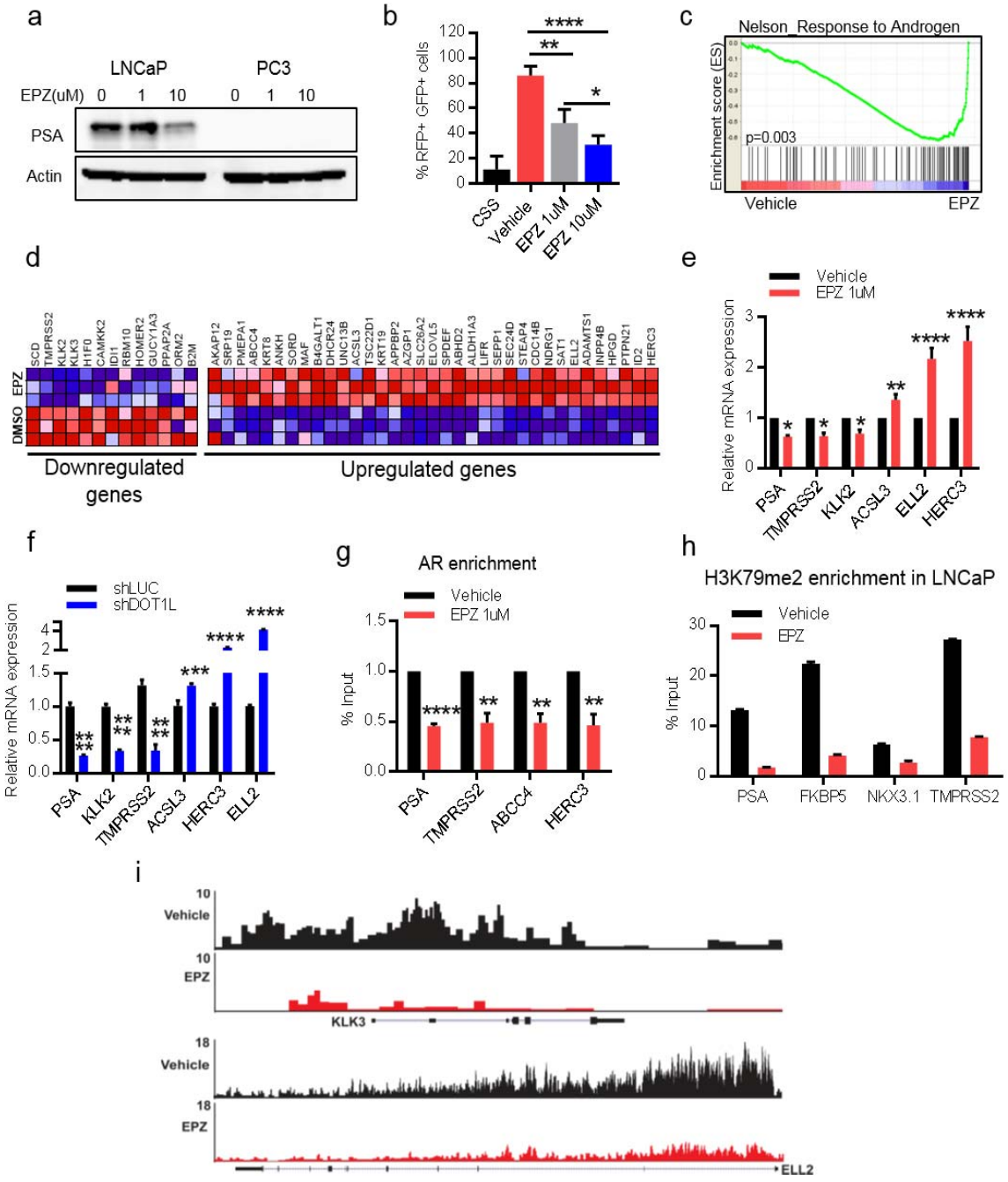

Figure 3.11: DOT1L inhibition leads to repression of a subset of AR genes but upregulation of a larger subset.

(a) PSA western blot analysis in LNCaP and PC3 cells treated with Vehicle and EPZ for 8 days. Representative image shown. (b) Percentage of RFP+GFP+ cells counted by Flow cytometry

after 8 days of Vehicle or EPZ treatment in LNCaP cells transfected with ARE-GFP reporter construct. (c) GSEA plot of Nelson_Response_to_Androgen geneset enriched in LNCaP cells treated with 1uM EPZ for 8 days compared to Vehicle treatment. (d) Heatmap of differentially expressed genes from Nelson_Response_To_Androgen dataset identified by GSEA analysis in LNCaP cells treated with Vehicle or 1uM EPZ. RNA expression of 6 AR target genes measured by qRT-PCR in LNCaP cells after 8 days of 1uM EPZ treatment (e) and transduction with shDOT1L or shControl lentivirus (f). (g) Relative enrichment of AR at 4 target genes measured by ChIP followed by qPCR in LNCaP cells treated with Vehicle or 1uM EPZ for 8 days. (h) H3K79me2 enrichment at AR target genes in LNCaP cells treated with Vehicle or 1uM EPZ for 8 days measured by ChIP-qPCR. (i) ChIP-seq plots of H3K79me2 at two AR target genes in LNCaP cells treated with Vehicle or 1uM EPZ.

The above results were even more surprising considering the fact that multiple androgen metabolism gene sets were upregulated upon EPZ treatment (**Figure 3.12 a-b**). We observed an upregulation of members of the UGT2B family of enzymes that are responsible for androgen glucuronidation leading to removal of androgens from the cell. UGT2B7, 15 and 17 are the main enzymes involved in the process (201, 202) and these were upregulated consistently in LNCaP and C42B cells upon EPZ treatment (**Figure 3.12 c-d**). Since these genes are negatively regulated by androgen bound AR, we confirmed that AR enrichment at UGT2B promoters was decreased upon EPZ treatment (**Figure 3.12 e**). Overall, these results indicate that, in addition to impairing AR protein stability, DOT1L inhibition may also lead to loss of androgen levels in prostate cancer cells by upregulating the UGT2B family of enzymes.

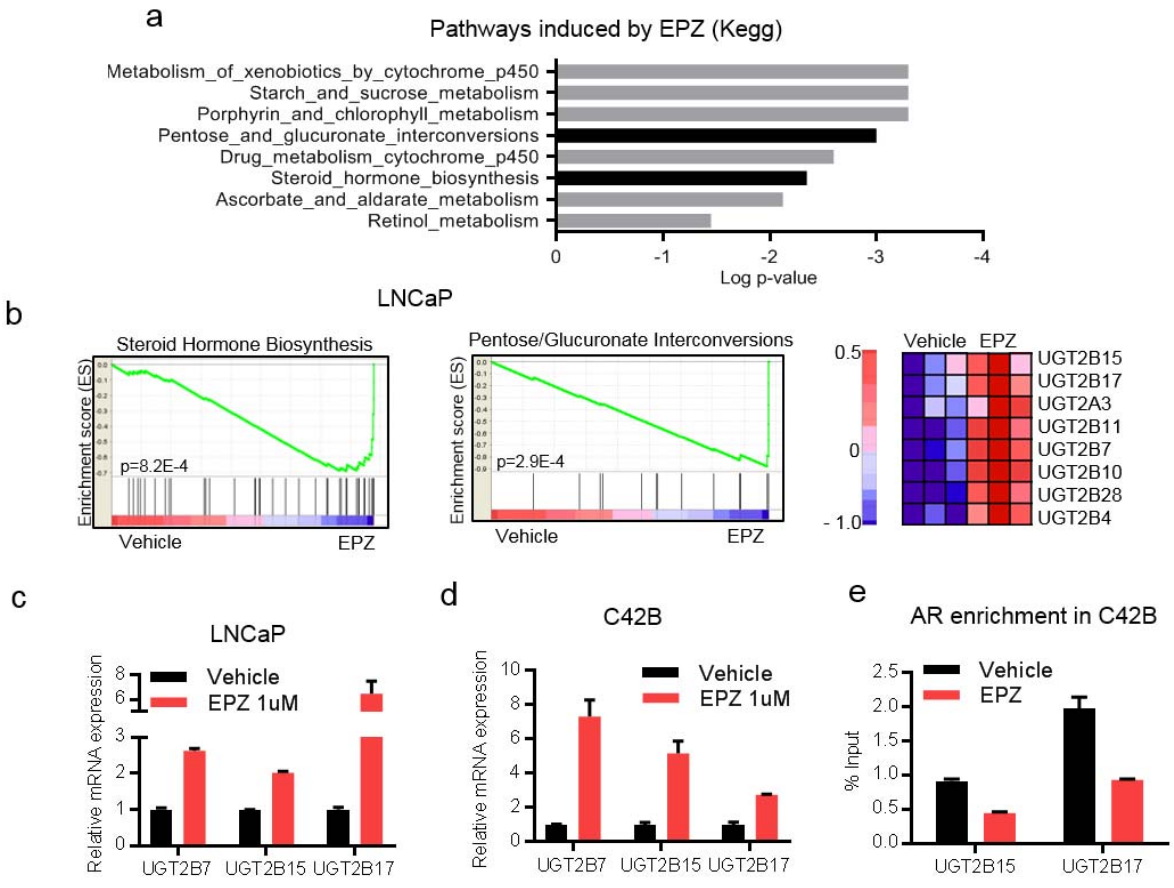

Figure 3.12: DOT1L inhibition leads to upregulation of androgen metabolism pathways.

(a) Top 8 Kegg pathways induced by EPZ identified by GSEA analysis in LNCaP cells after treatment with Vehicle or 1uM EPZ. Bars in black indicate gene-sets of interest. (b) GSEA plot of Steroid_Hormone_Biosynthesis geneset (left) and Pentose_Glucuronate_Interconversions geneset (middle) identified by GSEA analysis in LNCaP cells after treatment with Vehicle or 1uM EPZ. Heat map of UGT2B family of genes from leading edge of Pentose_Glucuronate_Interconversions gene set (right). mRNA expression of UGT2B7, 15, and 17 after 1uM EPZ treatment in LNCaP (c) and C42B cells (d). (e) AR enrichment at UGT2B

gene promoters after Vehicle/EPZ 1uM treatment for 8 days in C42B cells evaluated by ChIP-qPCR.

All of these changes should lead to a reduction in AR transcriptional activity; yet paradoxically we observed upregulation of a subset of AR activated genes as described above. These observations led us to hypothesize that expression of these discordant AR target genes may be regulated by another transcription factor that is modulated by DOT1L inhibition.

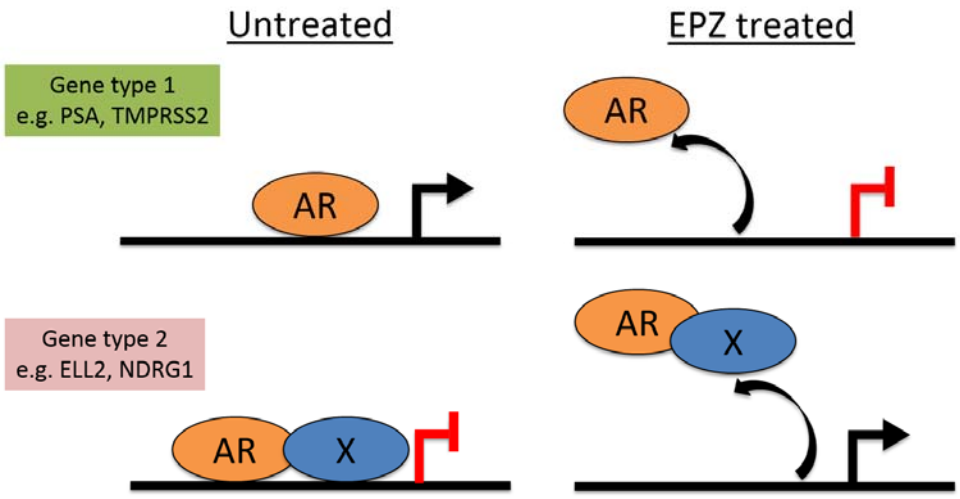

Figure 3.13: Two different types of AR target genes are altered upon DOT1L inhibition.

AR target genes belonging to type 1 are regulated by AR alone and are repressed upon EPZ treatment. AR target genes belonging to type 2 are regulated by AR and another factor 'X'. These genes are upregulated upon DOT1L inhibition.

3.4. DOT1L inhibition suppresses the MYC pathway

To search for a candidate DOT1L inhibitor regulated factor that may cross-regulate expression of the discordant AR target genes we examined GSEA datasets for EPZ-treated LNCaP and PC3 cells for significant transcription factor regulated gene sets. We found alterations in the MYC pathway with MYC target gene sets suppressed in EPZ-treated LNCaP but not PC3 cells (**Figure 3.14**). Interestingly, MYC has been shown to repress a subset of AR target genes in prostate cancer (21). We thus hypothesize that the discordant AR target genes we observed after EPZ treatment may be co-regulated by MYC, with loss of MYC induced by EPZ treatment leading to their upregulation, despite the reduction in AR levels. To examine this notion, we first compared the leading-edge genes from the 'Nelson' dataset from the above-mentioned study with the leading-edge genes from our own study and found a significant overlap (p value = 0.03) (**Figure 3.14** a).

Examination of gene expression profiling data by GSEA showed that MYC induced gene targets were repressed upon DOT1L inhibition in LNCaP cells but not PC3 cells (**Figure 3.14**). These data indicate that EPZ treatment suppresses the MYC pathway in LNCaP but not PC3 cells.

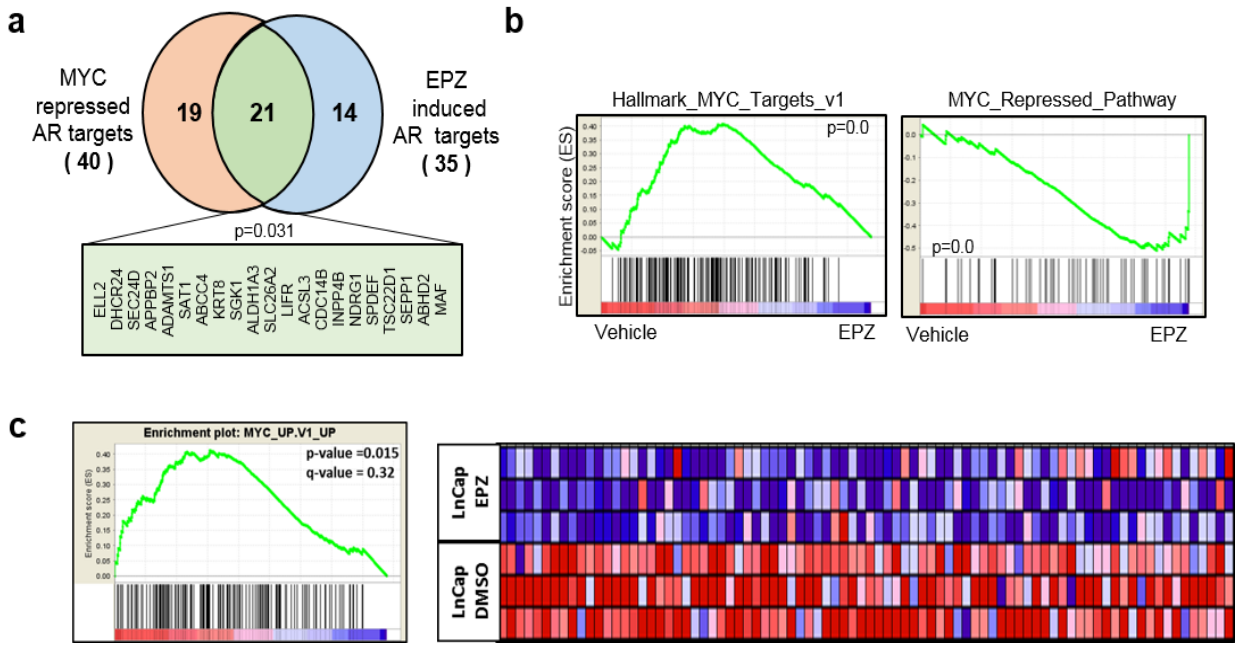

Figure 3.14: DOT1L inhibition leads to suppression of MYC induced target genes and upregulation of MYC repressed genes.

(a) Comparison of leading-edge genes from Nelson_Response_To_Androgen dataset in the present study (n=35) and Barfield study (n=40). P value determined by hypergeometric test. (b) GSEA plots of two MYC related datasets enriched in either Vehicle treated (left) or EPZ treated (right) LNCaP cells. Cells were treated with 1uM Vehicle or EPZ for 8 days prior to microarray analysis (n=3 biological replicates) (c) GSEA plot of two MYC_UP geneset and the associated heatmap of the leading edge genes.

By qRT-PCR analysis, we found that MYC mRNA levels were reduced in LNCaP & C42B cells but not PC3 cells after EPZ treatment (**Figure 3.15 a**). Furthermore, analysis of prostate cancer

patient datasets showed that MYC expression positively correlated with DOT1L expression in multiple datasets (**Figure 3.15 b**).

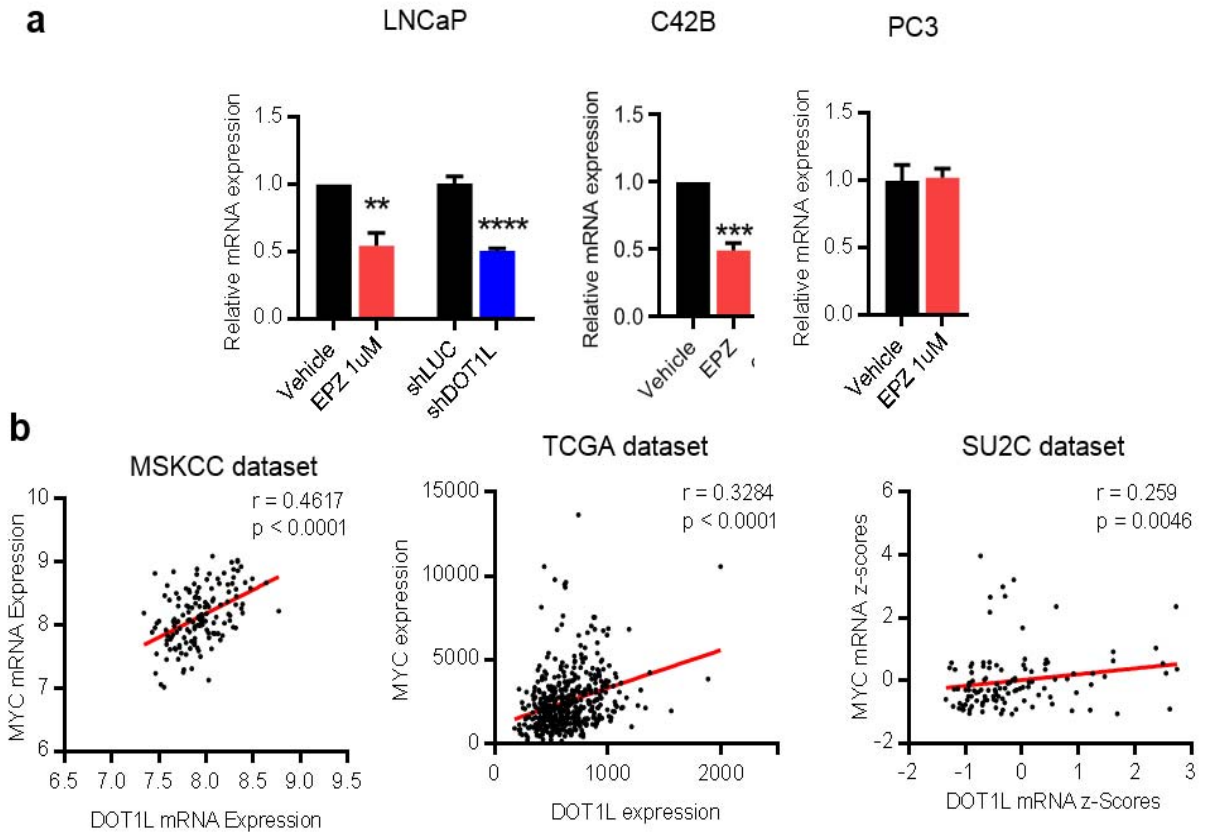

Figure 3.15: DOT1L regulates MYC mRNA expression.

(a) mRNA expression of MYC in (left) LNCaP and C42B (middle) cells treated with Vehicle or 1uM EPZ; and LNCaP cells transduced with shControl or shDOT1L lentivirus (right) PC3 cells treated with Vehicle or 1uM EPZ for 8 days. (d) Positive correlation between DOT1L and MYC expression in the MSKCC dataset (n=150), the SU2C dataset (n=118) and TCGA dataset (n=498). P-values were analyzed using Spearman's rank correlation. Data was obtained from cbioportal.org.

We next analyzed MYC protein levels in our prostate cancer cell lines and found that MYC protein was dramatically decreased upon DOT1L inhibition with EPZ in LNCaP but not PC3 cells (**Figure 3.16 a**). We confirmed these results by inhibiting DOT1L with EPZ5676 and DOT1L shRNA expression. We also observed that MYC levels increased upon upregulation of DOT1L (**Figure 3.16 b**). MYC protein levels were also decreased after long term treatment but not short-term 2 day treatment with EPZ in LNCaP cells (**Figure 3.16 c**). Next, we assessed the stability of MYC protein in both LNCaP and PC3 cells by the cycloheximide chase assay, and found decreased MYC protein stability in EPZ treated LNCaP but not PC3 cells (**Figure 3.16 d,f**). In addition, treatment with the proteasome inhibitor, MG132 restored MYC protein levels in EPZ treated LNCaP cells, implying that MYC is degraded through the proteasomal pathway upon EPZ treatment (**Figure 3.16 e**). These data suggest that DOT1L dependent MYC loss is dependent on AR activity as well.

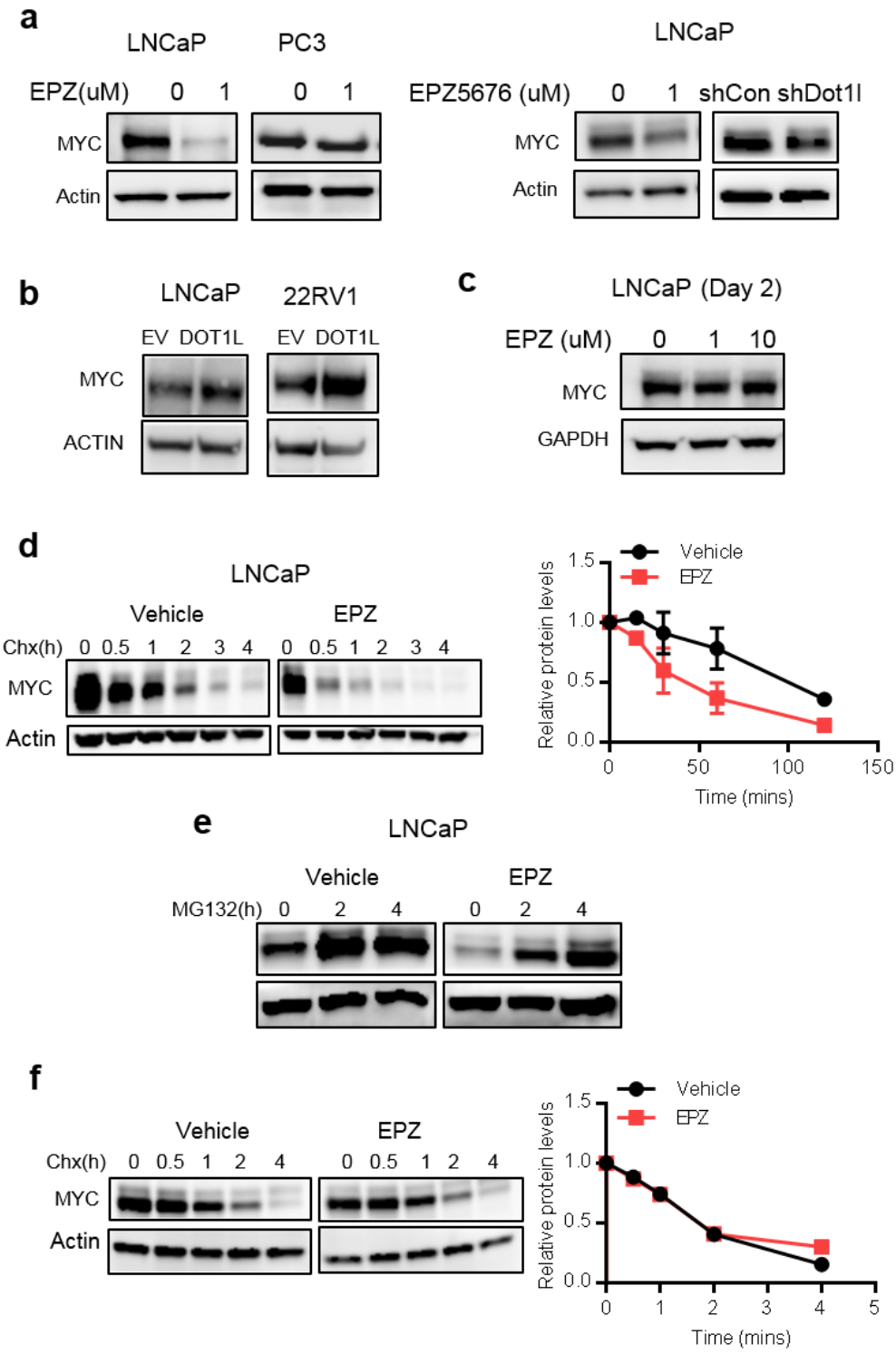
a
LNCaP
PC3
EPZ(uM) 0 1 0 1
MYC
Actin
LNCaP
EPZ5676 (uM) 0 1 shCon shDot1l
MYC
Actin
b
LNCaP
22RV1
EV DOT1L EV DOT1L
MYC
ACTIN
c
LNCaP (Day 2)
EPZ (uM) 0 1 10
MYC
GAPDH
d
LNCaP
Vehicle
EPZ
Chx(h) 0 0.5 1 2 3 4 0 0.5 1 2 3 4
MYC
Actin
Vehicle
EPZ
Relative protein levels
1.5
1.0
0.5
0.0
0
50
100
150
Time (mins)
e
LNCaP
Vehicle
EPZ
MG132(h) 0 2 4 0 2 4
f
Vehicle
EPZ
Chx(h) 0 0.5 1 2 4 0 0.5 1 2 4
MYC
Actin
Vehicle
EPZ
Relative protein levels
1.5
1.0
0.5
0.0
0
1
2
3
4
5
Time (mins)

Figure 3.16: DOT1L inhibition leads to loss of MYC stability.

(a) (left) Western blot analysis of MYC protein in LNCaP and PC3 cells treated with Vehicle or EPZ 1uM for 8 days. (right) Western blot analysis of MYC protein in LNCaP cells treated with EPZ5676 for 8 days (left) and LNCaP cells with DOT1L knockdown (b) Western blot analysis of MYC in LNCaP and 22rv1 cells with EV or DOT1L overexpression. (c)Western blot analysis of MYC in LNCaP cells treated with Vehicle or EPZ for 2 days. (d) Western blot analysis and quantitation of MYC protein after treatment with 50 ug/ml Cycloheximide in LNCaP cells treated with vehicle or 1uM EPZ for 8 days. (e) Western blot analysis of MYC protein after treatment with 10uM MG-132 in LNCaP cells treated with vehicle or 1uM EPZ for 8 days. (f) Western blot analysis and quantitation of MYC protein after treatment with 50 ug/ml Cycloheximide in PC3 cells treated with vehicle or 1uM EPZ for 8 days. Statistical tests: P value determined by Student's t-test.

3.5. EPZ-regulated E3 ligases target AR and MYC stability

Since both AR and MYC proteins were degraded at increased rates upon long-term DOT1L inhibition, we hypothesized that DOT1L inhibition and loss of H3K79 methylation might impact the expression of E3 ligases that regulate the stability of MYC and AR. A search of EPZ-regulated genes in LNCaP cells for known and putative E3 ubiquitin ligases identified 4 candidates: HERC3, HECTD4, MYCBP2 and TRIM49 (**Figure 3.17 a**). TRIM49 was decreased upon EPZ treatment while the others were increased. By qRT-PCR, we confirmed dysregulation of all 4 genes in LNCaP cells, while in PC3 cells, only TRIM49 was altered but in the opposite direction to the change in LNCaP cells (**Figure 3.17 b,c**). Similar results were seen with DOT1L knockdown as well (**Figure 3.17 c**). These results suggest that dysregulation of one or more of these candidate E3 ligases may mediate AR and MYC protein degradation.

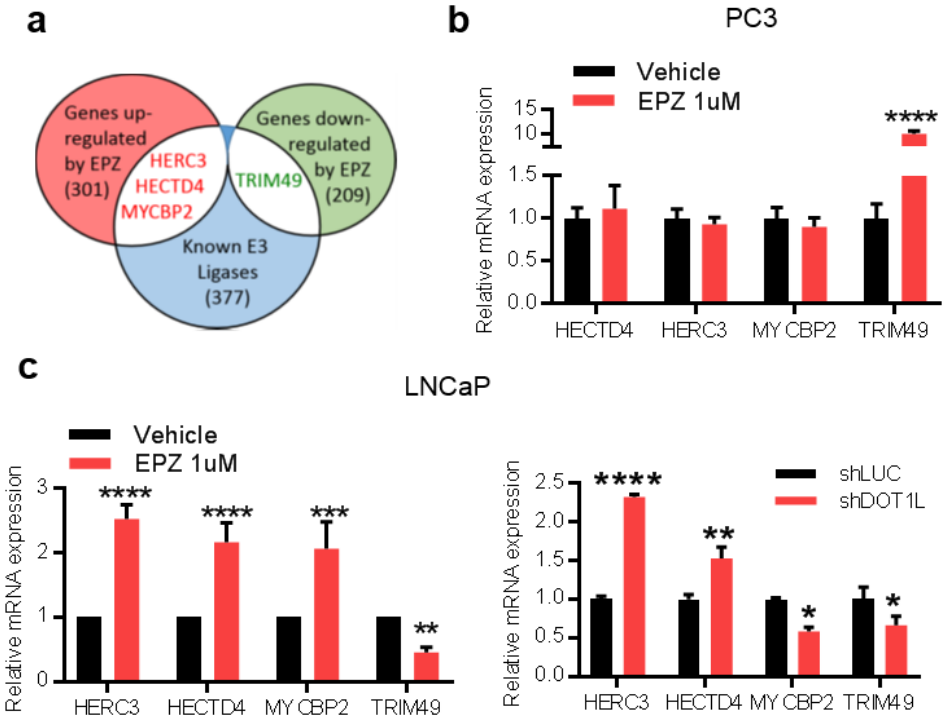

Figure 3.17: DOT1L inhibition leads to upregulation of key E3 ligases in AR positive cells.

(a) Comparison of genes that are differentially expressed by EPZ (n=510) and known E3 Ubiquitin ligases. mRNA expression of HERC3, HECTD4, MYCBP2 and TRIM49 in (b) PC3 and (c) LNCaP cells treated with vehicle or 1uM EPZ for 8 days and LNCaP cells with DOT1L knockdown.

Therefore, we performed a siRNA knockdown screen of the 4 candidate ligases and evaluated AR and MYC protein levels. (**Figure 3.18**). We did not detect any changes in AR or MYC protein levels after HERC3 knockdown. However, knockdown of HECTD4 and MYCBP2 led to an increase in both AR and MYC proteins while TRIM49 depletion reduced AR and MYC levels (**Figure 3.18 a**). We did not observe any changes in AR and MYC mRNA levels after

knockdown of HECTD4, MYCBP2 or TRIM49 supporting post-transcriptional regulation of AR and MYC by these ligases (**Figure 3.18 b, c, d**). These results suggest that EPZ-mediated upregulation of HECTD4 and MYCBP2 concomitant with downregulation of TRIM49 lead to a decrease in AR and MYC protein levels.

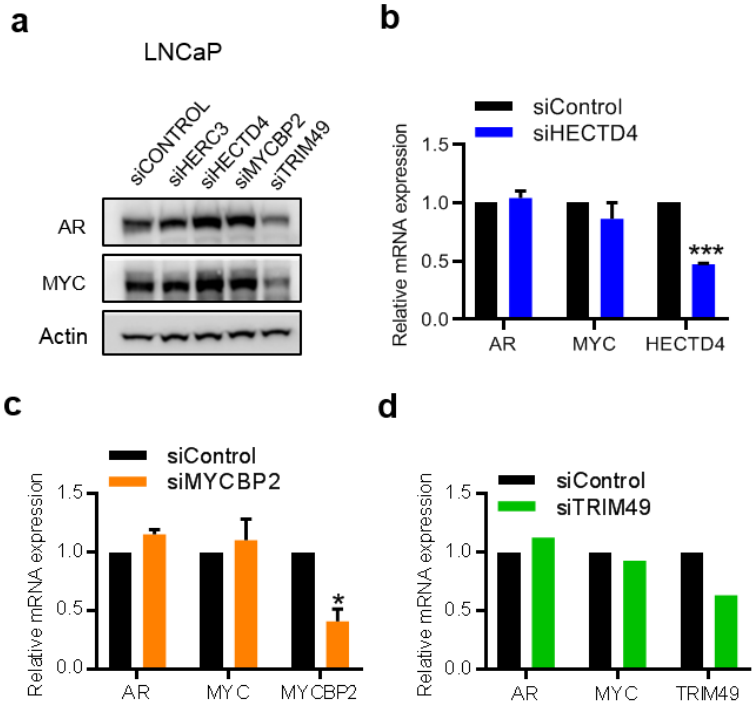

Figure 3.18: Knockdown of HECTD4 and MYCBP2 upregulate AR and MYC protein levels.

(a) AR and MYC protein levels in LNCaP cells 2 days after being transfected by Control, HERC3, HECTD4, MYCBP2 and TRIM49 targeting siRNA. AR and MYC mRNA expression in LNCaP cells transfected with Control or (b) HECTD4 targeting siRNA, (c) MYCBP2 targeting siRNA, (d) TRIM49 targeting siRNA for 2 days

To show this directly, we examined if knockdown of HECTD4 and MYCBP2 can rescue EPZ-mediated AR and MYC degradation. We thus treated LNCaP cells with EPZ or vehicle for 6 days, then transfected cells with siHECTD4 and siMYCBP2 and analyzed AR and MYC protein levels 2 days later. Both AR and MYC levels were restored after dual knockdown of HECTD4 and MYCBP2 in the EPZ treated cells (**Figure 3.19 a**). These data strongly suggest that HECTD4 and MYCBP2 are primarily responsible for the EPZ mediated loss of stability of AR and MYC proteins. To assess if the dual knockdown of HECTD4 and MYCBP2 could rescue the inhibitory effects of EPZ on cell viability, we repeated the same experiment, this time analyzing cell viability 6 days after siHECTD4+siMYCBP2 transfection. The results indicate that HECTD4 and MYCBP2 depletion significantly rescued the EPZ treatment induced loss of cell viability (**Figure 3.19 c**). To examine the functional role of TRIM49 in regulating MYC and AR after EPZ treatment, we overexpressed TRIM49 in LNCaP cells treated with EPZ or vehicle for 8 days. Analysis of AR and MYC protein levels 2 days later showed that TRIM49 overexpression can partially restore the levels of AR & MYC after EPZ treatment (**Figure 3.19 b**).

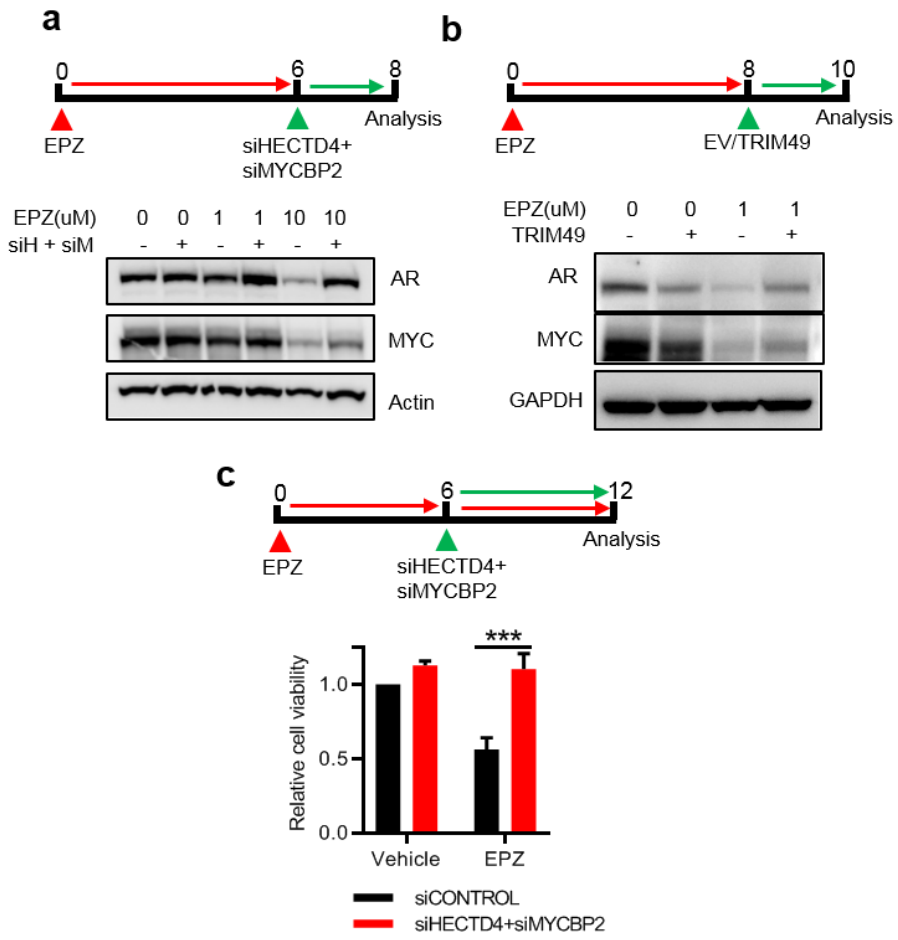

Figure 3.19: EPZ mediated upregulation of HECTD4 and MYCBP2 is required for AR and MYC protein loss.

(a) AR and MYC protein levels in LNCaP cells treated with Vehicle or EPZ for 6 days followed by transfection of Control or HECTD4 and MYCBP2 targeting siRNA for 2 days. Representative images shown from 3 independent experiments. (b) AR and MYC protein levels in LNCaP cells treated with Vehicle or EPZ for 8 days followed by transfection of EV or TRIM49 construct for 2 days. (c) Viability of LNCaP cells treated with Vehicle or EPZ for 6 days followed by

transfection of Control or HECTD4 and MYCBP2 targeting siRNA measured by CCK8 assay at Day 12.

We next examined if HECTD4 interacts with AR. MYCBP2 is an established E3 ubiquitin ligase that has been previously shown to interact with MYC (203, 204), and our mass spectrometry data for AR-interacting protein identified MYCBP2 (**Table 3**).

Table 3: Results from Mass spectrometry analysis

	Total spectra counts	
Protein ID	**DMSO normalized to IgG**	**EPZ normalized to IgG**
MYH10	260	132
MYO6	130	0
MYH14	73	20
MYO5A	64	11
AR	62	25
SEC16A	59	59
CDC42BPG	41	19
KRT18	38	52
KRT8	35	47
JUP	34	4
UBB	30	15
CLTC	28	17
TPM3	28	8
PSMD2	27	4
MYO1D	24	5
DSG2	24	0
PABPC1	24	4
EEF2	23	0
PCM1	23	0
EIF4A1	21	2
MCM7	20	0
TPM4	19	7
CDK1	19	0
MME	19	0
RAB11FIP1	19	5
TPM1	19	9
BRAT1	18	1
MAGED1	18	2
EPPK1	17	0
PRDX4	17	10
USP54	16	5

	Total spectra counts	
Protein ID	**DMSO normalized to IgG**	**EPZ normalized to IgG**
HSPD1	16	2
RACK1	16	0
PSMC4	14	3
GCN1	14	3
SQSTM1	13	6
PSMC1	13	2
CCT6A	12	4
CCDC51	12	5
XRN2	12	3
HSPA5	11	13
DDX3X	11	5
CAPZA1	10	0
MYO1C	10	3
SLC25A6	10	2
HSPA9	10	2
FOLH1	10	3
SLC25A5	9	11
DSP	9	0
HSPB1	9	3
PRKD1	9	0
RPL18A	9	8
KPNA2	9	0
HNRNPH1	9	4
PPP1CB	9	0
HAX1	9	2
AP1M2	9	1
NCOR1	9	0
PSMA7	9	0
NEK9	9	3
MYL6	8	21
FLII	8	2
ATP5A1	8	4
PSMD1	8	2
FLOT1	8	0
ENO1	8	3
ATP6V1A	8	4
MYO5B	8	2
PSMD11	8	0
CEP131	8	0
GNAI3	8	0
RPS11	7	1
NUP188	7	4
PSMC3	7	0
CKB	7	0
TOM1	7	0
GAPDH	7	3
RAN	7	1
PSMC2	7	0

	Total spectra counts	
Protein ID	**DMSO normalized to IgG**	**EPZ normalized to IgG**
ABCD3	7	8
PSMC6	7	1
MARC1	7	0
SEC23B	7	0
AAAS	7	3
UBXN6	7	0
ILF2	7	0
PKM	7	0
MYO5C	6	5
ACTR3	6	2
TKT	6	1
FLOT2	6	3
RPS23	6	3
SUMO2	6	0
HPS6	6	0
TCP1	6	5
AHCYL1	6	1
FADS2	6	3
PSMB5	6	1
MCM2	6	1
PSMC5	6	0
PSMD7	6	0
RRM2	6	0
PSMA2	5	0
TJP1	5	0
KRT3	5	9
CALM1	5	1
RPL24	5	4
GLUL	5	0
GDF15	5	0
DYNC1H1	5	3
GNB2	5	1
TELO2	5	1
CAPZA2	5	0
FAM83D	5	0
TOM1L2	5	0
GDI1	5	3
PSMB4	5	0
GNAI1	5	0
TSEN34	5	0
PSMA6	5	0
LRRC58	5	0
HNRNPH3	5	0
HIST1H4A	4	2
RPS8	4	3
RNF213	4	3
ACSL3	4	0
PHB2	4	4

	Total spectra counts	
Protein ID	**DMSO normalized to IgG**	**EPZ normalized to IgG**
LDHA	4	2
TARDBP	4	0
TOLLIP	4	0
ARPC1A	4	0
MYCBP2	4	0
KMT2D	4	1
RPS3	4	0
UBR5	4	0
PSMD14	4	0
CPSF7	4	4
CSE1L	4	1
HNRNPU	4	0
RPS6	4	2
LARP1	4	2
PSMD6	4	0
PGAM5	4	0
CDC42BPA	4	0
CCT4	4	0
RPS6KA1	4	1
RPL23	4	2
MLF2	4	2
APRT	4	1
PSMA1	4	1
CYFIP1	4	0
EXPH5	4	0
SNRNP200	4	0
ACY1	4	1
TXNRD1	4	0
DHX15	4	0
EFTUD2	4	0
SF3B1	4	0
MMS19	4	0
CSNK2A1	4	0
PRPF8	4	0
VPS51	4	0
RBM14	4	0
POLD1	4	0
YES1	4	0
MYO1B	3	2
LIMCH1	3	8
CAPZB	3	3
GNAS	3	3
TMOD3	3	0
PSMD12	3	0
HUWE1	3	0
TRIM25	3	0
RPS5	3	1
RPS4X	3	0

	Total spectra counts	
Protein ID	**DMSO normalized to IgG**	**EPZ normalized to IgG**
GNB1	3	0
CAND1	3	0
GRSF1	3	2
FAF2	3	2
MAOA	3	4
PSMB1	3	3
RPL27A	3	0
ASNS	3	0
RNF31	3	0
RPL3	3	2
DPY30	3	2
RPS7	3	1
DHX9	3	1
EIF3I	3	0
SEC13	3	2
SFPQ	3	2
RPS16	3	0
METTL13	3	0
PSMD3	3	0
NUBP2	3	0
ME1	3	0
PAICS	3	0
FANCG	3	0
TRIB3	3	0
G3BP1	3	0
DPH1	3	0
EIF2S1	3	0
PSMD13	3	0
TKFC	3	0
TYSND1	3	0
HNRNPM	3	0
UBAP2L	3	0
AURKB	3	0
RPS4Y1	3	0
FXR1	3	0
AP5B1	3	0
KIAA1217	3	0
PHGDH	2	0
H2AFJ	2	0
FARSA	2	1
ALDH16A1	2	1
ATP5B	2	1
IPO4	2	2
CTNNA1	2	1
ACTN4	2	0
VDAC1	2	0
POLR2H	2	0
YWHAZ	2	2

	Total spectra counts	
Protein ID	**DMSO normalized to IgG**	**EPZ normalized to IgG**
RAB10	2	0
TRAF4	2	1
GTF2H2C	2	0
RAP1A	2	0
TAF15	2	0
RPS9	2	0
RPS13	2	0
TRIM32	2	0
PRAME	2	0
PRKAG1	2	0
BAG6	2	0
PARP12	2	0
PSMB2	2	0
TONSL	2	0
DHFR	2	0
NVL	2	0
RPLP0P6	2	0
TBL1XR1	2	0
NPRL3	2	0
TEDC1	2	0
H3F3A	1	0
VPS13C	1	2
MYO18A	1	1
CGN	1	0
PSMB3	1	0
PCBP2	1	0
HRNR	1	0
ACTR2	1	0
CNDP2	1	0
MAGEA2	1	0
LMNB1	0	1
FN1	0	28
HIST1H2BC	0	1
MYL12B	0	3
H2AFY	0	3
SSFA2	0	4
TAX1BP1	0	1
UGT2B11	0	4

However, neither HECTD4 ubiquitin ligase function nor its interaction with AR has been established. By employing co-immunoprecipitation assays in cells expressing Flag-AR and Halotag-HECTD4, we observed robust interaction between HECTD4 and AR (**Figure 3.20 a**).

Furthermore, HECTD4 expression increased levels of ubiquitin conjugated AR protein (**Figure 3.20 b**). We used similar co-immunoprecipitation assays to show that in 293T cells expressing both MYC-tagged-MYCBP2 and Flag-AR, MYCBP2 is pulled down with the Flag-AR. Also, MYCBP2 expression increased levels of Ubiquinated AR in the cells, indicating that MYCBP2 is a novel E3 ligases targeting AR. (**Figure 3.20 c**).

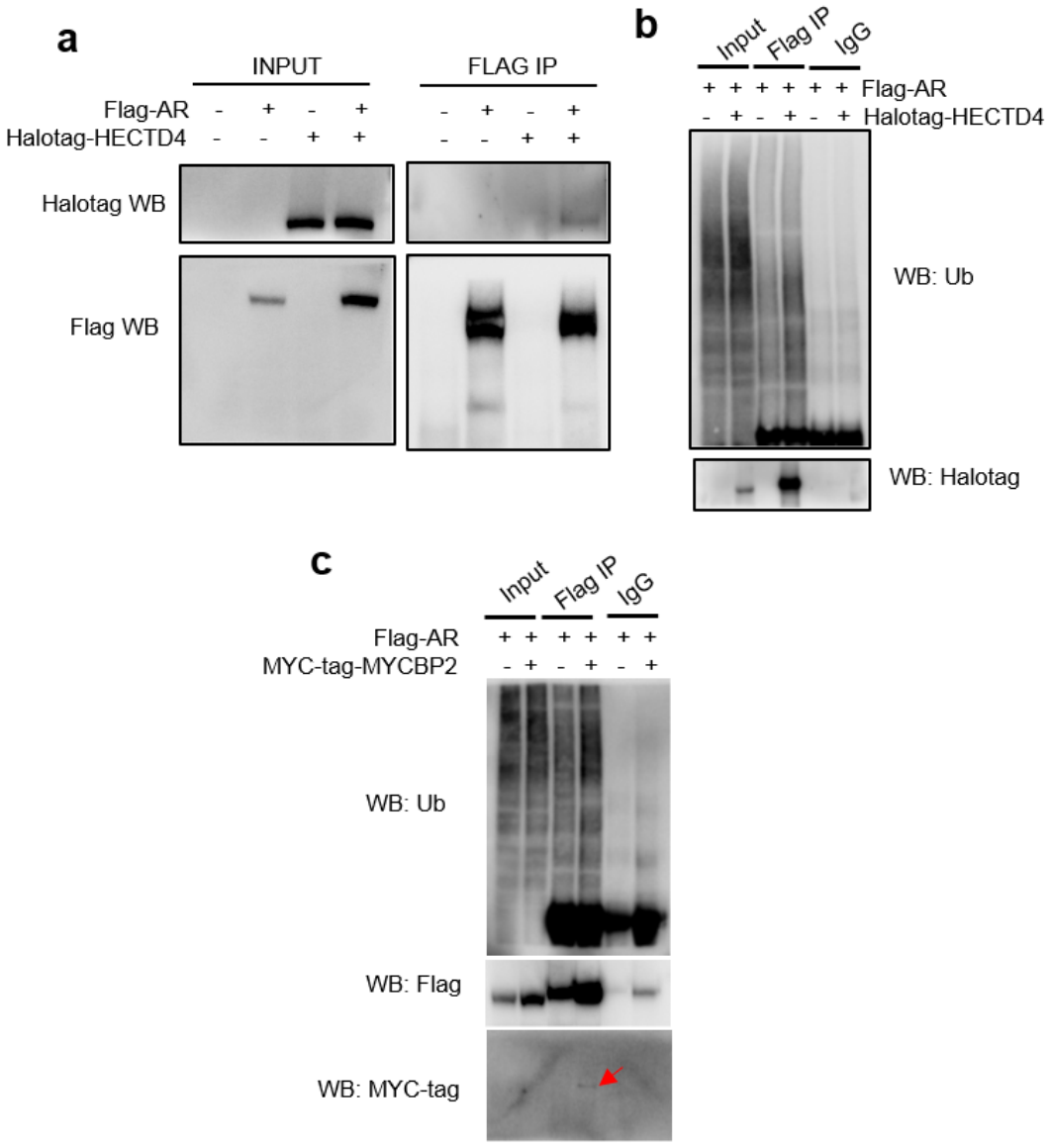

Figure 3.20: HECTD4 and MYCBP2 bind AR and play role in its ubiquitination.

(a) Co-immunoprecipitation assays performed with Flag-AR pulldown followed by western blot analysis in 293T cells transfected with Flag-AR and Halotag-HECTD4 constructs after 2 days. (h) Flag-AR pulldown followed by Ubiquitin western analysis in 293T cells transfected with both Flag-AR and HECTD4 constructs. (c) Co-immunoprecipitation assays performed with Flag-

AR pulldown followed by MYC-tag and Ubiquitin western blot analysis in 293T cells transfected with Flag-AR and Halotag-HECTD4 constructs after 2 days.

In sum, these results show that DOT1L inhibition coordinates loss of AR and MYC protein stability by modulating the expression of several E3 ligases.

3.6. MYC regulates E3 ligase expression

DOT1L inhibition selectively dysregulates the expression of HECTD4, MYCBP2 and TRIM49 E3 ligases in AR-positive but not AR-negative cells. To explore a direct role for AR in the regulation of these genes, we assessed their response to AR activation by DHT and AR inhibition by ENZA treatment (**Figure 3.21 a**). HECTD4 and TRIM49 did not behave as AR target genes, while MYCBP2 behaved like an AR stimulated target gene. Hence, these results did not recapitulate the expression profile seen upon EPZ treatment. We then examined the role of MYC in regulating the E3 ligases, including in the context of AR inhibition. Remarkably, depletion of MYC by siRNA in LNCaP cells resulted in upregulation of HECTD4 and MYCB2 both in the presence and absence of AR inhibitor enzalutamide (**Figure 3.21 b**). TRIM49 levels are upregulated upon MYC knockdown but suppressed in the presence of enzalutamide (**Figure 3.21 c**). The expression changes in HECTD4, MYCBP2 and TRIM49 observed upon MYC and AR inhibition in these experiments are remarkably similar to the changes seen after EPZ treatment. In AR-negative PC3 cells, MYC knockdown led to upregulation of HECTD4 and MYCBP2 and downregulation of TRIM49. These observations combined with the earlier results presented imply that EPZ-mediated loss of MYC expression triggers an increase in MYCBP2 and HECTD4 which then results in the loss of AR and MYC protein levels that ultimately lead to prostate cancer cell death. Since this pathway seems to be restricted to AR expressing prostate cancer cells, we asked the question – Why is MYC expression decreased in LNCaP cells but not PC3 cells? A simple model to explain this observation is that DOT1L and AR co-regulate MYC gene expression in AR positive cells.

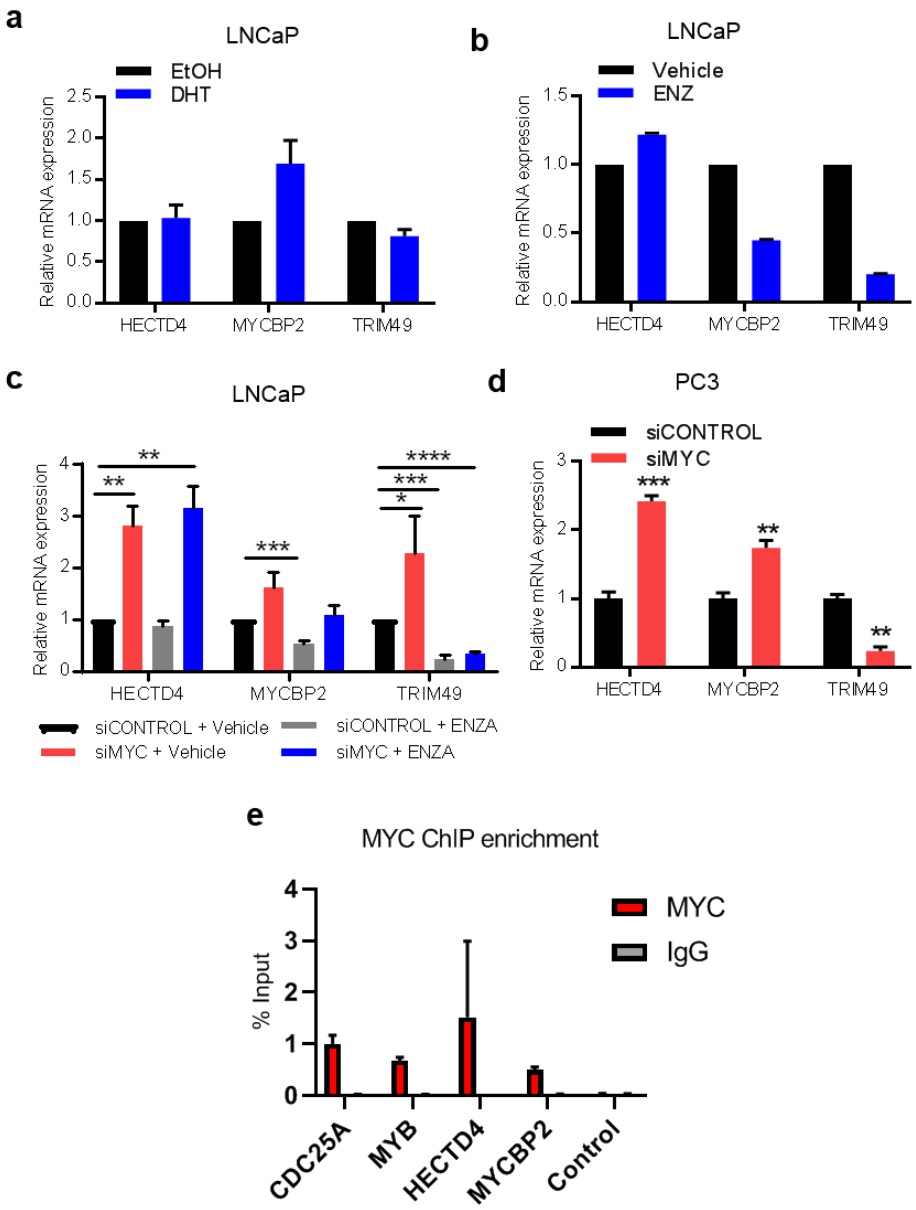

Figure 3.21: HECTD4 and MYCBP2 are MYC repressed targets.

(a) mRNA expression of HECTD4, MYCBP2 and TRIM49 in LNCaP treated with Control or 10nM DHT for 24 hours in Charcoal stripped media (b) mRNA expression of HECTD4, MYCBP2 and TRIM49 in LNCaP treated with Control or 20uM ENZA for 24 hours. (c) mRNA

expression of HECTD4, MYCBP2 and TRIM49 in LNCaP cells transfected with Control or MYC targeting siRNA (2 days) followed by treatment with Vehicle or 20uM ENZA (2 days). (d) mRNA expression of HECTD4, MYCBP2 and TRIM49 in PC3 cells transfected with Control or MYC targeting siRNA for 2 days. (e) MYC enrichment at the HECTD4 and MYCBP2 promoters in LNCaP cells with CDC25A and MYB as positive controls.

3.7. DOT1L and AR co-regulate MYC expression through a distal enhancer

To determine the role of DOT1L and AR in regulating MYC expression we first examined the H3K79me2 landscape at the MYC gene locus before and after EPZ treatment. H3K79me2 levels across the MYC gene were uniformly reduced in both LNCaP and PC3 cells. Examination of AR binding at the MYC locus revealed an AR bound enhancer 20 Kb downstream of the MYC gene that has been proposed to regulate MYC expression (**Figure 3.22**). Analysis of H3K79me2 ChIP-seq data showed a broad H3K79me2 peak at this site in LNCaP cells that is lost after EPZ treatment. Enhancer marks including H3K27ac overlapped with H3K79me2 and AR peaks at this site.

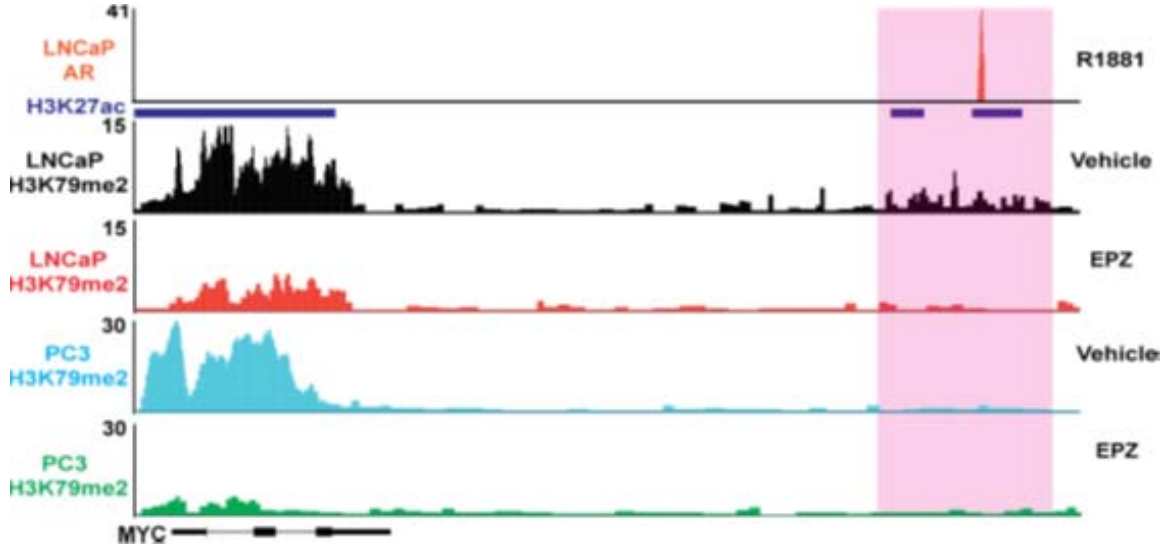

Figure 3.22: A downstream MYC enhancer is marked by H3K79me2 and is bound by AR. ChIP-seq tracks of AR in LNCaP cells treated with R1881, H3K27ac in LNCaP cells, H3K79me2 in Vehicle and EPZ treated LNCaP cells (EPZ 1uM, 8 days), H3K79me2 in Vehicle and EPZ treated PC3 cells (EPZ 1uM, 8 days) (top - bottom).

We confirmed AR binding to this enhancer by ChIP-qPCR in LNCaP cells treated with DHT or enzalutamide (**Figure 3.23 a**). We also found that MYC expression was decreased upon ENZA treatment (**Figure 3.23** b). Moreover, DOT1L overexpression in LNCaP cells rescued the loss of MYC expression seen upon ENZA treatment (**Figure 3.23 c**). These results imply that DOT1L and AR cooperate together to regulate MYC expression.

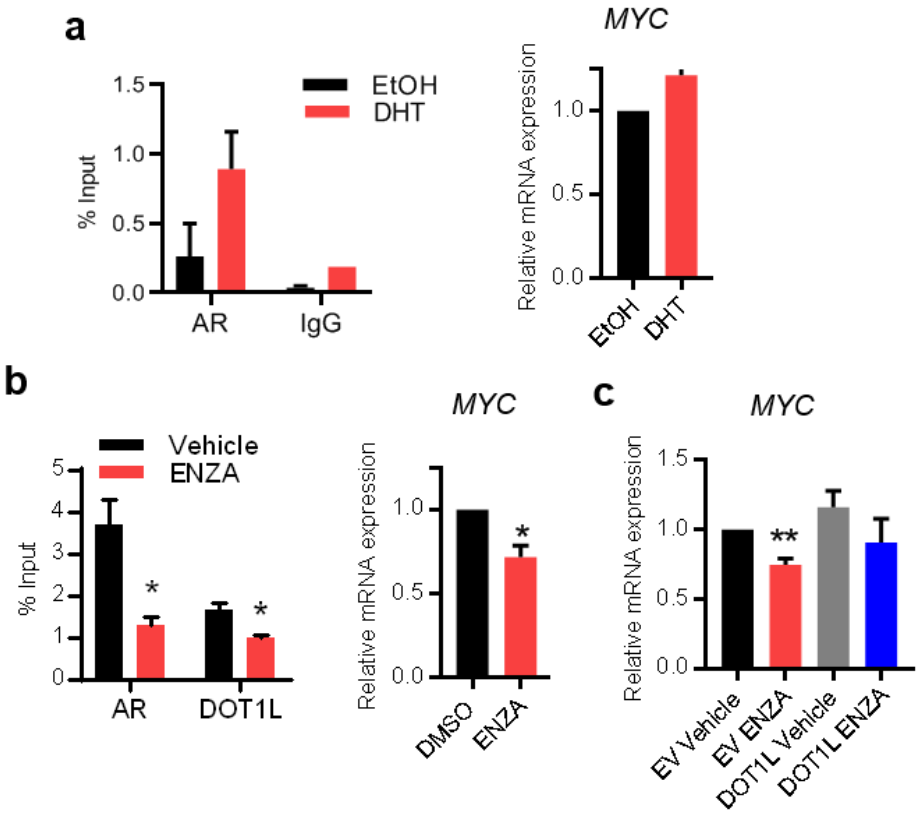

Figure 3.23: AR and DOT1L bind to the MYC enhancer.

(a) AR enrichment at MYC enhancer in LNCaP cells treated with Vehicle or DHT for 3 hours after 24 hours of hormone starvation in Charcoal stripped medium. (b) MYC expression in LNCaP cells treated with with Vehicle or DHT for 24 hours after 24 hours of hormone starvation in Charcoal stripped medium. (c) AR and DOT1L enrichment at MYC enhancer in LNCaP cells

treated with Vehicle or ENZA or 24 hours (d) MYC expression in LNCaP cells treated with MYC enhancer in LNCaP cells treated with Vehicle or ENZA for 24 hours.

We then performed ChIP-qPCR to assess the effect of DOT1L inhibition on enrichment of AR, DOT1L, enhancer marks H3K27ac and H3K4me2 as well as RNA Polymerase II (Pol II) (**Figure 3.24 a**). EPZ treatment of LNCaP cells led to a reduction in the recruitment of AR, DOT1L and Pol II as well as a reduction in H3K27ac, H3K4me2 and H3K79me2 marks at the MYC enhancer. These results indicate that DOT1L is required for AR enrichment at this distal MYC enhancer in order to regulate MYC expression in AR-positive cells. Next, we examined if AR overexpression can rescue the loss of enhancer marks and MYC mRNA expression after DOT1L inhibition. To this end, we performed ChIP-qPCR after EPZ treatment in control and AR-overexpressing LNCaP cells (**Figure 3.24 b**). In addition to increased enrichment of AR itself at the enhancer, we observed significantly higher enrichment of DOT1L, H3K79me2, H3K4me2, H3K27ac and Pol II in the AR overexpressing cells when compared to the control cells (**Figure 3.24 c**). Moreover, AR overexpression was able to rescue the loss of binding of DOT1L and Pol II as well as the loss of enhancer marks caused by EPZ treatment. Importantly, the reduction in MYC mRNA expression caused by EPZ treatment was also rescued in the AR overexpressing cells (**Figure 3.24 d**). Functionally, AR overexpressing LNCaP cells exhibited increased resistance to EPZ treatment (**Figure 3.24 e**). Overall, these results indicate that DOT1L and AR coregulation of MYC expression via a distal enhancer dictate sensitivity to DOT1L inhibition in prostate cancer cells.

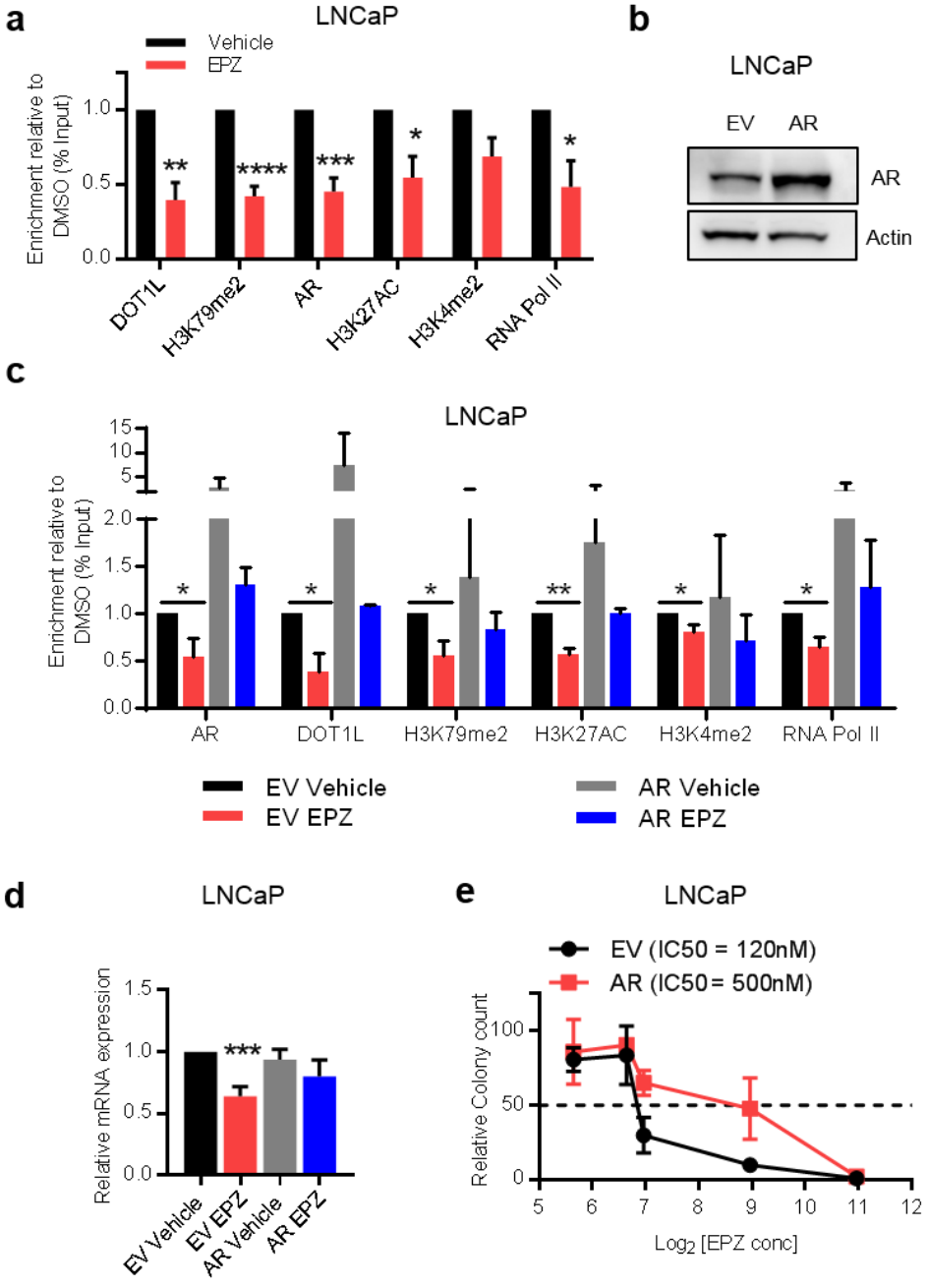

Figure 3.24: DOT1L is required at the MYC enhancer.

(a) Enrichment of AR, DOT1L, H3K79me2, H3K27ac, H3K4me2 and RNA Pol II at the MYC enhancer in LNCaP cells treated with Vehicle or 1uM EPZ for 8 days. (b) AR protein expression

in LNCaP cells transduced with EV or wild-type AR (c) MYC expression in LNCaP cells transduced with EV or AR and treated with Vehicle or EPZ for 8 days. (d) Enrichment of AR, DOT1L, H3K79me2, H3K27ac, H3K4me2 and RNA Pol II at the MYC enhancer in LNCaP cells transduced with EV or AR and treated with Vehicle or 1uM EPZ for 8 days. (e) Quantitation of colony formation assays in LNCaP cells transduced with EV or AR and treated with Vehicle or 1uM EPZ for 12 days.

Finally, to show that this enhancer is critical for MYC expression, we used CRISPR-Cas9 technology to knockout the AR binding sequence in the MYC enhancer by using a guide RNA pair flanking the AR binding site (**Figure 3.25 a)**. These gRNAs were cotransfected into LNCaP and PC3 cells expressing CRISPR-Cas9. We observed that after transfection, LNCaP cells with the transfected gRNAs experienced a substantial loss in viability whereas PC3 cells were virtually unaffected (**Figure 3.25 b)**. Successful CRISPR-Cas9–mediated deletion in a pooled population was confirmed through PCR of genomic DNA which showed a wild-type and a shorter, deleted PCR product (**Figure 3.25 c)**. Therefore, we concluded that the downstream enhancer is essential for MYC expression by AR and DOT1L.

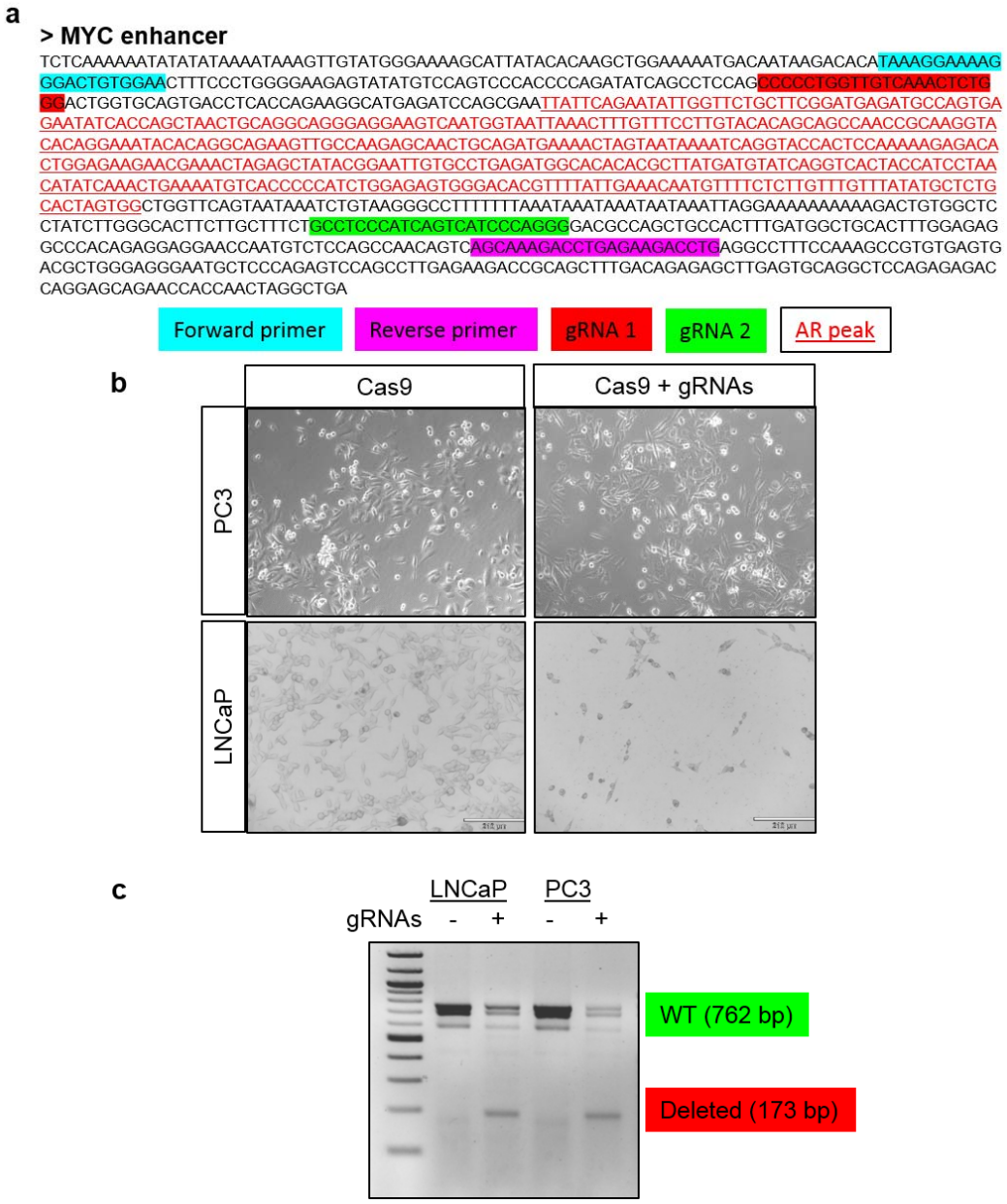

Figure 3.25: Deletion of AR binding sites at MYC enhancer impairs LNCaP cell viability. (a) The sequence of sgRNAs targeting sites on the AR binding region in AR enhancer are highlighted in red/green. Sequences of primers used for genomic DNA PCR are in blue/pink. The AR binding peak is underlined. (b) LNCaP cells and PC3 cells were infected with Cas9 and

then transfected with sgRNA1 and sgRNA2 and observed after 5 days. (c) Pooled populations were analyzed by genomic DNA PCR for CRISPR-Cas9–mediated deletion leading to a wild-type and a deleted band after 5 days.

3.8. An AR positive PDX model is sensitive to DOT1L inhibition

To further demonstrate that DOT1L inhibition is effective in AR+ positive prostate cancer, we used a patient-derived xenograft (PDX) human prostate cancer model, TM00298. We first developed in vitro PDX organoids to better recapitulate *in vivo* conditions. These organoids were treated with DOT1L inhibitors and allowed to grow for 12 days similar to the 2D cell line models. We observed that DOT1L inhibition induced a substantial loss in 3D cell viability (**Figure 3.26 a)**. Moreover, we confirmed that DOT1L inhibition led to a loss in both AR and MYC protein levels (**Figure 3.26 b)**. We also infected dissociated PDX cells with shControl or shDOT1L retrovirus and allowed them to form organoids. Again, we observed a dramatic loss in organoid viability after 12 days of treatment (**Figure 3.26 a)**. To confirm that MYC enhancer is active in this PDX model, we performed ChIP using PDX tumor tissue and checked the enrichment of H3K79me2 as well as other enhancer marks. We observed that similar to the LNCaP cell line, DOT1L and AR were enriched at the downstream enhancer along with other active marks (**Figure 3.26 c)**.

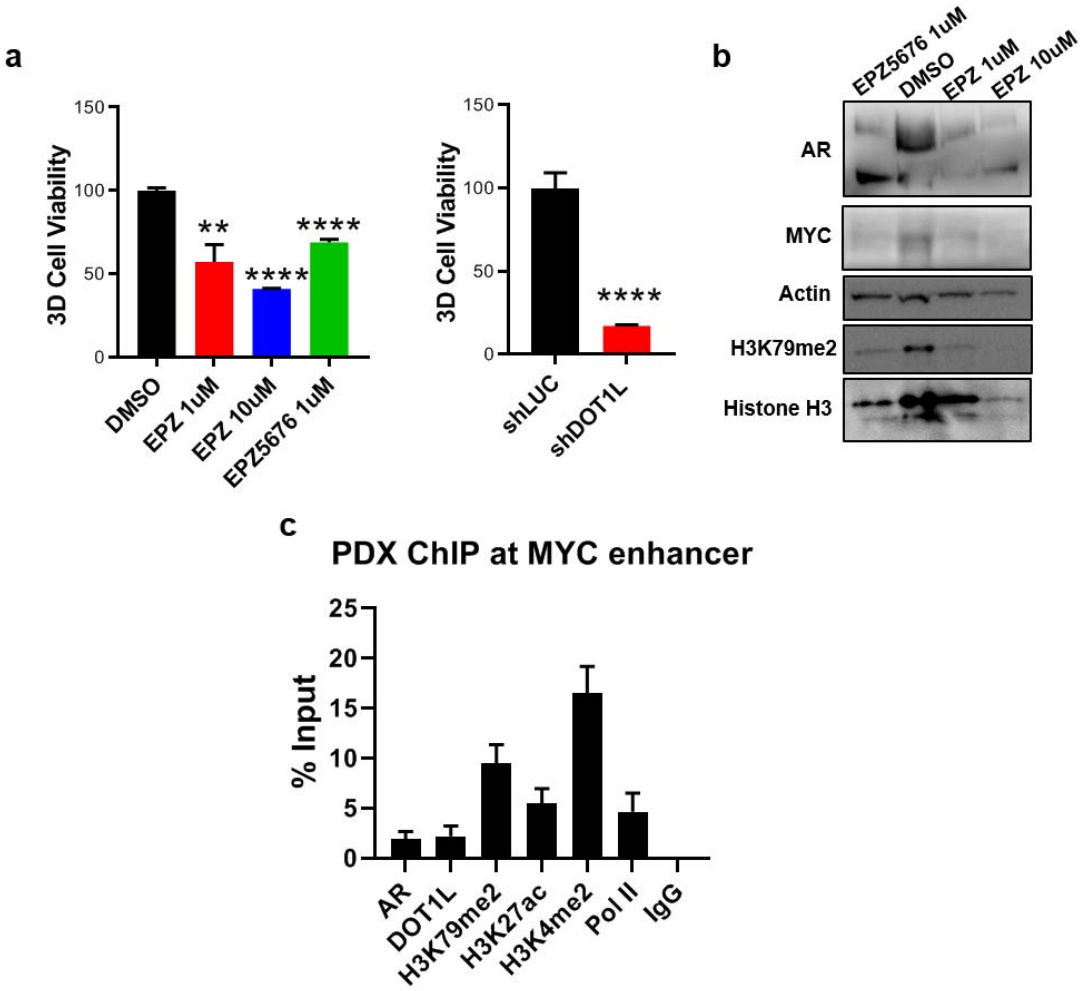

Figure 3.26: A PDX model of prostate cancer is sensitive to DOT1L inhibition.

(a) PDX organoids were treated for 12 days with DMSO, EPZ 1 or 10uM or EPZ5676 1uM (left). PDX cells were infected with shControl or shDOT1L virus and allowed to grow into organoids (right). (b) Western blot analysis of PDX organoids treated with DMSO or DOT1L inhibitors for 8 days. (c) Enrichment of AR, DOT1L, H3K79me2, H3K27ac, H3K4me2, RNA Pol II and IgG at the MYC enhancer in PDX tumors.

CHAPTER 4: DISCUSSION

In this study we have identified DOT1L as a promising therapeutic target whose inhibition selectively impairs the viability of AR-positive prostate cancer. We found pervasive upregulation of DOT1L expression in multiple cancers, including prostate cancer where high expression correlates with poor disease-free survival in multiple datasets. By targeting DOT1L using small molecule inhibitors and shRNA constructs *in vitro* and *in vivo*, we have shown that growth of AR expressing cells is selectively inhibited when compared to AR negative prostate cancer cells. We found that H3K79 methylation is severely inhibited upon DOT1L inhibition or knockdown in both AR positive and AR negative cells. Our findings indicate that while some H3K79me2 enriched sites are shared between the two, a majority are unique and correlate with transcriptional programs specific to each cell type. This study is also the first to shed light on the H3K79me2 landscape of AR positive and AR negative prostate cancer cells.

We found that the AR pathway is inhibited upon DOT1L loss and this was due to loss of protein stability. Similar to AR, MYC regulated pathways were also repressed due to shortened MYC protein half-life. We identified the E3 ligases responsible for AR and MYC protein loss as HECTD4, MYCBP2 and TRIM49. HECTD4 and MYCBP2 target AR and MYC for degradation while TRIM49 appears to promote AR and MYC stability. Other HECT domain containing ligases like NEDD4 have been known to target AR and MYC (205-207), however no targets are known for HECTD4. MYCBP2, on the other hand has been previously described as a MYC

binding E3 ligase. We have also identified a third novel ubiquitin ligase TRIM49 that may be involved in stabilizing AR and MYC protein. Very little is known about TRIM49, but other TRIM family members have been shown to play important roles in oncogenesis, especially in the prostate(208-210). We have shown that these E3 ligases in turn are regulated by MYC in a negative feedback loop.

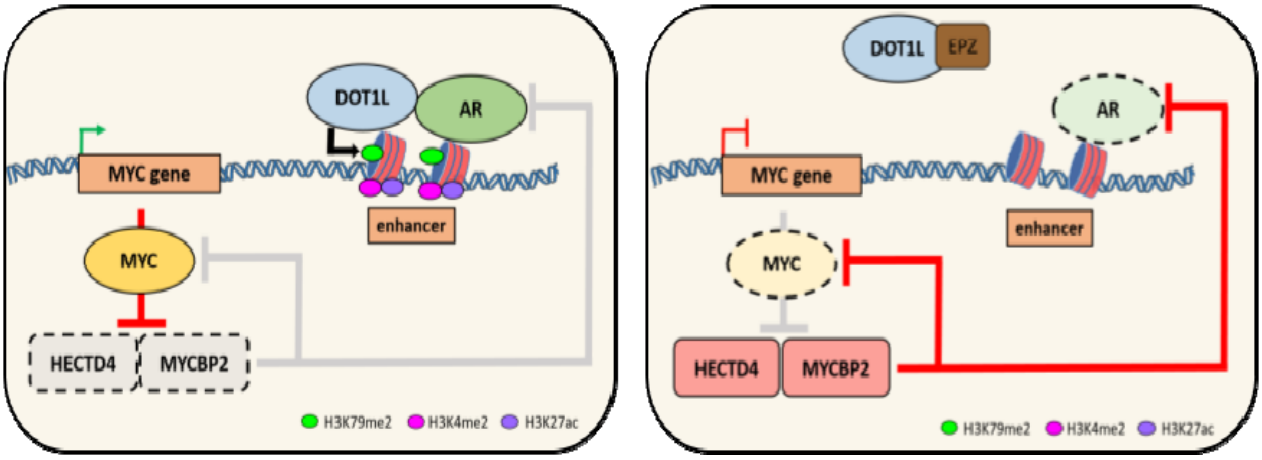

Figure 4.1. Graphical summary of DOT1L dependent regulation of MYC expression and its association with AR and MYC protein stability.

In cancer cells, DOT1L and AR cooperate at the MYC enhancer to regulate MYC expression. MYC expression leads to repression of the E3 ligases HECTD4 and MYCBP2, that can target both AR and MYC. When DOT1L is inhibited, MYC expression is lost leading to an upregulation of MYCBP2 and HECTD4 which further degrade MYC and AR proteins leading to

further MYC repression due to the negative forward loop. Dashed lines represent decreased abundance. Grey lines represent inactive pathways.

The basis for the increased sensitivity of AR-positive prostate cancer to DOT1L inhibition is the coregulation of MYC by DOT1L and AR at a distal enhancer active only in AR-positive prostate cancer cells. Our results showed that DOT1L inhibition suppresses both AR and MYC pathways via a negative feed forward loop (**Figure 4.1**). We showed that AR and DOT1L are bound to this enhancer and regulate its function. When DOT1L is inhibited, its displacement from the enhancer along with loss of AR and H3K79me2 at this site suppresses *MYC* expression. MYC in turn represses the expression of ubiquitin ligases, HECTD4 and MYCBP2 that promote AR and MYC protein degradation, further suppressing MYC and AR in a feed forward loop. We have also shown that increased AR expression can rescue the effects of DOT1L inhibition on cellular viability by restoring *MYC* expression. While DOT1L's role at enhancers is less known, a recent study (211) offered a model similar to ours wherein DOT1L mediated H3K79 methylation is critical for enhancer function in leukemia cells.

In summary, our studies indicate that DOT1L inhibition is a viable and more importantly, a selective therapeutic strategy in prostate cancer. We have shown that DOT1L's cooperation with AR, a prostate lineage factor to regulate MYC, an oncogenic driver of prostate tumorigenesis provides a specific cellular context for targeting prostate cancer cells. Indeed we have shown that CRPC cells including AR variant AR-V7 expressing cells as well as enzalutamide resistant

prostate cancer cells are sensitive to DOT1L inhibition. Currently, DOT1L inhibitors are being tested in the clinic particularly in leukemia (212). A phase I study of pinometostat (EPZ-5676) in adult patients with advanced acute leukemias, particularly MLL showed safety with modest efficacy as a single agent when dosed by continuous intravenous infusion in 28-day cycles. DOT1L inhibitors, particularly agents with improved pharmacokinetic properties warrant testing in prostate cancer.

REFERENCES

1. Mohammad HP, Barbash O, Creasy CL. Targeting epigenetic modifications in cancer therapy: erasing the roadmap to cancer. Nat Med. 2019;25(3):403-18.

2. Feng Q, Wang H, Ng HH, Erdjument-Bromage H, Tempst P, Struhl K, et al. Methylation of H3-lysine 79 is mediated by a new family of HMTases without a SET domain. Curr Biol. 2002;12(12):1052-8.

3. Huyen Y, Zgheib O, Ditullio RA, Jr., Gorgoulis VG, Zacharatos P, Petty TJ, et al. Methylated lysine 79 of histone H3 targets 53BP1 to DNA double-strand breaks. Nature. 2004;432(7015):406-11.

4. Okada Y, Feng Q, Lin Y, Jiang Q, Li Y, Coffield VM, et al. hDOT1L links histone methylation to leukemogenesis. Cell. 2005;121(2):167-78.

5. Bitoun E, Oliver PL, Davies KE. The mixed-lineage leukemia fusion partner AF4 stimulates RNA polymerase II transcriptional elongation and mediates coordinated chromatin remodeling. Hum Mol Genet. 2007;16(1):92-106.

6. Jones B, Su H, Bhat A, Lei H, Bajko J, Hevi S, et al. The histone H3K79 methyltransferase Dot1L is essential for mammalian development and heterochromatin structure. PLoS Genet. 2008;4(9):e1000190.

7. Steger DJ, Lefterova MI, Ying L, Stonestrom AJ, Schupp M, Zhuo D, et al. DOT1L/KMT4 recruitment and H3K79 methylation are ubiquitously coupled with gene transcription in mammalian cells. Mol Cell Biol. 2008;28(8):2825-39.

8. Daigle SR, Olhava EJ, Therkelsen CA, Majer CR, Sneeringer CJ, Song J, et al. Selective killing of mixed lineage leukemia cells by a potent small-molecule DOT1L inhibitor. Cancer Cell. 2011;20(1):53-65.

9. Miller KD, Nogueira L, Mariotto AB, Rowland JH, Yabroff KR, Alfano CM, et al. Cancer treatment and survivorship statistics, 2019. CA Cancer J Clin. 2019.

10. Shen HC, Balk SP. Development of androgen receptor antagonists with promising activity in castration-resistant prostate cancer. Cancer Cell. 2009;15(6):461-3.

11. Payton S. Prostate cancer: New insight into mechanisms of castration resistance. Nat Rev Urol. 2010;7(11):590.

12. Feldman BJ, Feldman D. The development of androgen-independent prostate cancer. Nat Rev Cancer. 2001;1(1):34-45.

13. Heidenreich A, Pfister D, Merseburger A, Bartsch G, German Working Group on Castration-Resistant Prostate C. Castration-resistant prostate cancer: where we stand in 2013 and what urologists should know. Eur Urol. 2013;64(2):260-5.

14. Joseph JD, Lu N, Qian J, Sensintaffar J, Shao G, Brigham D, et al. A clinically relevant androgen receptor mutation confers resistance to second-generation antiandrogens enzalutamide and ARN-509. Cancer Discov. 2013;3(9):1020-9.

15. Shen MM, Abate-Shen C. Molecular genetics of prostate cancer: new prospects for old challenges. Genes Dev. 2010;24(18):1967-2000.

16. Grasso CS, Cani AK, Hovelson DH, Quist MJ, Douville NJ, Yadati V, et al. Integrative molecular profiling of routine clinical prostate cancer specimens. Ann Oncol. 2015;26(6):1110-8.

17. DePrimo SE, Diehn M, Nelson JB, Reiter RE, Matese J, Fero M, et al. Transcriptional programs activated by exposure of human prostate cancer cells to androgen. Genome Biol. 2002;3(7):RESEARCH0032.

18. Claessens F, Helsen C, Prekovic S, Van den Broeck T, Spans L, Van Poppel H, et al. Emerging mechanisms of enzalutamide resistance in prostate cancer. Nat Rev Urol. 2014;11(12):712-6.

19. Antonarakis ES, Lu C, Wang H, Luber B, Nakazawa M, Roeser JC, et al. AR-V7 and resistance to enzalutamide and abiraterone in prostate cancer. N Engl J Med. 2014;371(11):1028-38.

20. Li Y, Chan SC, Brand LJ, Hwang TH, Silverstein KA, Dehm SM. Androgen receptor splice variants mediate enzalutamide resistance in castration-resistant prostate cancer cell lines. Cancer Res. 2013;73(2):483-9.

21. Barfeld SJ, Urbanucci A, Itkonen HM, Fazli L, Hicks JL, Thiede B, et al. c-Myc Antagonises the Transcriptional Activity of the Androgen Receptor in Prostate Cancer Affecting Key Gene Networks. Ebiomedicine. 2017;18:83-93.

22. Hawksworth D, Ravindranath L, Chen Y, Furusato B, Sesterhenn IA, McLeod DG, et al. Overexpression of C-MYC oncogene in prostate cancer predicts biochemical recurrence. Prostate Cancer Prostatic Dis. 2010;13(4):311-5.

23. Bernard D, Pourtier-Manzanedo A, Gil J, Beach DH. Myc confers androgen-independent prostate cancer cell growth. J Clin Invest. 2003;112(11):1724-31.

24. Kokontis J, Takakura K, Hay N, Liao S. Increased androgen receptor activity and altered c-myc expression in prostate cancer cells after long-term androgen deprivation. Cancer Res. 1994;54(6):1566-73.

25. Robinson D, Van Allen EM, Wu YM, Schultz N, Lonigro RJ, Mosquera JM, et al. Integrative Clinical Genomics of Advanced Prostate Cancer. Cell. 2015;162(2):454.

26. Rebello RJ, Pearson RB, Hannan RD, Furic L. Therapeutic Approaches Targeting MYC-Driven Prostate Cancer. Genes (Basel). 2017;8(2).

27. Yang L, Lin C, Jin C, Yang JC, Tanasa B, Li W, et al. lncRNA-dependent mechanisms of androgen-receptor-regulated gene activation programs. Nature. 2013;500(7464):598-602.

28. Prensner JR, Sahu A, Iyer MK, Malik R, Chandler B, Asangani IA, et al. The IncRNAs PCGEM1 and PRNCR1 are not implicated in castration resistant prostate cancer. Oncotarget. 2014;5(6):1434-8.

29. Bray F, Ferlay J, Soerjomataram I, Siegel RL, Torre LA, Jemal A. Global cancer statistics 2018: GLOBOCAN estimates of incidence and mortality worldwide for 36 cancers in 185 countries. CA Cancer J Clin. 2018;68(6):394-424.

30. Surveillance E, and End Results Program (SEER). SEER Stat Fact Sheets: Prostate Cancer Accessed 2015 Feb 5.

31. Stamey TA, Kabalin JN, Ferrari M, Yang N. Prostate specific antigen in the diagnosis and treatment of adenocarcinoma of the prostate. IV. Anti-androgen treated patients. The Journal of urology. 1989;141(5):1088-90.

32. Stamey TA, Kabalin JN. Prostate specific antigen in the diagnosis and treatment of adenocarcinoma of the prostate. I. Untreated patients. The Journal of urology. 1989;141(5):1070-5.

33. Stamey TA, Yang N, Hay AR, McNeal JE, Freiha FS, Redwine E. Prostate-specific antigen as a serum marker for adenocarcinoma of the prostate. The New England journal of medicine. 1987;317(15):909-16.

34. Huggins C. Effect of Orchiectomy and Irradiation on Cancer of the Prostate. Annals of surgery. 1942;115(6):1192-200.

35. Farooqi AA, Sarkar FH. Overview on the complexity of androgen receptor-targeted therapy for prostate cancer. Cancer Cell Int. 2015;15:7.

36. Gao L, Schwartzman J, Gibbs A, Lisac R, Kleinschmidt R, Wilmot B, et al. Androgen receptor promotes ligand-independent prostate cancer progression through c-Myc upregulation. PloS one. 2013;8(5):e63563.

37. Mulholland DJ, Tran LM, Li Y, Cai H, Morim A, Wang S, et al. Cell autonomous role of PTEN in regulating castration-resistant prostate cancer growth. Cancer cell. 2011;19(6):792-804.

38. McNeal JE, Redwine EA, Freiha FS, Stamey TA. Zonal distribution of prostatic adenocarcinoma. Correlation with histologic pattern and direction of spread. Am J Surg Pathol. 1988;12(12):897-906.

39. Yoo YA, Roh M, Naseem AF, Lysy B, Desouki MM, Unno K, et al. Bmi1 marks distinct castration-resistant luminal progenitor cells competent for prostate regeneration and tumour initiation. Nat Commun. 2016;7:12943.

40. Choi N, Zhang B, Zhang L, Ittmann M, Xin L. Adult murine prostate basal and luminal cells are self-sustained lineages that can both serve as targets for prostate cancer initiation. Cancer Cell. 2012;21(2):253-65.

41. Wang ZA, Toivanen R, Bergren SK, Chambon P, Shen MM. Luminal Cells Are Favored as the Cell of Origin for Prostate Cancer. Cell Rep. 2014;8(5):1339-46.

42. Shen MM, Abate-Shen C. Molecular genetics of prostate cancer: new prospects for old challenges. Gene Dev. 2010;24(18):1967-2000.

43. Bluemn EG, Coleman IM, Lucas JM, Coleman RT, Hernandez-Lopez S, Tharakan R, et al. Androgen Receptor Pathway-Independent Prostate Cancer Is Sustained through FGF Signaling. Cancer Cell. 2017;32(4):474-+.

44. Taylor BS, Schultz N, Hieronymus H, Gopalan A, Xiao YH, Carver BS, et al. Integrative Genomic Profiling of Human Prostate Cancer. Cancer Cell. 2010;18(1):11-22.

45. Grasso CS, Wu YM, Robinson DR, Cao XH, Dhanasekaran SM, Khan AP, et al. The mutational landscape of lethal castration-resistant prostate cancer. Nature. 2012;487(7406):239-43.

46. Tomlins SA, Rhodes DR, Perner S, Dhanasekaran SM, Mehra R, Sun XW, et al. Recurrent fusion of TMPRSS2 and ETS transcription factor genes in prostate cancer. Science. 2005;310(5748):644-8.

47. Iljin K, Wolf M, Edgren H, Gupta S, Kilpinen S, Skotheim RI, et al. TMPRSS2 fusions with oncogenic ETS factors in prostate cancer involve unbalanced genomic rearrangements and are associated with HDAC1 and epigenetic reprogramming. Cancer Research. 2006;66(21):10242-6.

48. Lin CR, Yang LQ, Tanasa B, Hutt K, Ju BG, Ohgi K, et al. Nuclear Receptor-Induced Chromosomal Proximity and DNA Breaks Underlie Specific Translocations in Cancer. Cell. 2009;139(6):1069-83.

49. Haffner MC, Aryee MJ, Toubaji A, Esopi DM, Albadine R, Gurel B, et al. Androgen-induced TOP2B-mediated double-strand breaks and prostate cancer gene rearrangements. Nat Genet. 2010;42(8):668-U45.

50. Klezovitch O, Risk M, Coleman I, Lucas JM, Null M, True LD, et al. A causal role for ERG in neoplastic transformation of prostate epithelium. P Natl Acad Sci USA. 2008;105(6):2105-10.

51. Carver BS, Tran J, Gopalan A, Chen Z, Shaikh S, Carracedo A, et al. Aberrant ERG expression cooperates with loss of PTEN to promote cancer progression in the prostate. Nat Genet. 2009;41(5):619-24.

52. He WW, Sciavolino PJ, Wing J, Augustus M, Hudson P, Meissner PS, et al. A novel human prostate-specific, androgen-regulated homeobox gene (NKX3.1) that maps to 8p21, a region frequently deleted in prostate cancer. Genomics. 1997;43(1):69-77.

53. Abdulkadir SA, Magee JA, Peters TJ, Kaleem Z, Naughton CK, Humphrey PA, et al. Conditional loss of Nkx3.1 in adult mice induces prostatic intraepithelial neoplasia. Mol Cell Biol. 2002;22(5):1495-503.

54. Asatiani E, Huang WX, Wang A, Ortner ER, Cavalli LR, Haddad BR, et al. Deletion, methylation, and expression of the NKX3.1 suppressor gene in primary human prostate cancer. Cancer Research. 2005;65(4):1164-73.

55. Bhatia-Gaur R, Donjacour AA, Sciavolino PJ, Kim M, Desai N, Young P, et al. Roles for Nkx3.1 in prostate development and cancer. Gene Dev. 1999;13(8):966-77.

56. Ouyang X, DeWeese TL, Nelson WG, Abate-Shen C. Loss-of-function of Nkx3.1 promotes increased oxidative damage in prostate carcinogenesis. Cancer Research. 2005;65(15):6773-9.

57. Wang SI, Parsons R, Ittmann M. Homozygous deletion of the PTEN tumor suppressor gene in a subset of prostate adenocarcinomas. Clinical Cancer Research. 1998;4(3):811-5.

58. Kim MJ, Cardiff RD, Desai N, Banach-Petrosky WA, Parsons R, Shen MM, et al. Cooperativity of Nkx3.1 and Pten loss of function in a mouse model of prostate carcinogenesis. P Natl Acad Sci USA. 2002;99(5):2884-9.

59. Kim J, Eltoum IEA, Roh M, Wang J, Abdulkadir SA. Interactions between Cells with Distinct Mutations in c-MYC and Pten in Prostate Cancer. Plos Genet. 2009;5(7).

60. Mulholland DJ, Dedhar S, Wu H, Nelson CC. PTEN and GSK3 beta: Key regulators of progression to androgen- independent prostate cancer. Oncogene. 2006;25(3):329-37.

61. Shen MM, Abate-Shen C. Pten inactivation and the emergence of androgen-independent prostate cancer. Cancer Research. 2007;67(14):6535-8.

62. Taplin ME, Bubley GJ, Shuster TD, Frantz ME, Spooner AE, Ogata GK, et al. Mutation of the androgen-receptor gene in metastatic androgen-independent prostate cancer. The New England journal of medicine. 1995;332(21):1393-8.

63. Visakorpi T, Hyytinen E, Koivisto P, Tanner M, Keinanen R, Palmberg C, et al. In vivo amplification of the androgen receptor gene and progression of human prostate cancer. Nat Genet. 1995;9(4):401-6.

64. Birrell SN, Hall RE, Tilley WD. Role of the androgen receptor in human breast cancer. Journal of mammary gland biology and neoplasia. 1998;3(1):95-103.

65. Miller WR, Telford J, Dixon JM, Hawkins RA. Androgen receptor activity in human breast cancer and its relationship with oestrogen and progestogen receptor activity. European journal of cancer & clinical oncology. 1985;21(4):539-42.

66. Boehmer AL, Brinkmann AO, Niermeijer MF, Halley DJ, Drop SL. [From gene to disease; androgen receptor gene, androgen insensitivity syndrome, and spinal and bulbar muscle atrophy]. Nederlands tijdschrift voor geneeskunde. 2001;145(48):2326-8.

67. La Spada AR, Wilson EM, Lubahn DB, Harding AE, Fischbeck KH. Androgen receptor gene mutations in X-linked spinal and bulbar muscular atrophy. Nature. 1991;352(6330):77-9.

68. Sawaya ME, Shalita AR. Androgen receptor polymorphisms (CAG repeat lengths) in androgenetic alopecia, hirsutism, and acne. Journal of cutaneous medicine and surgery. 1998;3(1):9-15.

69. Lonergan PE, Tindall DJ. Androgen receptor signaling in prostate cancer development and progression. Journal of carcinogenesis. 2011;10:20.

70. Grossmann ME, Huang H, Tindall DJ. Androgen receptor signaling in androgen-refractory prostate cancer. Journal of the National Cancer Institute. 2001;93(22):1687-97.

71. Jin HJ, Kim J, Yu J. Androgen receptor genomic regulation. Translational andrology and urology. 2013;2(3):157-77.

72. Bolton EC, So AY, Chaivorapol C, Haqq CM, Li H, Yamamoto KR. Cell- and gene-specific regulation of primary target genes by the androgen receptor. Genes & development. 2007;21(16):2005-17.

73. Chmelar R, Buchanan G, Need EF, Tilley W, Greenberg NM. Androgen receptor coregulators and their involvement in the development and progression of prostate cancer. International journal of cancer Journal international du cancer. 2007;120(4):719-33.

74. Jenster G, van der Korput JA, Trapman J, Brinkmann AO. Functional domains of the human androgen receptor. The Journal of steroid biochemistry and molecular biology. 1992;41(3-8):671-5.

75. Tan MH, Li J, Xu HE, Melcher K, Yong EL. Androgen receptor: structure, role in prostate cancer and drug discovery. Acta pharmacologica Sinica. 2015;36(1):3-23.

76. Hirawat S, Budman DR, Kreis W. The androgen receptor: structure, mutations, and antiandrogens. Cancer investigation. 2003;21(3):400-17.

77. Young CYF, Montgomery BT, Andrews PE, Qiu SD, Bilhartz DL, Tindall DJ. Hormonal-Regulation of Prostate-Specific Antigen Messenger-Rna in Human Prostatic Adenocarcinoma Cell-Line Lncap. Cancer Research. 1991;51(14):3748-52.

78. Cleutjens KBJM, vanderKorput HAGM, vanEekelen CCEM, vanRooij HCJ, Faber PW, Trapman J. An androgen response element in a far upstream enhancer region is essential for high, androgen-regulated activity of the prostate-specific antigen promoter. Mol Endocrinol. 1997;11(2):148-61.

79. Wang Q, Li W, Zhang Y, Yuan X, Xu K, Yu J, et al. Androgen receptor regulates a distinct transcription program in androgen-independent prostate cancer. Cell. 2009;138(2):245-56.

80. Sahu B, Laakso M, Ovaska K, Mirtti T, Lundin J, Rannikko A, et al. Dual role of FoxA1 in androgen receptor binding to chromatin, androgen signalling and prostate cancer. Embo J. 2011;30(19):3962-76.

81. Jin HJ, Zhao JC, Wu LT, Kim J, Yu JD. Cooperativity and equilibrium with FOXA1 define the androgen receptor transcriptional program. Nature Communications. 2014;5.

82. Pomerantz MM, Li FG, Takeda DY, Lenci R, Chonkar A, Chabot M, et al. The androgen receptor cistrome is extensively reprogrammed in human prostate tumorigenesis. Nat Genet. 2015;47(11):1346-+.

83. Shiota M, Yokomizo A, Naito S. Increased androgen receptor transcription: a cause of castration-resistant prostate cancer and a possible therapeutic target. Journal of molecular endocrinology. 2011;47(1):R25-41.

84. Dutt SS, Gao AC. Molecular mechanisms of castration-resistant prostate cancer progression. Future oncology. 2009;5(9):1403-13.

85. Waltering KK, Urbanucci A, Visakorpi T. Androgen receptor (AR) aberrations in castration-resistant prostate cancer. Molecular and cellular endocrinology. 2012;360(1-2):38-43.

86. Chang KH, Li R, Kuri B, Lotan Y, Roehrborn CG, Liu J, et al. A gain-of-function mutation in DHT synthesis in castration-resistant prostate cancer. Cell. 2013;154(5):1074-84.

87. Decker KF, Zheng D, He Y, Bowman T, Edwards JR, Jia L. Persistent androgen receptor-mediated transcription in castration-resistant prostate cancer under androgen-deprived conditions. Nucleic acids research. 2012;40(21):10765-79.

88. Locke JA, Guns ES, Lubik AA, Adomat HH, Hendy SC, Wood CA, et al. Androgen levels increase by intratumoral de novo steroidogenesis during progression of castration-resistant prostate cancer. Cancer research. 2008;68(15):6407-15.

89. Gioeli D, Paschal BM. Post-translational modification of the androgen receptor. Molecular and cellular endocrinology. 2012;352(1-2):70-8.

90. Rytinki MM, Kaikkonen S, Sutinen P, Palvimo JJ. Analysis of androgen receptor SUMOylation. Methods in molecular biology. 2011;776:183-97.

91. Faus H, Haendler B. Androgen receptor acetylation sites differentially regulate gene control. Journal of cellular biochemistry. 2008;104(2):511-24.

92. Chen Z, Lu W. Roles of ubiquitination and SUMOylation on prostate cancer: mechanisms and clinical implications. International journal of molecular sciences. 2015;16(3):4560-80.

93. Qi J, Fan L, Hussain A. Implications of ubiquitin ligases in castration-resistant prostate cancer. Curr Opin Oncol. 2015;27(3):172-6.

94. Li B, Lu W, Chen Z. Regulation of Androgen Receptor by E3 Ubiquitin Ligases: for More or Less. Receptors & clinical investigation. 2014;1(5).

95. Linn DE, Yang X, Xie Y, Alfano A, Deshmukh D, Wang X, et al. Differential regulation of androgen receptor by PIM-1 kinases via phosphorylation-dependent recruitment of distinct ubiquitin E3 ligases. The Journal of biological chemistry. 2012;287(27):22959-68.

96. Freeman MR. The ubiquitin ligase Siah2 is revealed as an accomplice of the androgen receptor in castration resistant prostate cancer. Asian journal of andrology. 2013;15(4):447-8.

97. Qi J, Tripathi M, Mishra R, Sahgal N, Fazli L, Ettinger S, et al. The E3 ubiquitin ligase Siah2 contributes to castration-resistant prostate cancer by regulation of androgen receptor transcriptional activity. Cancer cell. 2013;23(3):332-46.

98. Xu K, Shimelis H, Linn DE, Jiang R, Yang X, Sun F, et al. Regulation of androgen receptor transcriptional activity and specificity by RNF6-induced ubiquitination. Cancer cell. 2009;15(4):270-82.

99. Vogt PK. Retroviral oncogenes: a historical primer. Nat Rev Cancer. 2012;12(9):639-48.

100. Fleming WH, Hamel A, MacDonald R, Ramsey E, Pettigrew NM, Johnston B, et al. Expression of the c-myc protooncogene in human prostatic carcinoma and benign prostatic hyperplasia. Cancer Res. 1986;46(3):1535-8.

101. Lapointe J, Li C, Higgins JP, van de Rijn M, Bair E, Montgomery K, et al. Gene expression profiling identifies clinically relevant subtypes of prostate cancer. Proc Natl Acad Sci U S A. 2004;101(3):811-6.

102. Varambally S, Yu J, Laxman B, Rhodes DR, Mehra R, Tomlins SA, et al. Integrative genomic and proteomic analysis of prostate cancer reveals signatures of metastatic progression. Cancer Cell. 2005;8(5):393-406.

103. Yu YP, Landsittel D, Jing L, Nelson J, Ren B, Liu L, et al. Gene expression alterations in prostate cancer predicting tumor aggression and preceding development of malignancy. J Clin Oncol. 2004;22(14):2790-9.

104. Buttyan R, Sawczuk IS, Benson MC, Siegal JD, Olsson CA. Enhanced expression of the c-myc protooncogene in high-grade human prostate cancers. Prostate. 1987;11(4):327-37.

105. Beroukhim R, Mermel CH, Porter D, Wei G, Raychaudhuri S, Donovan J, et al. The landscape of somatic copy-number alteration across human cancers. Nature. 2010;463(7283):899-905.

106. Gabay M, Li Y, Felsher DW. MYC activation is a hallmark of cancer initiation and maintenance. Cold Spring Harb Perspect Med. 2014;4(6).

107. Kohl NE, Gee CE, Alt FW. Activated Expression of the N-Myc Gene in Human Neuroblastomas and Related Tumors. Science. 1984;226(4680):1335-7.

108. Nau MM, Brooks BJ, Battey J, Sausville E, Gazdar AF, Kirsch IR, et al. L-Myc, a New Myc-Related Gene Amplified and Expressed in Human Small Cell Lung-Cancer. Nature. 1985;318(6041):69-73.

109. Rabbitts TH, Hamlyn PH, Baer R. Altered nucleotide sequences of a translocated c-myc gene in Burkitt lymphoma. Nature. 1983;306(5945):760-5.

110. Tansey WP. Mammalian MYC Proteins and Cancer. New Journal of Science. 2014;2014:27.

111. Blackwood EM, Eisenman RN. Max - a Helix-Loop-Helix Zipper Protein That Forms a Sequence-Specific DNA-Binding Complex with Myc. Science. 1991;251(4998):1211-7.

112. Chen H, Liu HD, Qing GL. Targeting oncogenic Myc as a strategy for cancer treatment. Signal Transduct Tar. 2018;3.

113. Fernandez PC, Frank SR, Wang LQ, Schroeder M, Liu SX, Greene J, et al. Genomic targets of the human c-Myc protein. Gene Dev. 2003;17(9):1115-29.

114. Uribesalgo I, Buschbeck M, Gutierrez A, Teichmann S, Demajo S, Kuebler B, et al. E-box-independent regulation of transcription and differentiation by MYC. Nat Cell Biol. 2011;13(12):1443-U149.

115. Thomas LR, Wang QG, Grieb BC, Phan J, Foshage AM, Sun Q, et al. Interaction with WDR5 Promotes Target Gene Recognition and Tumorigenesis by MYC. Molecular Cell. 2015;58(3):440-52.

116. Lin CY, Loven J, Rahl PB, Paranal RM, Burge CB, Bradner JE, et al. Transcriptional Amplification in Tumor Cells with Elevated c-Myc. Cell. 2012;151(1):56-67.

117. Nie ZQ, Hu GQ, Wei G, Cui KR, Yamane A, Resch W, et al. c-Myc Is a Universal Amplifier of Expressed Genes in Lymphocytes and Embryonic Stem Cells. Cell. 2012;151(1):68-79.

118. Si JL, Yu XY, Zhang YJ, DeWille JW. Myc interacts with Max and Miz1 to repress C/EBP delta promoter activity and gene expression. Molecular Cancer. 2010;9.

119. Staller P, Peukert K, Kiermaier A, Seoane J, Lukas J, Karsunky H, et al. Repression of p15(INK4b) expression by Myc through association with Miz-1. Nat Cell Biol. 2001;3(4):392-9.

120. Jiang GC, Espeseth A, Hazuda DJ, Margolis DM. c-Myc and sp1 contribute to proviral latency by recruiting histone deacetylase 1 to the human immunodeficiency virus type 1 promoter. J Virol. 2007;81(20):10914-23.

121. Karn J, Watson JV, Lowe AD, Green SM, Vedeckis W. Regulation of cell cycle duration by c-myc levels. Oncogene. 1989;4(6):773-87.

122. Oster SK, Ho CS, Soucie EL, Penn LZ. The myc oncogene: MarvelouslY Complex. Adv Cancer Res. 2002;84:81-154.

123. Evan GI, Wyllie AH, Gilbert CS, Littlewood TD, Land H, Brooks M, et al. Induction of apoptosis in fibroblasts by c-myc protein. Cell. 1992;69(1):119-28.

124. Iritani BM, Eisenman RN. c-Myc enhances protein synthesis and cell size during B lymphocyte development. Proc Natl Acad Sci U S A. 1999;96(23):13180-5.

125. Grandori C, Gomez-Roman N, Felton-Edkins ZA, Ngouenet C, Galloway DA, Eisenman RN, et al. c-Myc binds to human ribosomal DNA and stimulates transcription of rRNA genes by RNA polymerase I. Nat Cell Biol. 2005;7(3):311-8.

126. Pourdehnad M, Truitt ML, Siddiqi IN, Ducker GS, Shokat KM, Ruggero D. Myc and mTOR converge on a common node in protein synthesis control that confers synthetic lethality in Myc-driven cancers. Cancer Research. 2013;73.

127. Hu S, Balakrishnan A, Bok RA, Anderton B, Larson PEZ, Nelson SJ, et al. C-13-Pyruvate Imaging Reveals Alterations in Glycolysis that Precede c-Myc-Induced Tumor Formation and Regression. Cell Metab. 2011;14(1):131-42.

128. Gao P, Tchernyshyov I, Chang TC, Lee YS, Kita K, Ochi T, et al. c-Myc suppression of miR-23a/b enhances mitochondrial glutaminase expression and glutamine metabolism. Nature. 2009;458(7239):762-U100.

129. Vafa O, Wade M, Kern S, Beeche M, Pandita TK, Hampton GM, et al. c-Myc can induce DNA damage, increase reactive oxygen species, and mitigate p53 function: A mechanism for oncogene-induced genetic instability. Molecular Cell. 2002;9(5):1031-44.

130. Felsher DW, Bishop JM. Transient excess of MYC activity can elicit genomic instability and tumorigenesis. P Natl Acad Sci USA. 1999;96(7):3940-4.

131. Frye M, Gardner C, Li ER, Arnold I, Watt FM. Evidence that Myc activation depletes the epidermal stem cell compartment by modulating adhesive interactions with the local microenvironment. Development. 2003;130(12):2793-808.

132. Smith AP, Verrecchia A, Faga G, Doni M, Perna D, Martinato F, et al. A positive role for Myc in TGFbeta-induced Snail transcription and epithelial-to-mesenchymal transition. Oncogene. 2009;28(3):422-30.

133. Ma L, Young J, Prabhala H, Pan E, Mestdagh P, Muth D, et al. miR-9, a MYC/MYCN-activated microRNA, regulates E-cadherin and cancer metastasis. Nat Cell Biol. 2010;12(3):247-56.

134. Jain M, Arvanitis C, Chu K, Dewey W, Leonhardt E, Trinh M, et al. Sustained loss of a neoplastic phenotype by brief inactivation of MYC. Science. 2002;297(5578):102-4.

135. Wang H, Hammoudeh DI, Follis AV, Reese BE, Lazo JS, Metallo SJ, et al. Improved low molecular weight Myc-Max inhibitors. Mol Cancer Ther. 2007;6(9):2399-408.

136. Soucek L, Helmer-Citterich M, Sacco A, Jucker R, Cesareni G, Nasi S. Design and properties of a myc derivative that efficiently homodimerizes. Oncogene. 1998;17(19):2463-72.

137. Delmore JE, Issa GC, Lemieux ME, Rahl PB, Shi JW, Jacobs HM, et al. BET Bromodomain Inhibition as a Therapeutic Strategy to Target c-Myc. Cell. 2011;146(6):903-16.

138. Chipumuro E, Marco E, Christensen CL, Kwiatkowski N, Zhang TH, Hatheway CM, et al. CDK7 Inhibition Suppresses Super-Enhancer-Linked Oncogenic Transcription in MYCN-Driven Cancer. Cell. 2014;159(5):1126-39.

139. Bjornsti MA, Houghton PJ. The TOR pathway: A target for cancer therapy. Nat Rev Cancer. 2004;4(5):335-48.

140. Yada M, Hatakeyama S, Kamura T, Nishiyama M, Tsunematsu R, Imaki H, et al. Phosphorylation-dependent degradation of c-Myc is mediated by the F-box protein Fbw7. Embo J. 2004;23(10):2116-25.

141. Popov N, Wanzel M, Madiredjo M, Zhang D, Beijersbergen R, Bernards R, et al. The ubiquitin-specific protease USP28 is required for MYC stability. Nat Cell Biol. 2007;9(7):765-U71.

142. Brockmann M, Poon E, Berry T, Carstensen A, Deubzer HE, Rycak L, et al. Small Molecule Inhibitors of Aurora-A Induce Proteasomal Degradation of N-Myc in Childhood Neuroblastoma (vol 24, pg 75, 2013). Cancer Cell. 2016;30(2):357-8.

143. Gravina GL, Ranieri G, Muzi P, Marampon F, Mancini A, Di Pasquale B, et al. Increased levels of DNA methyltransferases are associated with the tumorigenic capacity of prostate cancer cells. Oncol Rep. 2013;29(3):1189-95.

144. Lee E, Wang JC, Yumoto K, Jung YH, Cackowski FC, Decker AM, et al. DNMT1 Regulates Epithelial-Mesenchymal Transition and Cancer Stem Cells, Which Promotes Prostate Cancer Metastasis. Neoplasia. 2016;18(9):553-66.

145. Spans L, Van den Broeck T, Smeets E, Prekovic S, Thienpont B, Lambrechts D, et al. Genomic and epigenomic analysis of high-risk prostate cancer reveals changes in hydroxymethylation and TET1. Oncotarget. 2016;7(17):24326-38.

146. Brocks D, Assenov Y, Minner S, Bogatyrova O, Simon R, Koop C, et al. Intratumor DNA Methylation Heterogeneity Reflects Clonal Evolution in Aggressive Prostate Cancer. Cell Rep. 2014;8(3):798-806.

147. Festuccia C, Gravina GL, D'Alessandro AM, Muzi P, Millimaggi D, Dolo V, et al. Azacitidine improves antitumor effects of docetaxel and cisplatin in aggressive prostate cancer models. Endocr-Relat Cancer. 2009;16(2):401-13.

148. Varambally S, Dhanasekaran SM, Zhou M, Barrette TR, Kumar-Sinha C, Sanda MG, et al. The polycomb group protein EZH2 is involved in progression of prostate cancer. Nature. 2002;419(6907):624-9.

149. Chinnaiyan AM, Varambally S, Dhanasekaran SM, Fecko A, Sanda MG, Otte AP, et al. Genetic profiling of hormone refractory prostate cancer implicates EZH-2 as as a marker to distinguish cancers at risk for lethal progression from indolent prostate cancers. Modern Pathol. 2002;15(1):158a-a.

150. Kunderfranco P, Mello-Grand M, Cangemi R, Pellini S, Mensah A, Albertini V, et al. ETS Transcription Factors Control Transcription of EZH2 and Epigenetic Silencing of the Tumor Suppressor Gene Nkx3.1 in Prostate Cancer. Plos One. 2010;5(5).

151. Cao Q, Yu J, Dhanasekaran SM, Kim JH, Mani RS, Tomlins SA, et al. Repression of E-cadherin by the polycomb group protein EZH2 in cancer. Oncogene. 2008;27(58):7274-84.

152. Min J, Zaslavsky A, Fedele G, McLaughlin SK, Reczek EE, De Raedt T, et al. An oncogene-tumor suppressor cascade drives metastatic prostate cancer by coordinately activating Ras and nuclear factor-kappa B. Nature Medicine. 2010;16(3):286-U82.

153. Gao WL, Liu HL. [DOT1: a distinct class of histone lysine methyltransferase]. Yi Chuan. 2007;29(12):1449-54.

154. Nguyen AT, Zhang Y. The diverse functions of Dot1 and H3K79 methylation. Genes & development. 2011;25(13):1345-58.

155. Park JW, Kim KB, Kim JY, Chae YC, Jeong OS, Seo SB. RE-IIBP Methylates H3K79 and Induces MEIS1-mediated Apoptosis via H2BK120 Ubiquitination by RNF20. Sci Rep-Uk. 2015;5.

156. Frederiks F, Tzouros M, Oudgenoeg G, van Welsem T, Fornerod M, Krijgsveld J, et al. Nonprocessive methylation by Dot1 leads to functional redundancy of histone H3K79 methylation states. Nat Struct Mol Biol. 2008;15(6):550-7.

157. Singer MS, Kahana A, Wolf AJ, Meisinger LL, Peterson SE, Goggin C, et al. Identification of high-copy disruptors of telomeric silencing in Saccharomyces cerevisiae. Genetics. 1998;150(2):613-32.

158. Ng HH, Feng Q, Wang HB, Erdjument-Bromage H, Tempst P, Zhang Y, et al. Lysine methylation within the globular domain of histone H3 by Dot1 is important for telomeric silencing and Sir protein association. Gene Dev. 2002;16(12):1518-27.

159. Jones B, Su H, Bhat A, Lei H, Bajko J, Hevi S, et al. The Histone H3K79 Methyltransferase Dot1L Is Essential for Mammalian Development and Heterochromatin Structure. Plos Genet. 2008;4(9).

160. Kim SK, Jung I, Lee H, Kang K, Kim M, Jeong K, et al. Human histone H3K79 methyltransferase DOT1L protein [corrected] binds actively transcribing RNA polymerase II to regulate gene expression. J Biol Chem. 2012;287(47):39698-709.

161. Worden EJ, Hoffmann NA, Hicks CW, Wolberger C. Mechanism of Cross-talk between H2B Ubiquitination and H3 Methylation by Dot1L. Cell. 2019;176(6):1490-+.

162. Chang MJ, Wu H, Achille NJ, Reisenauer MR, Chou CW, Zeleznik-Le NJ, et al. Histone H3 lysine 79 methyltransferase Dot1 is required for immortalization by MLL oncogenes. Cancer Res. 2010;70(24):10234-42.

163. Bernt KM, Armstrong SA. A role for DOT1L in MLL-rearranged leukemias. Epigenomics. 2011;3(6):667-70.

164. Bernt KM, Zhu N, Sinha AU, Vempati S, Faber J, Krivtsov AV, et al. MLL-rearranged leukemia is dependent on aberrant H3K79 methylation by DOT1L. Cancer cell. 2011;20(1):66-78.

165. Nguyen AT, Taranova O, He J, Zhang Y. DOT1L, the H3K79 methyltransferase, is required for MLL-AF9-mediated leukemogenesis. Blood. 2011;117(25):6912-22.

166. Chen CW, Koche RP, Sinha AU, Deshpande AJ, Zhu N, Eng R, et al. DOT1L inhibits SIRT1-mediated epigenetic silencing to maintain leukemic gene expression in MLL-rearranged leukemia. Nat Med. 2015;21(4):335-43.

167. Campbell JD, Alexandrov A, Kim J, Wala J, Berger AH, Pedamallu CS, et al. Distinct patterns of somatic genome alterations in lung adenocarcinomas and squamous cell carcinomas. Nat Genet. 2016;48(6):607-16.

168. Kim W, Kim R, Park G, Park JW, Kim JE. Deficiency of H3K79 histone methyltransferase Dot1-like protein (DOT1L) inhibits cell proliferation. J Biol Chem. 2012;287(8):5588-99.

169. MacLeod G, Bozek DA, Rajakulendran N, Monteiro V, Ahmadi M, Steinhart Z, et al. Genome-Wide CRISPR-Cas9 Screens Expose Genetic Vulnerabilities and Mechanisms of Temozolomide Sensitivity in Glioblastoma Stem Cells. Cell Rep. 2019;27(3):971-86 e9.

170. Qu Y, Liu L, Wang J, Xi W, Xia Y, Bai Q, et al. Dot1l expression predicts adverse postoperative prognosis of patients with clear-cell renal cell carcinoma. Oncotarget. 2016;7(51):84775-84.

171. Kryczek I, Lin Y, Nagarsheth N, Peng D, Zhao L, Zhao E, et al. IL-22(+)CD4(+) T cells promote colorectal cancer stemness via STAT3 transcription factor activation and induction of the methyltransferase DOT1L. Immunity. 2014;40(5):772-84.

172. Cho MH, Park JH, Choi HJ, Park MK, Won HY, Park YJ, et al. DOT1L cooperates with the c-Myc-p300 complex to epigenetically derepress CDH1 transcription factors in breast cancer progression. Nat Commun. 2015;6:7821.

173. Lee JY, Kong G. DOT1L: a new therapeutic target for aggressive breast cancer. Oncotarget. 2015;6(31):30451-2.

174. Nassa G, Salvati A, Tarallo R, Gigantino V, Alexandrova E, Memoli D, et al. Inhibition of histone methyltransferase DOT1L silences ER alpha gene and blocks proliferation of antiestrogen-resistant breast cancer cells. Sci Adv. 2019;5(2).

175. Zhang L, Deng LS, Chen FJ, Yao Y, Wu BL, Wei LP, et al. Inhibition of histone H3K79 methylation selectively inhibits proliferation, self-renewal and metastatic potential of breast cancer. Oncotarget. 2014;5(21):10665-77.

176. Oktyabri D, Ishimura A, Tange S, Terashima M, Suzuki T. DOT1L histone methyltransferase regulates the expression of BCAT1 and is involved in sphere formation and cell migration of breast cancer cell lines. Biochimie. 2016;123:20-31.

177. Salvati A, Gigantino V, Nassa G, Giurato G, Alexandrova E, Rizzo F, et al. The Histone Methyltransferase DOT1L Is a Functional Component of Estrogen Receptor Alpha Signaling in Ovarian Cancer Cells. Cancers. 2019;11(11):1720.

178. Liu D, Zhang XX, Li MC, Cao CH, Wan DY, Xi BX, et al. C/EBPbeta enhances platinum resistance of ovarian cancer cells by reprogramming H3K79 methylation. Nat Commun. 2018;9(1):1739.

179. Zhang X, Liu D, Li M, Cao C, Wan D, Xi B, et al. Prognostic and therapeutic value of disruptor of telomeric silencing-1-like (DOT1L) expression in patients with ovarian cancer. J Hematol Oncol. 2017;10(1):29.

180. Wang X, Wang H, Xu B, Jiang D, Huang S, Yu H, et al. Depletion of H3K79 methyltransferase Dot1L promotes cell invasion and cancer stem-like cell property in ovarian cancer. Am J Transl Res. 2019;11(2):1145-53.

181. Grasso CS, Wu YM, Robinson DR, Cao X, Dhanasekaran SM, Khan AP, et al. The mutational landscape of lethal castration-resistant prostate cancer. Nature. 2012;487(7406):239-43.

182. Chandran UR, Ma C, Dhir R, Bisceglia M, Lyons-Weiler M, Liang W, et al. Gene expression profiles of prostate cancer reveal involvement of multiple molecular pathways in the metastatic process. BMC Cancer. 2007;7:64.

183. Taylor BS, Schultz N, Hieronymus H, Gopalan A, Xiao Y, Carver BS, et al. Integrative genomic profiling of human prostate cancer. Cancer Cell. 2010;18(1):11-22.

184. Roudier MP, Winters BR, Coleman I, Lam HM, Zhang X, Coleman R, et al. Characterizing the molecular features of ERG-positive tumors in primary and castration resistant prostate cancer. Prostate. 2016;76(9):810-22.

185. Gulzar ZG, McKenney JK, Brooks JD. Increased expression of NuSAP in recurrent prostate cancer is mediated by E2F1. Oncogene. 2013;32(1):70-7.

186. Beltran H, Prandi D, Mosquera JM, Benelli M, Puca L, Cyrta J, et al. Divergent clonal evolution of castration-resistant neuroendocrine prostate cancer. Nat Med. 2016;22(3):298-305.

187. Zhao H, Langerod A, Ji Y, Nowels KW, Nesland JM, Tibshirani R, et al. Different gene expression patterns in invasive lobular and ductal carcinomas of the breast. Mol Biol Cell. 2004;15(6):2523-36.

188. Gaedcke J, Grade M, Jung K, Camps J, Jo P, Emons G, et al. Mutated KRAS results in overexpression of DUSP4, a MAP-kinase phosphatase, and SMYD3, a histone methyltransferase, in rectal carcinomas. Genes Chromosomes Cancer. 2010;49(11):1024-34.

189. Murat A, Migliavacca E, Gorlia T, Lambiv WL, Shay T, Hamou MF, et al. Stem cell-related "self-renewal" signature and high epidermal growth factor receptor expression associated with resistance to concomitant chemoradiotherapy in glioblastoma. J Clin Oncol. 2008;26(18):3015-24.

190. Hong Y, Downey T, Eu KW, Koh PK, Cheah PY. A 'metastasis-prone' signature for early-stage mismatch-repair proficient sporadic colorectal cancer patients and its implications for possible therapeutics. Clin Exp Metastasis. 2010;27(2):83-90.

191. Haferlach T, Kohlmann A, Wieczorek L, Basso G, Kronnie GT, Bene MC, et al. Clinical utility of microarray-based gene expression profiling in the diagnosis and subclassification of

leukemia: report from the International Microarray Innovations in Leukemia Study Group. J Clin Oncol. 2010;28(15):2529-37.

192. Kim WJ, Kim EJ, Kim SK, Kim YJ, Ha YS, Jeong P, et al. Predictive value of progression-related gene classifier in primary non-muscle invasive bladder cancer. Mol Cancer. 2010;9:3.

193. Luca BA, Brewer DS, Edwards DR, Edwards S, Whitaker HC, Merson S, et al. DESNT: A Poor Prognosis Category of Human Prostate Cancer. Eur Urol Focus. 2018;4(6):842-50.

194. Ross-Adams H, Lamb AD, Dunning MJ, Halim S, Lindberg J, Massie CM, et al. Integration of copy number and transcriptomics provides risk stratification in prostate cancer: A discovery and validation cohort study. EBioMedicine. 2015;2(9):1133-44.

195. Cancer Genome Atlas Research N. The Molecular Taxonomy of Primary Prostate Cancer. Cell. 2015;163(4):1011-25.

196. Robinson D, Van Allen EM, Wu YM, Schultz N, Lonigro RJ, Mosquera JM, et al. Integrative clinical genomics of advanced prostate cancer. Cell. 2015;161(5):1215-28.

197. Unno K, Roh M, Yoo YA, Al-Shraideh Y, Wang L, Nonn L, et al. Modeling African American prostate adenocarcinoma by inducing defined genetic alterations in organoids. Oncotarget. 2017;8(31):51264-76.

198. Kim JY, Banerjee T, Vinckevicius A, Luo Q, Parker JB, Baker MR, et al. A role for WDR5 in integrating threonine 11 phosphorylation to lysine 4 methylation on histone H3 during androgen signaling and in prostate cancer. Mol Cell. 2014;54(4):613-25.

199. Anker JF, Naseem AF, Mok H, Schaeffer AJ, Abdulkadir SA, Thumbikat P. Multi-faceted immunomodulatory and tissue-tropic clinical bacterial isolate potentiates prostate cancer immunotherapy. Nat Commun. 2018;9(1):1591.

200. Yoo YA, Vatapalli R, Lysy B, Mok H, Desouki MM, Abdulkadir SA. The Role of Castration-Resistant Bmi1+Sox2+ Cells in Driving Recurrence in Prostate Cancer. J Natl Cancer Inst. 2019;111(3):311-21.

201. Nadeau G, Bellemare J, Audet-Walsh E, Flageole C, Huang SP, Bao BY, et al. Deletions of the Androgen-Metabolizing UGT2B Genes Have an Effect on Circulating Steroid Levels and Biochemical Recurrence after Radical Prostatectomy in Localized Prostate Cancer. J Clin Endocr Metab. 2011;96(9):E1550-E7.

202. Chouinard S, Barbier O, Belanger A. UDP-glucuronosyltransferase 2B15 (UGT2B15) and UGT2B17 enzymes are major determinants of the androgen response in prostate cancer LNCaP cells. Journal of Biological Chemistry. 2007;282(46).

203. Ge Z, Guo X, Li JY, Hartman M, Kawasawa YI, Dovat S, et al. Clinical Significance of High C-MYC and Low MYCBP2 Expression and Their Association with Ikaros Dysfunction in Adult Acute Lymphoblastic Leukemia. Blood. 2015;126(23).

204. Guo QB, Xie JW, Dang CV, Liu ET, Bishop JM. Identification of a large Myc-binding protein that contains RCC1-like repeats. P Natl Acad Sci USA. 1998;95(16):9172-7.

205. Liu PY, Xu N, Malyukova A, Scarlett CJ, Sun YT, Zhang XD, et al. The histone deacetylase SIRT2 stabilizes Myc oncoproteins. Cell Death Differ. 2013;20(3):503-14.

206. Li H, Xu LL, Masuda K, Raymundo E, McLeod DG, Dobi A, et al. A feedback loop between the androgen receptor and a NEDD4-binding protein, PMEPA1, in prostate cancer cells. J Biol Chem. 2008;283(43):28988-95.

207. Farrell AS, Sears RC. MYC degradation. Cold Spring Harb Perspect Med. 2014;4(3).

208. Hatakeyama S. TRIM proteins and cancer. Nature reviews Cancer. 2011;11(11):792-804.

209. Groner AC, Cato L, de Tribolet-Hardy J, Bernasocchi T, Janouskova H, Melchers D, et al. TRIM24 Is an Oncogenic Transcriptional Activator in Prostate Cancer. Cancer Cell. 2016;29(6):846-58.

210. Fujimura T, Inoue S, Urano T, Takayama K, Yamada Y, Ikeda K, et al. Increased Expression of Tripartite Motif (TRIM) 47 Is a Negative Prognostic Predictor in Human Prostate Cancer. Clin Genitourin Cancer. 2016;14(4):298-303.

211. Godfrey L, Crump NT, Thorne R, Lau IJ, Repapi E, Dimou D, et al. DOT1L inhibition reveals a distinct subset of enhancers dependent on H3K79 methylation. Nat Commun. 2019;10(1):2803.

212. Stein EM, Garcia-Manero G, Rizzieri DA, Tibes R, Berdeja JG, Savona MR, et al. The DOT1L inhibitor pinometostat reduces H3K79 methylation and has modest clinical activity in adult acute leukemia. Blood. 2018;131(24):2661-9.